



THE INDIAN CONCRETE JOURNAL

Published by **ACC** Limited

Volume 95 • Number 4 • April 2021 • Pages 73 • ₹ 175

**ICJ BEST PAPER AWARDS - 2020  
winners announced**

## **CORROSION AND ITS CONTROL IN CONCRETE STRUCTURES**





# BUILDING A NEW AND STRONG INDIA



☎ 1800 1033 444

**ACC**

CEMENT ■ READY MIX CONCRETE ■ BUILDING MATERIALS

Cementing Relationships



THE INDIAN CONCRETE JOURNAL

Volume 95 • Number 4 • April 2021 • Pages 72

ISSN (Digital) : 0019-4565

## Founded in 1927

Published by ACC Limited, L.B. Shastri Road, Near Teen Haath Naka, Thane (West) 400 604. The contents of this journal are contributions of individual authors, and reflect their independent opinions, findings, conclusions and recommendations, and do not necessarily imply that they reflect the views of the Publisher, ACC Limited. The Publishers are not liable for any damage or inconvenience caused to anyone who may have acted on the information contained in the publication.

This is a **Scopus®** indexed journal.



### Cover image source:

Mr. Zameel D. Veedu  
from Radhe Structorepair  
Pvt. Ltd., India.

### Cover

The cover page shows a 10-year-old clarifier from a power plant in Gujarat in India. The clarifier is an essential component in the pre-treatment of seawater for use in the plant. The structure was observed to have durability issues in terms of leakage through the joints as well as corrosion of rebars. The structure is undergoing its first major repair for which a combination of various repair strategies along with the galvanic cathodic protection of steel bars is incorporated on the structure.

## 04 EDITORIAL

## 06 ICJ BEST PAPER AWARDS - 2020

### PART I : FEATURES

## 07 NEWS and EVENTS

### PART II : PERSPECTIVES ON TRENDS

## 08 Hydrophobic treatment for control of deterioration in reinforced concrete structures

Joanitta Ndawula, Hans Beushausen,  
Mark Alexander

## 17 Optimal dosage of $\text{Fe}_2\text{O}_3$ nanoparticles to enhance chloride resistance and microstructural properties of concrete- A comprehensive study

Raghava Kumar Vanama, Harinee Addepalli,  
Balaji Ramakrishnan

## 29 Performance of organic and inorganic functional groups as corrosion inhibitors in concrete experiencing extreme corrosive environment

Himanshu Guleria, Purnima, Ashish Kumar Tiwari,  
Shweta Goyal

## 38 Corrosion inhibiting admixture for corrosion prevention in small scale reinforced concrete structures

S. Shafeer Ahamed, J. Sherin Mariya, V. Roopa,  
M.S. Haji Sheik Mohammed

## 52 Mechanical and electrochemical aspects of microalloyed steel

B. Bhuvaneshwari, P. Prabha, S. Sandhiya,  
G. S. Palani

## 61 Cathodic protection of steel reinforcement: Past experience, performance and future opportunities

George Sergi

The Indian Concrete Journal, ISSN 0019-4565 Copyright © 2020 ACC Limited. All copyright in all materials published in The Indian Concrete Journal are owned by ACC Limited. None of this material may be used for any commercial or public use, other than for the purpose of fair dealing, research or private study, or review of the contents of the journal, in part or in whole, and may not be reproduced or stored in any media for mass circulation without the prior written consent of the publisher.

**CIRCULATION OFFICE:** The Indian Concrete Journal, ACC Limited, L.B. Shastri Road, Near Teen Haath Naka, Next to Eternity Mall, Thane (West) 400 604, Maharashtra, INDIA.  
Website: <http://www.icjonline.com>; e-mail: [info@icjonline.com](mailto:info@icjonline.com), [editor@icjonline.com](mailto:editor@icjonline.com)



Dear Readers,

Our special themed edition covering research papers on various aspects of corrosion and its control in concrete structures (C3S) was very well received. We are pleased to share with you a sequel edition guest edited by Dr Radhakrishna G. Pillai and Dyana Joseline.

Dr Pillai is an associate professor in the Department of Civil Engineering at Indian Institute of Technology (IIT) Madras. He earned B.E. degree in Civil Engineering from the M. N. Regional Engineering College (now MNNIT), Allahabad. Then, he earned M.S. and Ph.D. degrees in Civil Engineering at Texas A & M University, U.S.A. and has been passionate to combat corrosion of steel in reinforced and prestressed concrete structures. Beyond teaching in the areas of construction materials, concrete technology, and maintenance/repair of concrete structures, recently, he has been extending his research towards the extension of the residual service life of concrete structures through durable repair techniques such as cathodic protection. Most of his projects contribute to address the practical challenges and enhancing standards and specifications. He is also an active volunteer contributing to various association bodies like the Indian Concrete Institute (ICI), the NACE International Gateway India Section (NIGIS), and the International Union of Laboratories and Experts in Construction Materials, Systems and Structures (RILEM).

Dyana Joseline is a senior Ph. D. student in the Department of Civil Engineering at IIT Madras, Chennai, India. She holds an M. Tech. Degree in Structural Engineering from B.S. Abdur Rahman University, Chennai. Her Ph. D. work focusses on the scientific understanding of the corrosion mechanisms of prestressed steel in concrete, and the modification of existing practices of service life-based design and assessment of prestressed concrete structures. She aspires to build a career in academic research, conduct purpose-driven research and take it from lab to field. She has been involved in various technical activities of RILEM and NIGIS.

Production Editor  
Indian Concrete Journal



Dear Colleagues,

Now-a-days, durability and/or service life based design of concrete structures is gaining acceptance worldwide. This is because of the realization that about 80% of structural failures are occurring due to the poor materials design of concrete, lack of timely inspections and repair, and eventual steel corrosion. In other words, the durability considerations in many structures today are severely inadequate and need significant improvements so that the onset of corrosion of steel reinforcement can be delayed. With this in mind, we bring you the second special edition of the Indian Concrete Journal (ICJ) focusing exclusively on the various aspects of corrosion and its control in concrete structures. This edition provides results from original research conducted in India and abroad on various approaches to combat corrosion in both existing and upcoming concrete structures.

India and many other countries have a large inventory of concrete structures that have not yet reached their desired service life (say, original design life) and are already experiencing severe corrosion damage (say, premature corrosion). According to the NACE IMPACT report published in 2016, such corrosion and subsequent repairs incur a total direct "cost of corrosion" of about 3.4% of global GDP; this is a higher value of 4.2% of GDP for India<sup>[1]</sup>. Moreover, if true data from all the concrete structures in India are collected, this cost could be much larger. Also, the

indirect 'cost of corrosion' could be about 10 times more than that of the direct cost<sup>[1]</sup>. These are serious issues that need to be addressed by the civil engineers by bringing in durability and/or service life based design and construction approaches. Also, the condition of many structures indicates that soon, a large number of structures may experience severe corrosion and face the need of repair and repeated repairs – leading to significant replacement of materials and systems. Through personal discussions with top personnel in steel and cement industries, we came to know the 'hard-to-believe' facts that about 25% steel and cement made are used for repair, rehabilitation, and retrofitting works at various constructed facilities. If the repairs do not address the root cause of problems, they may fail in short time (say, within 5 years)<sup>[2]</sup>, which can be avoided with the use of various corrosion control technologies.

Corrosion control can be implemented, and repairs can be made durable if both the structural/mechanical and electrochemical/chemical aspects of steel-concrete systems are adequately addressed by the repair materials and systems. If regular maintenance is done with suitable repair strategy, the number of structures that need repair can be reduced by about 80%. This means significant advantage in terms of the savings of natural resources (materials used) and money<sup>[3]</sup>, and associated carbon footprint. Hence, it is high time that the stakeholders, especially the clients, ask for the desired service life of repair work and facilitate the necessary implementation strategies by changing the contract specifications appropriately. For this, the engineers of clients can be encouraged to adopt not only BIS but also other worldwide standard documents on best practices so that the desired life of structures can truly be achieved with minimal implications on life cycle cost. This approach is essential when some of the new technologies are to be implemented.

We have witnessed the continued use of many structures with severe corrosion – increasing the probability of failure and associated risk. The civil engineering fraternity must start perceiving the high risk associated with corrosion-induced



failures and start allocating larger budgets for frequent condition assessment and preventive maintenance measures. Such approach will help to ensure adequate safety of the users and minimize the life cycle cost and life-cycle material usage – better sustainability. Also, the efforts to ensure durability for the structures is of utmost importance because the money saved by avoiding repairs can be diverted to the development of new infrastructure. The design-for-durability strategy involves the use of high-performance materials, a change in the approach from prescriptive to performance-based specifications, and the adoption of regular condition assessment and preventive maintenance strategies. This special edition sequel will address these issues through various articles.

The six papers in edition have been ordered in the following subthemes: Service life design approaches for new structures, performance of various technologies available for “avoidance of deterioration”, and cathodic protection for electrochemical repair of existing structures. The first paper of this edition is authored by Joanitta Ndawula, Dr Hans Beushausen and Dr Mark Alexander from the University of Cape Town, South Africa. This paper discusses the various approaches of service life design of concrete structures and then presents a detailed discussion on the “avoidance of deterioration” approach. A state-of-the art review of hydrophobic surface treatments for avoidance of corrosion and opportunities for further research in this area are also presented.

Then, four papers on the performance of various technologies available for “avoidance of deterioration” are provided. Usage of any new technology should be preferred only if there are no detrimental effects on the performance of the reinforced concrete system as a whole. The second paper by Mr. Raghava Kumar Vanama, Ms. Harinee Adepalli and Dr Balaji Ramakrishnan from IIT Bombay presents a comprehensive study on the influence of synthesized nano-hematite on the durability and microstructural characteristics of concrete. Through a systematic evaluation of various properties like workability, compressive strength, electrical resistivity, depth of chloride ingress, pore structure and microstructure, the authors have determined the optimum dosage of the nano-hematite. With a conclusion that a ‘higher dosage’ did not necessarily provide ‘better performance’, the general take-away from the paper is that it is important to select the optimum dosage of any new concrete additive by evaluating multiple aspects-including corrosion aspects, as shown in the next three papers. The third paper by Mr. Himanshu Guleria and others from Thapar Institute of Engineering and Technology in Patiala, Punjab, provides insights on the performance of corrosion inhibiting admixtures with Aminobenzoic Acid and Triethylphosphate functional groups in resisting carbonation and carbonation-induced

corrosion. The fourth paper is by Mr. Shafeer Ahamed and others from B.S. Abdur Rahman Crescent Institute of Science and Technology in Chennai, Tamil Nadu. They have evaluated the effect of commercial corrosion inhibiting admixtures on the engineering and corrosion properties of reinforced concrete systems with flyash and slag-based cements. The fifth paper by Dr Bhuvaneshwari and others from IIT Kanpur and CSIR-Structural Engineering Research Centre in Chennai, Tamil Nadu presents a preliminary evaluation of Titanium microalloyed steel, commonly used in automotive industry worldwide, for potential use as a concrete reinforcement. In addition, the editors believe that chloride diffusion coefficient and carbonation coefficient (along with the critical chloride threshold and critical pH) should always be determined and used to estimate the service life before utilizing new technologies in the field.

The sixth paper is authored by Dr George Sergi, a pioneering and leading researcher in the area of cathodic protection in concrete structures, and the technical director at Vector Corrosion Technologies, UK. It provides an overview of past experience and future opportunities in the usage of cathodic protection technology for extending the service life of concrete structures.

In short, this special edition calls for a major change in the mindset among the various stakeholders in the following lines: (i) utilize emerging technologies for avoidance of corrosion only if all relevant performances have been evaluated and (ii) utilize electrochemical repair methodologies (such as cathodic protection) to repair existing structures instead of conventional patch repair. The photos on the front cover page of this edition show the use of cathodic protection with embedded galvanic anodes in a power plant.

We thank the opportunity given in guest-editing this ICJ special edition on *corrosion and its control in concrete structures*. Journals like ICJ are well-read by the practicing engineers and decision makers in the concrete industry, especially in India. Such knowledgeable and wide readership (outside the academia and research community) has a huge role in implementing the latest technologies in the field of construction. Hence, we request the readers (the concrete technologists and researchers) to consider publishing in ICJ to take the results from the *purpose-driven research* in laboratories to the construction sites and thereby make a positive impact on the concrete construction sector.

Regards,

**Dr Radhakrishna G Pillai** (pillai@civil.iitm.ac.in)

**Dyana Joseline** (dyanajoseline@gmail.com)

Guest Editors

The Indian Concrete Journal

## REFERENCES

- [1] Koch, G., Varney, J., Thompson, N., Moghissi, O., Gould, M., Payer, J. (2016) International Measures of Prevention, Application, and Economics of Corrosion Technologies Study, *NACE IMPACT Report*, NACE International, Houston, Texas, USA, <http://impact.nace.org/documents/Nace-International-Report.pdf>
- [2] Raupach, M. (2006). “Patch repairs on reinforced concrete structures - Model investigations on the required size and practical consequences.” *Cement and Concrete Composites*, Vol. 2, No. 8, pp 679–684.
- [3] Polder, R. B., Peelen, W. H. A., and Courage, W. M. G. (2012). “Non-traditional assessment and maintenance methods for aging concrete structures - Technical and non-technical issues.” *Materials and Corrosion*, Vol. 63, No. 12, pp 1147–1153.

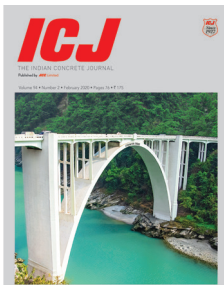
## Congratulations to the winners!

To enrich the contribution and to honour the contributors of outstanding merit, the ICJ Best Paper Awards were launched starting 2020. All papers published from January to December 2020 were considered for this annual award. Applying the key criteria of novel concept and well-documented paper, of the 92 published papers, the top fifteen papers were shortlisted. These selected top fifteen papers were further evaluated by an independent jury panel consisting of three faculty members from academia with vast research experience and association with reputed international journals.

The jury panel carefully evaluated these shortlisted papers in categories such as : i) Numerical analysis ii) Experimental research iii) Experiments and model development and iv) Review papers.

We are pleased to share with you top three ICJ Best Paper Awards - 2020 winners:

1<sup>st</sup>



Authors



**DAMANI K. PANESAR**  
University of Toronto,  
Canada



**KARINA E. SETO**  
University of Toronto,  
Canada



**CAMERON J. CHURCHILL**  
McMaster University,  
Canada



**RUNXIAO ZHANG**  
University of Toronto,  
Canada

Title: **Life cycle assessment and environmental disturbance indicators to evaluate the sustainability of concrete mix designs**

Published in February 2020 edition.

Read full paper on our website: <https://icjonline.com/award1>

2<sup>nd</sup>



Authors



**KOMATHI MURUGAN**  
Indian Institute of  
Technology (IIT) Madras, India



**AMLAN K. SENGUPTA**  
Indian Institute of  
Technology (IIT) Madras, India

Title: **Performance of high-strength concrete as jacket material in strengthening applications**

Published in May 2020 edition.

Read full paper on our website: <https://icjonline.com/award2>

3<sup>rd</sup>



Authors



**PREETHY MARY  
ARULANANDAM**  
National Institute of Technology  
(NIT) Puducherry, India



**S. B. SINGH**  
Birla Institute of  
Technology and Science  
(BITS) Pilani, India



**TOSHIYUKI KANAKUBO**  
University of Tsukuba,  
Japan.



**MADAPPA V.R.  
SIVASUBRAMANIAN**  
National Institute of  
Technology (NIT)  
Puducherry, India

Title : **Behavior of engineered cementitious composite structural elements – A review**

Published in June 2020 edition.

Read full paper on our website: <https://icjonline.com/award3>

We congratulate the winners and thank our jury panel who took time off their busy schedule to carefully evaluate each contribution and select the top three ICJ Best Papers - 2020. We also thank Dr Radhakrishna Pillai who has been instrumental in conceptualizing and instituting the ICJ Best Paper Awards.

We have made all these papers open access and available for our readers to read them online. Please visit our website to read these and many other open access papers.





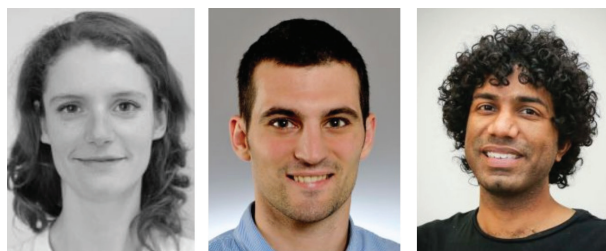
## RILEM UPDATE

The International Union of Laboratories and Experts in Construction Materials, Systems and Structures

### 2021 RILEM Medallists

We are glad to announce the 2021 RILEM Medallists!

- Robert L'Hermite Medallist: **Prof. Klaartje de Weerd**, Norwegian University of Science and Technology (NTNU)
- Gustavo Colonnetti Medallist: **Dr Emilio Martínez-Pañeda**, Imperial College London, UK
- Gustavo Colonnetti Medallist: **Dr Prannoy Suraneni**, University of Miami, USA (Dr Suraneni obtained a B.Tech. Civil Engineering from the Indian Institute of Technology Madras, India, in 2008)



These young and fabulous scientists will present their research at the 75<sup>th</sup> RILEM Annual Week, in September this year. Stay tuned as their presentations will be shared for free on our YouTube Channel [youtube.com/user/RILEMChannel](https://youtube.com/user/RILEMChannel).

### RILEM FAQ

There are no excuses to miss crucial information related to RILEM, its publications and events! We are proud to announce the new Frequently Asked Questions page, [rilem.net/article/faq](https://rilem.net/article/faq), where you will quickly find the answers to the most common questions like, for instance, how to access the numerous free RILEM publications and how to join a TC! Here you will also find some useful short videos about our website and organization.



Frequently Asked Questions

### RTL closed volume

There are so many interesting papers in the 2020 volume of RILEM Technical Letters like, to mention a few, the ones about geopolymers mortar, fungi to produce biosandstone, printable cement-based materials and corrosion of steel in carbonated concrete! These letters are all Open Access! The new 2021 volume will be opened soon with exciting articles! [letters.rilem.net](https://letters.rilem.net)



### Roc&Tok webinars

Have you missed the RILEM webinars released so far in 2021? You can watch them all FOR FREE on our YouTube Channel here [bit.ly/3qweacj](https://bit.ly/3qweacj).

April webinar: *Corrosion and electrochemistry of steel in concrete* - Professor Ueli Angst, Durability of Engineering Materials Research Lab, ETH Zurich, Switzerland.

March webinar: *Hydration and performance of Limestone Calcined Clay Cement* - Prof. Shashank Bishnoi, Indian Institute of Technology, Delhi, India and Prof. José Fernando Martirena-Hernandez, Universidad Central de las Villas, CIDEM, Cuba.

February webinar: *Thermodynamic modelling: a tool to understand hydrated cements* - Professor Barbara Lothenbach, Group Leader Cement Chemistry and Thermodynamics, Empa, Switzerland.



# HYDROPHOBIC TREATMENT FOR CONTROL OF DETERIORATION IN REINFORCED CONCRETE STRUCTURES

JOANITTA NDAWULA\*,  
HANS BEUSHAUSEN,  
MARK ALEXANDER

## Abstract

The durability of a reinforced concrete structure or structural element relates to its capacity to withstand its exposure environment, without the need for major repair over its service life. Realising concrete durability may be achieved using service life design. Service life design methods are used to ensure sufficient resistance of concrete structures to the exposure environmental actions. Avoidance of deterioration is a highly favourable option for the service life design of new structures. Surface treatment of reinforced concrete using hydrophobic impregnation (e.g. using silanes) may effectively be used for both corrosion control and avoidance of deterioration of reinforced concrete structures susceptible to chloride-induced corrosion. However, further studies are required to generate the statistical data and input variables required for the calibration and validation of service life prediction models for silane-treated structures.

## 1. INTRODUCTION

The durability of a reinforced concrete structure or structural element may be defined as its capacity to withstand its exposure environment, without the need for major repair over its service life<sup>[1]</sup>. In other words, for durable concrete, the resistance of the material to deterioration must be greater than the environmental load causing the degradation<sup>[2]</sup>. Ensuring the durability of concrete structures is fundamental to achieving sustainability<sup>[3]</sup>. Demis & Papadakis (2019)<sup>[4]</sup> describe durability as “an ability ‘given’ to a reinforced concrete structure, through correct conceptual design, planning, selection of materials and sound construction, and maintenance of the structure.” Realising concrete durability through correct conceptual and detailed design may be achieved using service life design (SLD).

Service life design methods are used to ensure sufficient resistance of concrete structures to the exposure environmental actions and are normally included in concrete standards such as the fib Model Code for Service Life Design<sup>[2]</sup>, the ACI Guide to Durable Concrete<sup>[5]</sup> and the ISO standard 16204: Durability –

Service Life Design of Concrete Structures<sup>[6]</sup>. Service life design is typically based on service life prediction models (SLM) which may be mathematical, numerical, or empirical simulations of the deterioration behaviour of the reinforced concrete structure or structural element<sup>[1]</sup>. The prediction of deterioration phenomena using a SLM requires rigorous interrogation of the processes involved. Therefore, understanding of the influencing factors and governing mechanisms of the deterioration process is crucial to the development and implementation of quantitative SLMs with high reliability<sup>[7]</sup>. SLMs may also be used to predict the remaining service life of existing structures in order to plan for maintenance, repair and rehabilitation as required.

While a large number of reinforced concrete structures are sufficiently durable, evidence has shown that various deterioration mechanisms may shorten their service life. The most severe of these mechanisms is corrosion of the reinforcing steel, which accounts for up to 90% of practical cases of premature deterioration of reinforced concrete structures<sup>[8]</sup>.

Steel is naturally prone to corrosion in atmospheric conditions. However, in reinforced concrete, the high alkalinity of the hydrated cement paste (typically with a pH above 12.5) enables the formation of a thermodynamically stable protective oxide layer on the steel surface that prevents the steel from corroding<sup>[9]</sup>. The formation of this protective layer on the steel surface is known as steel passivation<sup>[10]</sup>. The concrete cover provides additional protection by preventing ingress of aggressive agents such as carbon dioxide and chloride ions to the steel surface. The effectiveness of the protection provided by the concrete cover, therefore, depends on various factors such as the pH of the pore solution, the cover depth, the porosity of the concrete and the presence of cracks in the concrete cover. Depassivation of steel occurs when the passive oxide layer on the steel surface is broken down, leaving the steel vulnerable to corrosion<sup>[9]</sup>. Depassivation may occur as a result of carbonation of the concrete cover or due to the ingress of chloride ions to the level of the reinforcing steel, or a combination of both.



Carbonation of concrete occurs when carbon dioxide from the atmosphere diffuses into the concrete cover and reacts with the hydrated cement paste in the presence of moisture<sup>[9]</sup>. During the carbonation reaction, hydroxyl ions ( $OH^-$ ) are consumed, resulting in a reduction of the pH of the pore solution from a value greater than 12.5 to a value of about 9 for fully carbonated concrete. The carbonation reaction progresses as a front from the concrete surface exposed to the atmosphere towards the steel surface<sup>[10]</sup>. When the carbonation front reaches the steel surface, the reduction of pH results in destabilisation of the passive oxide layer on the steel surface and corrosion is initiated.

Chloride-induced corrosion is caused by chloride ions, typically from the marine environment or de-icing salts, penetrating into the concrete cover.. Chloride ingress is a complex process; however, it is often idealised as a pure diffusion process so that it may be described using *Fick's second law of diffusion*<sup>[10]</sup>. Chloride ions in concrete may be either 'fixed' or 'free' chlorides. Fixed chlorides are either physically or chemically bound to the hydrated cement paste, while free chlorides are present in the concrete pore water. Free chloride ions decrease the resistivity of the concrete cover and break down the passive layer on the reinforcing steel<sup>[9]</sup>. Chloride-induced corrosion is the more severe form of reinforcement corrosion and is therefore often the critical concern for service life design.

The corrosion reactions may be divided into four processes namely<sup>[10]</sup>

- the anodic process resulting in an anodic current,  $I_a$
- the cathodic process resulting in a cathodic current,  $I_c$
- the flow of electrons from the anode to the cathode through the steel resulting in a metallic current,  $I_m$ , and finally
- the flow of ionic current from the anode to the cathode through the concrete,  $I_{con}$

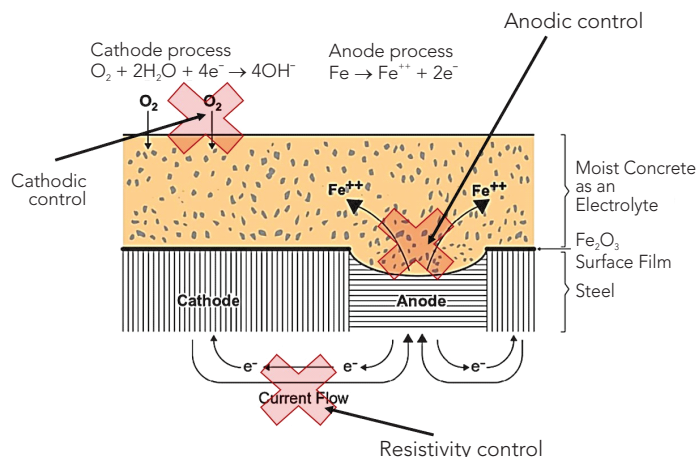


Figure 1: Reinforcement corrosion control methods, adapted from Mehta & Monteiro (2006)<sup>[12]</sup>

The rate of corrosion,  $I_{corr}$  describes the volume of metal lost per unit of area and unit of time, and may also be referred to as the corrosion current density, with units  $\mu A/cm^2$ <sup>[11]</sup>. The four corrosion processes occur simultaneously, such that<sup>[10]</sup>

$$I_a = I_c = I_m = I_{con} = I_{corr} \quad (1)$$

The result is that the overall corrosion rate,  $I_{corr}$  is regulated by the slowest process. Steel naturally has low resistivity that may be considered negligible in comparison to the resistivity of the concrete, and therefore the flow of electrons from the anode to the cathode through the steel ( $I_m$ ) is never the slowest process. However, any of the other three processes may limit the corrosion rate depending on the prevailing conditions shown in Figure 1, resulting in different methods of corrosion control<sup>[10]</sup>.

Before the carbonation front or chloride ions reach the steel surface and while the reinforcing steel remains passive, the rate of the anodic process is negligible. When the anodic process is the rate-controlling process, corrosion is said to be under anodic (passive) control<sup>[10]</sup>.

The rate of the cathodic process is negligible when the rate of diffusion of oxygen into concrete is low, as in the case of water saturated concrete. When the cathodic process is the slowest, the corrosion rate is said to be under cathodic (oxygen diffusion) control<sup>[10]</sup>.

The flow of ions from the anode to the cathode, through the concrete, is greatly influenced by the electrical resistivity and moisture content of the concrete. In cases where the resistivity of concrete is high, typically in concrete of low relative humidity, the flow of ions may become negligible. In this case, the corrosion rate is under resistivity (ohmic) control<sup>[10]</sup>.

Techniques used for corrosion control may also be utilized to avoid deterioration. These two concepts are closely associated and full understanding of both is essential for designing and maintaining durable reinforced concrete structures.

## 2. PRINCIPLES OF SERVICE LIFE DESIGN

The fib Bulletin No 34. Model Code for Service Life Design<sup>[2]</sup> gives the four approaches to service life design as: the full probabilistic approach; the semi-probabilistic approach (partial factor design); the deemed-to-satisfy (DtS) rules; and avoidance of deterioration.

Using the full probabilistic approach for service life design, the required service life is calculated based on statistical data for the material's resistance to deterioration and environmental load with a specified level of reliability<sup>[13]</sup>. The full probabilistic SLD method requires a large number of input variables and the quantification of the associated uncertainties<sup>[2]</sup>. This in addition to the complexities involved in the validation of full probabilistic

SLMs, may make this approach unwieldy for the design of new structures. It may however be considered more applicable to the prediction of the remaining service life of existing structures where data might be derived from the actual structure<sup>[14]</sup>.

Due to the complexity of the full probabilistic approach, a semi-probabilistic approach known as the partial factor approach may be employed instead, for less critical concrete structures or structural elements. Using the partial factor approach, the statistical distribution of the material's resistance to deterioration and the environmental load are characterized by partial factors or characteristic values<sup>[4, 13]</sup>.

The deemed-to-satisfy method employs a set of requirements (normally w/c, cover to the reinforcement, crack width, air entrainment, etc.) that have been determined through research and experience and are defined by a standard design code to satisfy the service life requirements if adhered to<sup>[13]</sup>. The durability achieved using this method has historically been inconsistent, with some structures attaining sufficient durability and others showing premature deterioration<sup>[14]</sup>.

The avoidance of deterioration method aims to ensure that deterioration is not initiated during the service life of the structure. This can be achieved in a number of ways including; insulation (or isolation) of the structure or element from environmental action, using non-reactive materials, isolation of reactants and inhibiting the deleterious reactions<sup>[2]</sup>.

The avoidance of deterioration approach can provide excellent durability with high reliability<sup>[14]</sup>. Nevertheless, this design methodology is not widely used for non-critical structures due to its misconceived high initial cost and a lack of understanding or awareness of the techniques available for using this approach. In the case of reinforcement corrosion, avoidance of deterioration may be achieved if depassivation of the steel i.e. corrosion initiation, can be prevented or suppressed.

An important point to highlight here is that the fib Bulletin No 34, Model Code for Service Life Design<sup>[2]</sup>, recommends that the calibration of the partial factor and DtS methods be performed either by using the full probabilistic method or based on long-term field data. Thus, it may be deduced that the precision of the partial factor and DtS SLD methods is dependent on the full probabilistic model used for the calibration. This limitation does not apply to the avoidance of deterioration approach, making it a more a pragmatic option than the other SLD methods.

The fib Model Code 2010<sup>[15]</sup> presumes that the DtS and avoidance of deterioration approaches will imminently be the preferred options for SLD of new structures, and therefore the following section highlights the latter as a key concept for achieving the durability of reinforced concrete structures, including those susceptible to chloride-induced reinforcement corrosion.

### 3. AVOIDANCE OF DETERIORATION

The following sections provide more details on the methods used to achieve concrete durability by preventing the initiation of degradation.

#### 3.1 Insulation of the structure or element from environmental action

This principle is based on providing a physical barrier between the aggressive exposure environment and the affected structure. This barrier can be in the form of cladding or surface coatings for concrete.

Various materials with different textures and colours such as stone, bricks and engineered materials may be used as cladding for concrete. The choice of material typically depends on the prevailing industry trends; however it is important to keep in mind that the cladding material has to be supported and restrained on the structure when making this choice.

Coatings for concrete are compounds that form a continuous, impervious layer on the surface of concrete and block the ingress (and egress) of water, carbon dioxide and chloride ions<sup>[10]</sup>. These compounds are typically composed of bituminous materials or organic polymers such as acrylates, polyurethanes, epoxy resins, dissolved in solvents and may contain pigments and fine aggregate (usually of grain size  $\leq 1$  mm).

#### 3.2 Using non-reacting materials

For reinforcement corrosion, the principle of using non-reacting materials relies on the use of reinforcing steels impervious to corrosion such as stainless steel.

#### 3.3 Inhibiting the deleterious reactions

During steel corrosion, deleterious chemical reactions take place on anodic and cathodic sites on the steel surface. Iron is oxidised at the anodic sites and oxygen is reduced at the cathodic sites to form hydroxyl ions<sup>[16]</sup>. Inhibiting the deleterious reactions may therefore be achieved by controlling cathodic (cathodic protection) or anodic areas on the steel.

##### 3.3.1 Cathodic protection

Since the dissolution of iron occurs at anodic sites, cathodic protection aims to prevent reinforcement corrosion by making the whole steel bar a cathode<sup>[17]</sup>. This is typically done by electrically connecting another metal to the reinforcing steel and making this the anode, with or without the application of a small current. Cathodic protection systems without application of a current are known as sacrificial or passive anode systems, while those employing a current are known as impressed current cathodic protection (ICCP) systems<sup>[17]</sup>.



Sacrificial anode systems are achieved using metals that are more electronegative than reinforcing steel, e.g. zinc, magnesium, and aluminium. When these metals are electrically connected to the steel, a galvanic cell is formed in which the metal with the more negative potential becomes the anode and begins to corrode. The steel becomes the cathode in the cell, and therefore is protected from corrosion<sup>[18]</sup>. Zinc and its alloys are the most commonly used sacrificial anodes. Because sacrificial anodes are consumed during this type of cathodic protection, their service life is limited. Sacrificial anodes do not require the application of an external current, and therefore have lower installation and maintenance costs than ICCP<sup>[10, 18]</sup>.

Impressed current systems use an external power supply to drive a small current through the reinforcing steel and reverse the flow of the corrosion current<sup>[17]</sup>. The system typically requires current densities lower than 20 mA/m<sup>2</sup> of total surface area of steel, and this requirement decreases as the corrosion rate decreases over time<sup>[10]</sup>. Unlike sacrificial anodes, ICCP anodes are made of metals with a less negative potential than steel, and that are not prone to corrosion (i.e. titanium and platinum). If such metals are electrically connected to the reinforcing steel without an external current being supplied, the reinforcing steel will severely corrode<sup>[18]</sup>. The anodes used in ICCP systems are not consumed during corrosion, and therefore these systems have a longer service life than sacrificial anodes. However, these systems require constant monitoring to ensure their effective functioning.

### 3.3.2 Control of anodic areas on the steel

Halting the anodic reaction may also be used to prevent corrosion<sup>[10]</sup>. The most common methods of implementing this principle are coating the reinforcing steel and using corrosion inhibitors<sup>[18]</sup>.

Coatings may be applied to the reinforcing steel at the initial construction phase or while conducting patch repairs. These coatings may contain corrosion inhibitors, may function as sacrificial anodes (active coatings), or may provide a physical barrier between the steel and aggressive environment (barrier coatings). To ensure maximum efficiency of the method, it is vital to ensure that the reinforcing steel is thoroughly cleaned and corrosion free, before being completely covered with the coating<sup>[10]</sup>. Coatings may affect the bond properties between steel and concrete<sup>[18]</sup>.

Corrosion inhibitors are products that either form a passive film on the reinforcing steel or modify the electrochemical behaviour of its surface<sup>[10]</sup>. The inhibitor may be applied on the concrete surface, from where it migrates towards the steel surface, or it may be mixed into the repair mortar<sup>[18]</sup>. For maximum efficiency of corrosion inhibitors, there needs to be sufficient product at

the steel surface. The efficacy of migrating (surface-applied) corrosion inhibitors may therefore be limited for concrete elements with low permeability or a high cover depth as this condition may not be met<sup>[10]</sup>.

### 3.4 Isolation of reactants

The initiation of corrosion in reinforced concrete structures requires the penetration of carbon dioxide, chloride ions, moisture, and oxygen to the steel surface. Chloride-induced corrosion of the reinforcing steel requires sufficient chloride ion concentration at the steel surface, moisture, and dissolved oxygen. If there is insufficient quantity of any of these reactants at the steel surface, the corrosion reaction is restricted. Hence isolating the steel surface from any of the reactants, including moisture or oxygen may be employed to avoid corrosion-induced degradation.

Isolation of the reactants is typically achieved using surface protection systems, namely coatings (as described previously), sealants and hydrophobic impregnations, and operates on similar principles to insulation of the structure or element from environmental action.

Sealants are also known as impregnations or pore blockers. These products reduce the porosity of the concrete cover by partially or fully blocking the concrete pores. Sealants may change the appearance of the concrete surface on which they are applied and may be chemically composed of organic polymers (i.e. epoxy, polyurethane and acrylics), or inorganic compounds such as silicates and silico-fluorides<sup>[10, 18]</sup>.

Hydrophobic impregnations are silanes or siloxanes dissolved in a solvent such as water or alcohol<sup>[19, 20]</sup>. They penetrate the concrete pores where their hydrophobic action prevents moisture ingress, while allowing water vapour and gases to either penetrate or escape from the concrete surface<sup>[21]</sup>. Hydrophobic impregnations contain no pigments and therefore clear-dry. The main advantage of hydrophobic impregnations is that they provide a water-repellent surface without affecting the appearance of the concrete and do not hinder the movement of water vapour in and out of the concrete<sup>[10]</sup>.

The methods that may be used to achieve concrete durability as described above all have various advantages and disadvantages. Upon careful consideration, hydrophobic impregnation may be considered to be a very advantageous solution as it does not change the appearance of the concrete structure, does not require expert knowledge for application, is easy to apply, is a low-cost option, does not require support or restraint, and has documented efficacy<sup>[20, 22, 23]</sup>. A summary of relevant research studies conducted on the influence of hydrophobic impregnations on reinforced concrete is presented in Table 1.

Table 1: Summary of research studies conducted on the application of hydrophobic impregnations on reinforced concrete structures

ARTICLE TITLE (AUTHOR, DATE)	PARAMETER(S) INVESTIGATED	MAJOR FINDINGS
1 Determining the effective service life of silane treatments in concrete bridge decks (Moradillo <i>et al.</i> , 2016) <sup>[24]</sup>	<ul style="list-style-type: none"> <li>Silane impregnation service life</li> </ul>	<ol style="list-style-type: none"> <li>Durability of silane impregnations varied from 6 to 20 years</li> <li>Silane surface impregnations were not susceptible to abrasion</li> <li>Deterioration of the silane began in the bulk paste and migrated to the exposure surface</li> </ol>
2 Influence of exposure environments and moisture content on water repellency of surface impregnation of cement-based materials (Bao <i>et al.</i> , 2020) <sup>[25]</sup>	<ul style="list-style-type: none"> <li>Silane penetration depth</li> <li>Water absorption</li> </ul>	<ol style="list-style-type: none"> <li>Maximum silane penetration depth and hydrophobicity was attained when the initial relative humidity of treated specimens was 50%.</li> <li>Silane penetration depth increased with increasing water/binder ratios of mortar specimens</li> </ol>
3 Influence of silane-based water repellent on the durability properties of recycled aggregate concrete (Zhu <i>et al.</i> , 2013) <sup>[26]</sup>	<ul style="list-style-type: none"> <li>Capillary water absorption</li> <li>Carbonation depth</li> <li>Chloride ion penetration</li> </ul>	<ol style="list-style-type: none"> <li>Surface silane treatment reduced water absorption by up to 81% for natural aggregate concrete and up to 96% for recycled aggregate concrete compared to the control samples.</li> <li>The carbonation depths of surface silane treated recycled aggregate concrete samples was only half of the carbonation depths of untreated recycled aggregate concrete samples.</li> <li>The resistance to chloride ion penetration was up to 68% higher for silane treated recycled aggregate concrete than that for untreated recycled aggregate concrete</li> </ol>
4 Long-term performance of surface impregnation of reinforced concrete structures with silane (Christodoulou <i>et al.</i> , 2013) <sup>[23]</sup>	<ul style="list-style-type: none"> <li>Capillary absorption</li> </ul>	<ol style="list-style-type: none"> <li>Silane impregnation on real structures was effective for up to 20 years on real structures</li> </ol>
5 Water repellent surface impregnation for extension of service life of reinforced concrete structures in marine environments: The role of cracks (Dai <i>et al.</i> , 2010) <sup>[27]</sup>	<ul style="list-style-type: none"> <li>Silane penetration depth</li> <li>Water absorption</li> <li>Chloride ion penetration</li> </ul>	<ol style="list-style-type: none"> <li>The long-term performance of silane impregnations depends on the penetration depth</li> <li>Silane impregnation is most effective when applied after the formation of cracks, unless the cracks are less than 0.1 mm</li> <li>Impregnation was less effective when applied before the formation of cracks</li> </ol>
6 Efficacy of surface hydrophobic agents in reducing water and chloride ion penetration in concrete (Medeiros & Helene, 2006) <sup>[28]</sup>	<ul style="list-style-type: none"> <li>Immersion absorption</li> <li>Capillary water absorption</li> <li>Chloride diffusion</li> </ul>	<ol style="list-style-type: none"> <li>Hydrophobic impregnation is effective when capillary suction is the dominant water transport mechanism.</li> <li>Surface hydrophobic agents do not have sufficient capacity for stopping water penetration under pressure.</li> <li>Silanes allow evaporation of water from the concrete surface</li> <li>Hydrophobic impregnation reduced the chloride diffusion coefficient by up to 17%</li> </ol>
7 The effect of hydrophobic (silane) treatment on concrete durability characteristics (Sohawon & Beushausen, 2018) <sup>[29]</sup>	<ul style="list-style-type: none"> <li>Oxygen Permeability Index (OPI)</li> <li>Water Sorptivity Index (WSI)</li> <li>Chloride Conductivity Index (CCI)</li> <li>Silane penetration depth</li> <li>Bulk diffusion</li> </ul>	<ol style="list-style-type: none"> <li>A linear relation was observed between OPI values and silane penetration depths</li> <li>The silane penetration depth was higher in specimens with higher porosity</li> <li>Silane treated concrete specimens showed reduced sorptivity and chloride conductivity</li> <li>Surface chloride concentrations and chloride penetration depths were lower in treated specimens than in untreated specimens</li> </ol>

(Contd...)



ARTICLE TITLE (AUTHOR, DATE)	PARAMETER(S) INVESTIGATED	MAJOR FINDINGS
8 Use of surface treatment materials to improve concrete durability (Ibrahim <i>et al.</i> , 1999) <sup>[22]</sup>	<ul style="list-style-type: none"> <li>Chloride profiles</li> <li>Carbonation depth</li> <li>Half-cell potential</li> <li>Corrosion current density</li> </ul>	<ol style="list-style-type: none"> <li>Silane treatment reduced the chloride diffusion coefficient of concrete to only half of the untreated specimens.</li> <li>Test specimens treated with silanes showed slightly lower carbonation depths than untreated specimens</li> <li>Of all the surface treatments tested, silane impregnations showed the highest decrease in corrosion potential and corrosion current densities</li> </ol>
9 Protection provided by surface treatments against chloride induced corrosion (Basheer <i>et al.</i> , 1997) <sup>[21]</sup>	<ul style="list-style-type: none"> <li>Chloride content</li> <li>Silane penetration depth</li> <li>Half-cell potential</li> <li>Macrocell current</li> </ul>	<ol style="list-style-type: none"> <li>Silane treatment significantly reduced chloride ion penetration into the treated concrete</li> <li>The corrosion initiation period for silane treated specimens was 2-3 times longer than for untreated specimens</li> <li>Silane treated specimens showed reduced corrosion activity compared to untreated specimens</li> </ol>
10 The Effect of Water Repellent Surface Impregnation on Durability of Cement-Based Materials (Peng <i>et al.</i> , 2017) <sup>[30]</sup>	<ul style="list-style-type: none"> <li>Capillary suction</li> <li>Chloride ion penetration</li> <li>Carbonation depth</li> <li>Half-cell potential</li> <li>Corrosion current density</li> </ul>	<ol style="list-style-type: none"> <li>Hydrophobic impregnation significantly reduced the capillary suction of treated specimens</li> <li>Silane impregnation provided an effective barrier to chloride ion penetration into treated specimens</li> <li>At high application rates and exposure relative humidity of 70%, high application rates of silane impregnation reduced the carbonation rate by up to 50% of the control specimens.</li> <li>The corrosion risk for silane treated specimens was found to be 10%, while that of untreated specimens was 95% for the same exposure conditions.</li> </ol>

## 4. HYDROPHOBIC IMPREGNATION FOR AVOIDANCE OF DETERIORATION

From Table 1, it is evident that the most investigated parameters are water absorption by capillary suction, chloride ion penetration and silane penetration depth, as these are reasonably considered to be the most relevant parameters for preventing corrosion initiation and therefore avoiding deterioration using hydrophobic impregnation. The major findings of the studies presented in this regard may be summed up by concluding that hydrophobic impregnations are highly effective at reducing water absorption and consequently the penetration of dissolved chloride ions into uncracked concrete.

However, some studies note that the efficacy of the impregnations depends on the penetration depth and the application rate of the product <sup>[27, 21, 25]</sup>. The penetration depth of the silane is affected by the initial moisture content of the treated concrete <sup>[25]</sup>, and the porosity of the treated concrete <sup>[29]</sup>. Medeiros & Helene (2006) <sup>[28]</sup> note that silane impregnations are much less effective when subjected to significant hydrophobic pressure and consequently are more suited for application to verticle surfaces or where ponding of water does not occur.

In a study conducted by Sohawon (2018) <sup>[20]</sup>, hydrophobic impregnation of cracked concrete specimens resulted in lower chloride contents than for untreated cracked concrete

specimens as shown in Figure 2. Regarding the results presented, it was observed that the chloride concentration initially reduced with increasing depth from the exposure surface before gradually increasing with increasing depth. From this observation, it may be deduced that the hydrophobic impregnation is only effective up to a certain depth within the cracked concrete, since this phenomenon was not observed in the uncracked concrete. Furthermore, research by Dai *et al.* (2010) <sup>[27]</sup> and Sohawon (2018) <sup>[20]</sup> suggested that silane impregnations are most effective when applied after

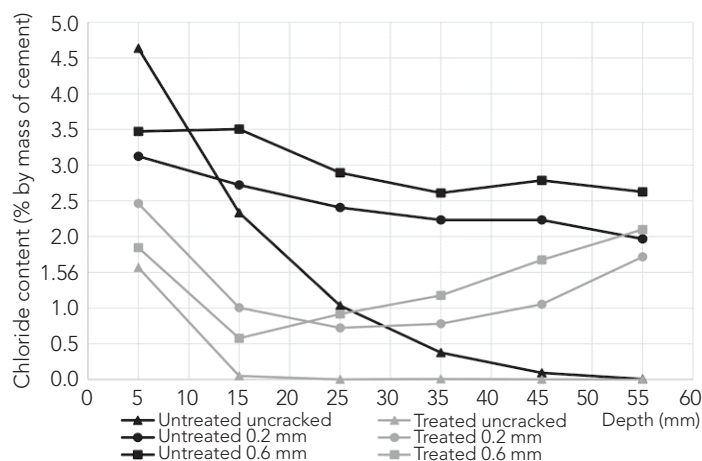


Figure 2: Effect of silane impregnation on the chloride content of cracked and uncracked concrete specimens <sup>[20]</sup>. Specimens were immersed in a 16% sodium chloride solution for 80 days

the formation of cracks. This has significant implications for real concrete structures which are susceptible to various forms of cracking. Cracking in concrete is known to increase both corrosion initiation and corrosion propagation<sup>[31]</sup>. It is therefore recommended that the movement of existing cracks be evaluated before application of a hydrophobic impregnation.

In the study by Zhu *et al.* (2013)<sup>[26]</sup>, surface silane impregnation was found to substantially reduce capillary water absorption, chloride ion penetration and carbonation depths of recycled aggregate concrete specimens. The reduction recorded was greater in recycled aggregate concrete than in natural aggregate concrete when compared with their respective controls. These results were corroborated by the observations of Sohawon (2018)<sup>[20]</sup> and Bao *et al.* (2020)<sup>[25]</sup>, that silane penetration depth was higher in concrete with higher water/binder ratios. Practically, this means that silane impregnation may successfully be employed to retrospectively reinstate the durability of poor quality concrete with insufficient material resistance to chloride-rich exposure conditions, and therefore extend their service life.

A few studies extended their investigations to include the measurement of corrosion activity in the form of half-cell potential, macrocell current or corrosion current density measurements. In these studies, hydrophobic impregnations were found to significantly reduce both the measured corrosion potential and corrosion current densities, indicating that silane impregnation may be successfully employed to halt corrosion even after corrosion initiation. This extends their applicability beyond avoidance of deterioration to corrosion control. However, the exact mechanisms by which silane impregnation may control corrosion (as previously described) have not been sufficiently investigated.

## 5. OPPORTUNITIES FOR FURTHER RESEARCH

While various studies have investigated the effect of hydrophobic impregnations on capillary absorption of water, their influence on other transport mechanisms such as migration and permeation have not been sufficiently addressed in existing literature. In reality, reinforced concrete structures are subjected to a combination of these transport mechanisms and the informed use of these products on real structures requires a more comprehensive evaluation of their effects.

There exists a lack of understanding of the mechanisms by which silanes control reinforcement corrosion. This may be because surface treatments are more commonly recommended for use before corrosion initiation. In the corrosion propagation phase, sufficient chloride ion concentration and moisture content have been attained at the steel surface to achieve an active corrosion rate. Application of silanes would prevent further ingress of both moisture and chloride ions while allowing water vapour

to escape, and therefore provide moisture control. Lowering the moisture content of concrete increases its resistivity and therefore induces resistivity control of the corrosion rate.

Determining the effectiveness of silane impregnation for corrosion control of structures in an intermediate state of corrosion therefore requires measuring the corrosion rate and resistivity of the concrete after silane application. These may then be used to quantify the service life extension using an appropriate service life model.

The development of appropriate service life prediction models for silane-treated structures especially using the full probabilistic approach, necessitates that further studies be conducted to generate the statistical data and relevant input variables required for the calibration and validation of models.

## 6. CONCLUDING REMARKS

The durability of reinforced concrete structures depends on the resistance of the material to degradation being greater than the load from environmental action. Achieving durable concrete begins with service life design.

Current service life design approaches include the full probabilistic, semi-probabilistic, deemed-to-satisfy and avoidance of deterioration methods. While full probabilistic service life models are more comprehensive, their complexity and validation challenges make them impractical for application to a large number of concrete structures. Considering that the semi-probabilistic and deemed-to-satisfy techniques often need to be calibrated against full probabilistic models, the most practical approach to service life design may therefore, in many cases, be avoidance of deterioration.

Chloride-induced reinforcement corrosion is the leading cause of premature deterioration of reinforced concrete structures. This makes chloride-induced corrosion the critical concern during service life design. The avoidance of deterioration approach to service life design for reinforced concrete structures aims to prevent the initiation of steel corrosion. This can be achieved in a number of ways including; insulation of the structure or element from environmental action, using non-reactive materials, isolation of reactants and inhibiting the deleterious reactions<sup>[2]</sup>.

This paper has discussed the various techniques used to avoid the initiation of chloride-induced corrosion, focussing on silane impregnation. Silane impregnation prevents the ingress of moisture and chloride ions into the concrete cover while allowing the egress of gases and vapour. Numerous studies have been conducted investigating the influence of silane impregnation on corrosion, with results indicating that silanes are highly effective at preventing corrosion initiation for up to 20 years. Based on this evidence, it may be concluded that

silane impregnation is a very viable option for avoiding the deterioration of reinforced concrete structures susceptible to chloride-induced corrosion. In addition, silane impregnation may be used for corrosion control after corrosion initiation; however, the specific mechanisms of control need further investigation.

## REFERENCES

- [1] M. Alexander and H. Beushausen, (2019). "Durability, service life prediction, and modelling for reinforced concrete structures – review and critique," *Cement and Concrete Research*, Vol. 122, pp. 17-29.
- [2] fib – fédération internationale du béton, fib Bulletin No 34. Model Code for Service Life Design, Lausanne: International Federation for Structural Concrete, 2006.
- [3] R. D. Hooton and J. A. Bickley, (2014). "Design for durability: The key to improving concrete sustainability," *Construction and Building Materials*, Vol. 67, pp. 422-430.
- [4] S. Demis and V. Papadakis, (2019). "Durability design process of reinforced concrete structures - Service life estimation, problems and perspectives," *Journal of Building Engineering*, Vol. 26.
- [5] ACI 201.2R-08, Guide to Durable Concrete, Farmington, Michigan: American Concrete Institute, 2008.
- [6] ISO 16204:, Durability – Service Life Design of Concrete Structures, Geneva, (2012).
- [7] U. M. Angst, (2019). "Predicting the time to corrosion initiation in reinforced concrete structures exposed to chlorides," *Cement and Concrete Research*, Vol. 115, pp. 559-567.
- [8] U. Angst, (2018). "Challenges and opportunities in corrosion of steel in concrete," *Materials and Structures*, Vol. 51, No. 4.
- [9] Y. Ballim, M. Alexander and H. Beushausen, "Durability of concrete," in *Fulton's concrete technology*, 9 ed., G. Owens, Ed., Cement and Concrete Institute, 2009, pp. 155-188.
- [10] L. Bertolini, B. Elsner, P. Pedferri, E. Redaelli and R. Polder, Corrosion of steel in concrete: Prevention, Diagnosis, Repair., Wiley-VCH Verlag GmbH & Co. KGaA, 2013.
- [11] RILEM TC 154-EMC, (2004). "Test methods for on-site corrosion rate measurement of steel reinforcement in concrete by means of the polarization resistance method," *Materials and Structures*, Vol. 33, pp. 603-611.
- [12] P. K. Mehta and P. J. M. Monteiro, Concrete: microstructure, properties, and materials, 3rd ed., McGraw-Hill, 2006.
- [13] S. Helland, (2013). "Design for service life: Implementation of fib Model Code 2010 rules in the operational code ISO 16204," *Structural Concrete*, Vol. 14, No. 1, pp. 10-18.
- [14] F. Papworth, (2015). "A Whole of Life Approach to Concrete Durability – The CIA Concrete," in *International Conference on Concrete Repair, Rehabilitation and Retrofitting (ICCRRR)*, Leipzig.
- [15] fib - fédération Internationale du Béton, Model Code for Concrete Structures 2010, Berlin: Wilhelm Ernst & Sohn, Verlag für Architektur und technische Wissenschaften GmbH & Co. KG, 2013.
- [16] M. F. Montemor, A. M. P. Simoes and M. G. S. Ferreira, (2003). "Chloride-induced corrosion on reinforcing steel: from the fundamentals to the monitoring techniques," *Cement & Concrete Composites*, Vol. 25, pp. 491-502.
- [17] ACI 546R-04, Guide for Evaluation of Concrete Structures before Rehabilitation., Farmington, Michigan: American Concrete Institute, 2004.
- [18] M. Raupach and T. Buettner, Concrete Repair to EN 1504: Diagnosis, Design, Principles and Practice., CRC Press, 2014.
- [19] A. Bentur, N. Berke and S. Diamond, "Corrosion control," in *Steel Corrosion in Concrete: Fundamentals and Civil Engineering practice*, E & FN Spom, 1997, pp. 94-145.
- [20] H. Sohawon, *Service life extension of reinforced concrete structures using hydrophobic*, University of Cape Town, 2018.
- [21] L. Basheer, C. D. J. and A. E. Long, (1997). "Protection provided by surface treatments against chloride induced corrosion," *Materials and Structures*, Vol. 31, pp. 459-464,
- [22] M. Ibrahim, A. S. Al-Gahtani, M. Maslehuddin and F. H. Dakhil, (1999). "Use of surface treatment materials to improve concrete durability," *Materials in Civil Engineering*, Vol. 11, No. 1, pp. 36-40.
- [23] C. Christodoulou, C. Goodier, S. Austin, J. Webb and G. Glass, (2013). "Long-term performance of surface impregnation of reinforced concrete structures with silane," *Construction and Building Materials*, Vol. 48, pp. 708 -716.
- [24] M. K. Moradillo, B. Sudbrink and M. T. Ley, (2016). "Determining the effective service life of silane treatments in concrete bridge decks," *Construction and Building Materials*, Vol. 116, pp. 121-127.
- [25] J. Bao, S. Li, P. Zhang, S. Xue, Y. Cui and T. Zhao, (2020). "Influence of exposure environments and moisture content on water repellency of surface impregnation of cement-based materials," *Journal of Materials Research and Technology*, Vol. 9, No. 6, pp. 12115-12125.



- [26] Y. Zhu, S. Kou, C. Poon, J. Dai and L. Q., (2013). "Influence of silane-based water repellent on the durability properties of recycled aggregate concrete," *Cement and Concrete Composites*, Vol. 35, No. 1, pp. 32-38.
- [27] J. Dai, Y. Akira, F. Wittmann, H. Yokota and P. Zhang, (2010). "Water repellent surface impregnation for extension of service life of reinforced concrete structures in marine environments: The role of cracks," *Cement and Concrete Composites*, Vol. 32, No. 2, pp. 101-109.
- [28] M. Medeiros and P. Helene, (2006). "Efficacy of surface hydrophobic agents in reducing water and chloride ion penetration in concrete," *Materials and Structures*, Vol. 41, pp. 59-71.
- [29] H. Sohawon and H. Beushausen, "The effect of hydrophobic (silane) treatment on concrete durability characteristics," in *International Conference on Concrete Repair, Rehabilitation and Retrofitting (ICCRRR)*, Cape Town, 2018.
- [30] Z. Peng, S. Huaishuai, H. Dongshuai, G. Siyao and Z. Tiejun, "The Effect of Water Repellent Surface Impregnation on Durability of Cement-Based Materials," *Advances in Materials Science and Engineering*, 2017.
- [31] M. Otieno, H. Beushausen and M. Alexander, (2016). "Chloride-induced corrosion of steel in cracked concrete – Part I: Experimental studies under accelerated and natural marine environments," *Cement and Concrete Research*, Vol. 79, pp. 373-385.



**JOANITTA NDAWULA** is a Ph.D. candidate at the University of Cape Town in South Africa. Her research focusses on mitigating chloride-induced reinforcement corrosion propagation. Her research interests include condition assessment, non-destructive testing and service life extension of existing concrete structures. She is currently the chairperson of the RILEM Youth Council. Email: NDWJOA001@myuct.ac.za



**HANS BEUSHAUSEN** is Professor for Structural and Materials Engineering at the University of Cape Town, UCT. After completing his first degree in Structural Engineering in Hamburg, Germany, he obtained his MSc (2000) and Ph.D. (2005) from UCT. His research interests concern advanced concrete technology, assessment and repair of concrete structures, durability design and service life modelling, recycled aggregate concrete, and concrete with low clinker contents for improved sustainability. He is the Head of the fib National Member Group South Africa and Chairman of the Development Activity Committee of RILEM. Email: hans.beushausen@uct.ac.za



**MARK ALEXANDER** is a Senior Research Scholar in the University of Cape Town. He co-authored "Aggregates in Concrete" (2005), "Alkali-Aggregate Reaction and Structural Damage to Concrete" (2011), and "Durability of concrete – design and construction" (2017) (CRC Press) and was Editor of "Marine concrete structures. Design, durability and performance" (Woodhead Publishers (2016)). He is involved in (CoMSIRU) at UCT, which focuses on infrastructure performance and renewal research. Email: mark.alexander@uct.ac.za

Cite this article: Ndawula, J., Beushausen, H. and Alexander, M. (2021). "Hydrophobic treatment for control of deterioration in reinforced concrete structures", *The Indian Concrete Journal*, Vol. 95, No. 4, pp. 8-16.

# OPTIMAL DOSAGE OF $\text{Fe}_2\text{O}_3$ NANOPARTICLES TO ENHANCE CHLORIDE RESISTANCE AND MICROSTRUCTURAL PROPERTIES OF CONCRETE- A COMPREHENSIVE STUDY

RAGHAVA KUMAR VANAMA,  
HARINEE ADDEPALLI,  
BALAJI RAMAKRISHNAN\*

## Abstract

Majority of reinforced concrete port structures in India are experiencing premature failures due to chloride-induced corrosion. The use of concrete that possesses higher chloride penetration resistance and better compact microstructure can potentially increase the corrosion initiation period and thereby, the service life of the structure. The present study investigates the influence of  $\text{Fe}_2\text{O}_3$  nanoparticles in improving the durability and microstructural characteristics of concrete. Hematite nanoparticles were synthesised and comprehensively characterised. The characteristics of nano hematite blended concrete have been widely studied by rapid chloride migration, electrical resistivity against chloride migration, mercury intrusion porosimetry and XRD tests. FEG-SEM micrographs of hardened nano blended concrete indicated the strengthening of the Interfacial Transition Zone. Based on the comprehensive study, cement replaced by 0.5 weight percentage of hematite nanoparticles found to be an optimum dosage for a durable concrete in the marine environment.

**Keywords:** Chloride-induced corrosion, Concrete, Microstructure, Nanoparticles, Permeability.

## 1. INTRODUCTION

Corrosion degrades the properties of steel rebar<sup>[1]</sup> and its bond with concrete, thereby disturbing the composite action and service life of the structure. Chloride induced corrosion is the main reason behind the premature failures of reinforced concrete structure in the coastal and marine environment<sup>[2]</sup>. Resistance to chloride penetration and compact pore structure increases the durability of concrete and delays the corrosion initiation period, thereby increases the service life of the structure<sup>[3,4]</sup>. Nanotechnology is emerging in recent years,

shedding light on enhancing the overall performance of cement and concrete composites<sup>[5-8]</sup>. Several researchers in the past have studied the effect of incorporating the nanomaterials in improving the properties of cementitious composites by partially replacing the cement with various nanoparticles. Among the different types of nanoparticles,  $\text{Fe}_2\text{O}_3$  is available abundantly, which can be synthesised in different morphologies without using any (toxic) surfactants. Hence, it has a wide range of adaptability/performance and is safe to use on the site as it is non-toxic in nature. Limited studies<sup>[9-11]</sup> have explored the effect of  $\text{Fe}_2\text{O}_3$  nanoparticles partially replacing the cement content on the properties of concrete, to the best of authors' knowledge. Some of the previous works focus on improving the mechanical properties<sup>[12-15]</sup> of nano blended cement composites. Nanoparticles strongly influence the mechanical properties of cementitious materials subjected to the well dispersion, as they have a high surface area and chemical reactivity<sup>[16]</sup>. Researchers have reported that  $\text{Fe}_2\text{O}_3$  nanoparticles increase the compressive strength of concrete, 1 wt.% being the optimum dosage<sup>[15]</sup>. However, a comprehensive investigation exploring the chloride resistance, electrical resistivity, formation of hydration products, pore structure, Interfacial Transition Zone (ITZ) and microstructural characteristics of concrete incorporated with  $\text{Fe}_2\text{O}_3$  nanoparticle have not been reported in the literature, which motivated the present study. All the parameters mentioned above influence the durability of concrete in the marine environment; however, they cannot be interrelated to the compressive strength of concrete alone, therefore, requires a comprehensive experimental investigation. Thus, the present study focusses on finding the optimal dosage of  $\text{Fe}_2\text{O}_3$  nanoparticles from a durability perspective to enhance the chloride resistance of the nano hematite blended concrete based on a comprehensive study, which was never attempted in any of the previous studies. The main objective of the study

\*Corresponding author : Balaji Ramakrishnan, Email: rbalaji@iitb.ac.in

is to improve the microstructure and durability performance of conventional concrete in the marine environment using synthesised nano-hematite, based on a comprehensive experimental investigation. To meet this objective, the pore size distribution, ITZ and microstructural characteristics of concrete at different nanoparticles dosages have been investigated. A comparative study by Mercury Intrusion Porosimetry (MIP) and by Field Emission Gun Scanning Electron Microscopic (FEG-SEM) analysis was conducted to understand the pore structure, micropores and cracks present in the concrete matrix with and without nanoparticles.

## 2. EXPERIMENTAL PROGRAM

Synthesis of  $\text{Fe}_2\text{O}_3$  nanoparticles, characterisation of materials used in the study, test methodologies and instrumentation adopted for evaluating the mechanical, durability and microstructural properties of nano blended concrete have been discussed in this section.

### 2.1 Materials

In the present study, Ordinary Portland Cement (OPC-53 grade)<sup>[17]</sup> having a specific gravity of 3.15 and specific surface area (Blaine's method) of  $2913 \text{ cm}^2/\text{g}$  was used. Coarse aggregate (CA) of 10 mm nominal maximum size and fine aggregate (FA) conforms to Zone II of IS 383<sup>[18]</sup> were used for the investigation. The physical properties of coarse and fine aggregates are specified in Table 1. Potable water was used at a temperature of  $27 \pm 2^\circ\text{C}$  in the preparation of concrete. Polycarboxylate Ether (PCE) based superplasticiser (SP) with a solids content of 21.76% was used for improving the workability of the concrete mixture.

### 2.2 Synthesis of hematite nanoparticles

The  $\alpha\text{-Fe}_2\text{O}_3$  nanoparticles were synthesised by the hydrothermal method to obtain better crystallinity, high purity and stabilisation. In a typical procedure, a solution of 0.1 M  $\text{FeCl}_3 \cdot 6 \text{H}_2\text{O}$  was attained by diluting 4.05 g of  $\text{FeCl}_3$  in 150 ml of de-ionised water under magnetic stirring. 50 ml of 2.0 M  $\text{NH}_4\text{OH}$  was used as reducing/precipitating agent. The base solution ( $\text{NH}_4\text{OH}$ ) was then added gradually to obtain a pH of 13.0. The precipitate was then transferred to a Teflon-

lined stainless-steel autoclave and kept in an oven at  $180^\circ\text{C}$  for 12 hours. After 12 hours, the obtained powder was subject to calcination at  $500^\circ\text{C}$  for 2 hours followed by annealing at  $800^\circ\text{C}$  for 20 minutes.

### 2.3 Characterisation of synthesised nanoparticles

Synthesised nanoparticles were comprehensively characterised to ensure their form, nature, purity and morphology. X-ray diffraction (XRD) patterns of synthesised nanoparticles (Figure 1a) were recorded at an accelerating voltage of 45 kV and accelerating current of 40 mA with a step interval of  $0.0263^\circ$  ( $2\theta$ ) using  $\text{Cu K}\alpha$  radiation. Diffraction peaks are observed to be broad, indicating the crystalline nature of the samples. All the intense peaks are indexed with  $\alpha\text{-Fe}_2\text{O}_3$  mineral indicating the high purity of synthesised nanoparticles. The average crystallite size of nanoparticles normal to the reflection planes estimated by the Scherer equation was found to be 66.8 nm. Besides, the functional group and quality of synthesised nanoparticles were confirmed by Fourier-Transform Infrared Spectroscopy (FTIR), as shown in Figure 1b. FT-IR spectrum of nanoparticles was in the range of  $400\text{--}4000 \text{ cm}^{-1}$  wavenumber, identifying the chemical bonds as well as functional groups in the compound. The influential bands below  $700 \text{ cm}^{-1}$  were assigned to the Fe-O stretching mode<sup>[19]</sup>. Therefore, prominent bands at  $628 \text{ cm}^{-1}$ ,  $457 \text{ cm}^{-1}$  and  $417 \text{ cm}^{-1}$  observed in the spectrum attribute to Fe-O vibrational modes. The broad absorption band centred at  $3133 \text{ cm}^{-1}$  and reaching the peak at  $1640 \text{ cm}^{-1}$  attribute to the stretching and bending vibrations of the hydroxyl groups and water molecules, respectively<sup>[20,21]</sup>.

FEG-SEM micrographs were taken at different magnification levels up to  $75000\times$  and presented in Figure 1 (c, d, e and f). Synthesised nanoparticles possess a mixture of distorted spherical and nanorod (NR) shaped morphology. The average size of the  $\text{Fe}_2\text{O}_3$  nanoparticles was 26.8 nm, whereas the nanorods were in the range of 40.2 to 337 nm. This scenario is due to the incomplete growth of NRs due to the conditions maintained during the synthesis process. Furthermore, Energy-dispersive X-ray spectroscopy (EDS) analysis was conducted for a better understanding of the elemental composition of synthesised nanoparticles (Figure 1g). Results indicate the presence of iron (Fe) and Oxygen (O) elements and confirms the absence of any impurities during the synthesis of the desired material. The additional peaks observed in the spectrum are corresponding to the Platinum element, which was coated over the specimens for FEG-SEM analysis.

### 2.4 Mixture proportion

Five different concrete mixture proportions are adopted in the study, replacing cement by 0, 0.5, 1.0, 1.5 and 2.0 weight

Table 1: Physical properties of aggregates

PROPERTIES	FA	CA
Specific Gravity	2.70	2.78
Bulk density ( $\text{kg}/\text{m}^3$ )	1688.3	1610.9
Voids (%)	37.5	42.1
Water absorption (%)	4.10	1.41



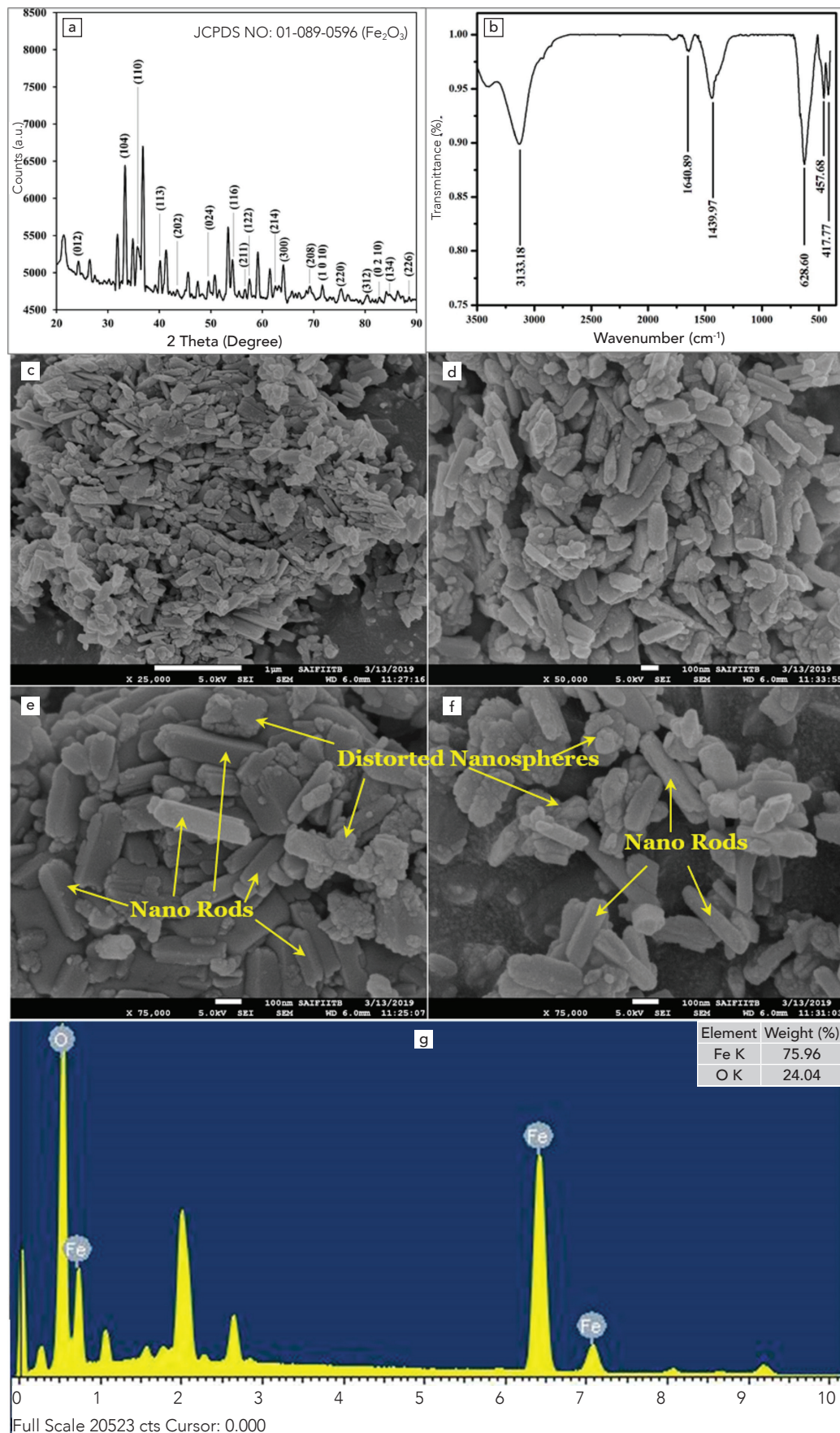


Figure 1: (a) X-Ray Diffraction pattern, (b) FT-IR, (c-f) FEG-SEM micrographs, and (g) Energy-dispersive X-ray spectroscopy of synthesised nanoparticles

percentage of synthesised nanoparticles. Water to powder ratio of 0.3 and a total powder content (Cement + nanoparticles) of 430 kg/m<sup>3</sup> was maintained constant across all the concrete mixtures. For the adopted nominal maximum size of coarse aggregate, as per IS 10262<sup>[22]</sup>, the volume of CA per unit volume of total aggregate was considered as 0.46. For better workability, superplasticiser (SP) was added by 1.2 weight per cent of total powder content. SP dosage was unvaried across the mixtures to understand the effect of nano dosage on the workability of the concrete mixture. Concrete specimens without nanoparticles will henceforth be regarded as a control specimen (0.0NH). Specimen with nanoparticles will be referred to 0.5NH, 1.0NH, 1.5NH and 2.0NH for cement replaced by 0.5, 1.0, 1.5 and 2.0 weight percentage of synthesised nano-hematite, respectively.

## 2.5 Production of specimens

As agglomeration reportedly affecting the workability, mechanical and durability properties<sup>[23]</sup>, in the present study, nanoparticles were pre-dispersed in water by the method of sonication before blending with concrete to avoid accumulations<sup>[24]</sup>. A horizontal pan mixer of 60-litre capacity was used for mixing concrete. Firstly, dry aggregates were mixed for a minute, then the cement, one-half of the total quantity of water (with nanoparticles) were added to dry mixture and mixed for 3 minutes. Finally, the remaining water containing nanoparticles and SP were added and mixed for another 4 minutes. After thorough mixing, the slump test was conducted. Blended concrete was well compacted to cubes of 15 cm × 15 cm × 15 cm size and cylinders of 10 cm diameter and 20 cm height suitable for compression, chloride migration, MIP and XRD tests. Compaction was achieved through the vibration of the specimens using a vibrating table. After 24 hours, concrete specimens were demoulded and cured in a water tank at 23 ± 2 °C for the next 27 days. The water in the curing tank was saturated with 3 g/L of calcium hydroxide to prevent leaching<sup>[25]</sup>. Servo-hydraulically controlled compression testing machine of 3000 kN capacity was used for testing of cubical concrete specimens at a rate of 140 kg/cm<sup>2</sup>/min<sup>[26]</sup>.

## 2.6 Rapid chloride migration test (RCMT)

For the RCMT tests, specimens of 100 mm diameter and 50 mm thick were prepared from cast cylinders using a water-cooled diamond saw, after 28 days of curing. Sample preparation, preconditioning and RCMT tests were conducted in accordance with NT Build 492<sup>[27]</sup>. According to the standard, a constant DC voltage of 25.0 V was maintained for all specimens (0.0NH, 0.5NH, 1.0NH, 1.5NH and 2.0NH) using a voltage regulator. The actual voltage supplied and corresponding current drawn by each specimen were recorded for every five minutes using a data logger<sup>[28]</sup> with a precision of 10 mV and 0.1 mA respectively.

During RCMT tests, the temperature and relative humidity levels were varying in the range of 30.75 to 33.14 °C and 54.20 to 73.31%, respectively, as recorded by the data logger<sup>[28]</sup>.

## 2.7 Mercury Intrusion Porosimetry (MIP) test

Due to its wide range of measuring the pore sizes, Mercury Intrusion porosimetry (MIP) method was extensively used to assess the total connected porosity, volume and size distribution of pores present in concrete<sup>[29,30]</sup>. MIP test was conducted to understand the pore structure, and total connected porosity of control and nano blended concrete specimens, as they majorly influence the mechanical and durability properties of concrete<sup>[31]</sup>. In the present study, MIP tests were performed on concrete. A number of factors affect the MIP results. Most important among them are the method of sampling and sample conditioning. Thereby, concrete samples representative of the overall quality of concrete in the cylinders specimens were collected following the procedure given in the literature<sup>[32,33]</sup>. Concrete chunk samples required for MIP testing were cut from the core of the hardened concrete cylindrical specimen cured for 28 days. The small test specimens were immersed in anhydrous ethanol solution for 24 hours to stop the further hydration, then dried at 100 °C until a constant mass was reached. An automatic mercury intrusion porosimeter with a low-pressure range up to 0.345 MPa and a high-pressure range of 0.138 MPa to 413.69 MPa was used for investigating the pore structures of concrete. The applied pressures were converted to equivalent pore diameter using the Washburn equation<sup>[34]</sup>, as expressed in Equation 1.

$$d = - \frac{(4\gamma Hg \cos\theta)}{P} \quad (1)$$

Where  $d$  is the pore diameter;  $\gamma Hg$  is the surface tension of mercury (480 mN/m);  $\theta$  is the contact angle between mercury and concrete (assumed as 140°), and  $P$  is the applied pressure.

## 3. RESULTS AND DISCUSSIONS

### 3.1 Workability and Compressive strength

The slump and compressive strength of nano blended concrete are summarised in Figure 2. For the same amount of SP used across the mixtures, slump values observed to decrease with an increase in the percentage of nanoparticles replacing the cement. With reference to the control specimen, concrete mixture with 0.5, 1.0, 1.5 and 2 wt.% of nanoparticles show nearly 23, 40, 46 and 63% decrease in slump value respectively. In the present study, as the dosage of SP was kept constant, the variation in the slump values was only influenced by the dosage of nanoparticles. The decrease in workability of concrete with the increase in dosage of nanoparticles was because of two reasons. First, due to the larger surface area to volume ratio

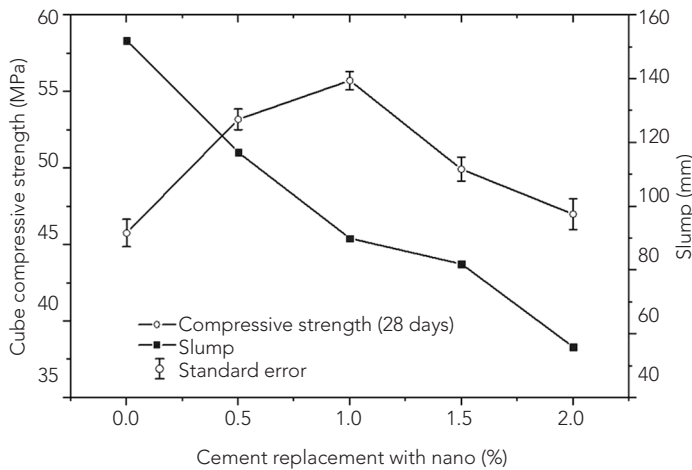


Figure 2: Slump and compressive test results

of nanoparticles, more water gets adsorbed on their surface and reduce the quantity of water available for lubricating the aggregate surface. Second, nanoparticles are usually charged due to their fineness; thereby, the total quantity of SP added was not only adsorbed to cement particles but also nanoparticles. Thus, the nanoparticles affected the workability of the concrete mixture with an increase in its dosage.

Compared to the control specimen, the increase in compressive strength was observed in all mixtures containing nano-hematite (Figure 2); out of which 1.0NH specimen with an increment of 21.76%, being highest. The enhancement of compressive strength is due to high activity and well dispersion of synthesised nano-hematite in the concrete mixture. Whereas for a higher dosage of nanoparticles, i.e., 1.5NH and 2.0NH specimens, an increment of only 9.1 and 2.7% were observed respectively, due to agglomeration of nanoparticles, which is explained through the pore structure, XRD and morphological characteristics of nano blended concrete, in later sections.

## 3.2 Electrical resistivity

Few studies reported that the addition of nanoparticles contributes to the enhanced chloride resistance and improves the electrical resistivity of the cementitious system<sup>[31,35,36]</sup>. The electrical resistance offered by specimen against the chloride migration were estimated from the data logged during RCMT tests, namely, supplied voltage (V) and current drawn by each specimen (I). The electrical resistivity ( $\rho$ ) of the specimens was then estimated as  $\rho = R.A/L$  where, R is the resistance offered by concrete specimen against chloride migration =  $V/I$ , A is the cross-sectional area of the specimen and L is the thickness of the specimen. Thickness and diameter of each specimen were measured by a digital calliper with 0.01mm precision. Electrical resistivity was estimated for all the specimen throughout the migration test, and their variation with time (Figure 3). It can be observed from the figure that 0.5NH specimens have shown the

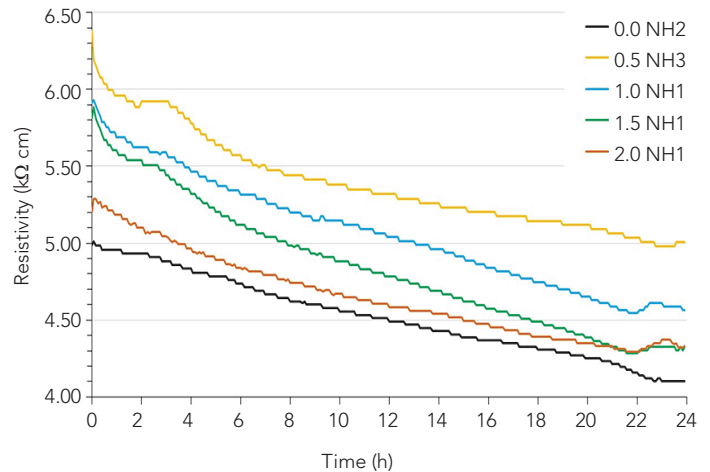


Figure 3: Variation of electrical resistivity during RCMT test

highest electrical resistivity, followed by 1.0NH. 1.5NH, 2.0NH and control specimen, indicating that concrete with 0.5 wt.% of  $Fe_2O_3$  nanoparticles has lesser chances of corrosion due to its higher electrical resistivity among all the tested specimens. The electrical resistivity of concrete is majorly influenced by the porosity and pore structure<sup>[15,16,35,37,38]</sup>. The porosity decrease due to use of nanoparticles, results in higher resistivity which delays the penetration of chlorides into the system<sup>[35]</sup>. The cementitious system with a denser microstructure and lesser porosity offers maximum resistance to chloride penetration, thereby increasing the chloride resistivity<sup>[16,39]</sup>. To understand the porosity, pore structure and microstructural morphology, MIP and FEG-SEM analyses were conducted.

## 3.3 Chloride ingress

At the end of RCMT test, specimens were split into two parts and sprayed with 0.1 M Silver nitrate solution on both surfaces. Silver nitrate reacts with the chlorides present on the split surface and turns to white Silver chloride precipitate. The chloride penetration depth can be measured from the visible white silver chloride precipitation, as shown in Figure 4. Chloride ingress depth in each split of the specimen subjected to RCMT tests was measured using a digital calliper with 0.01 mm precision. Figure 4 also shows the typical chloride penetration depth traced on a split specimen for each nano dosage for a better comparison among the tested specimens. It can be observed from the typical chloride penetration pattern that, 0.5NH specimen showed least chloride ingress in concrete among all the tested specimen. The performance of 1.0NH specimen is also better compared to the control specimen. However, the migration depth was more than that of the control specimen for the concrete with 2.0 wt.% of nanoparticles. Based on the ingress depth, the non-steady-state migration coefficient ( $D_{nssm}$ ) and the apparent coefficient of chloride diffusion ( $D_{app}$ ) were estimated in accordance with NT BUILD 492



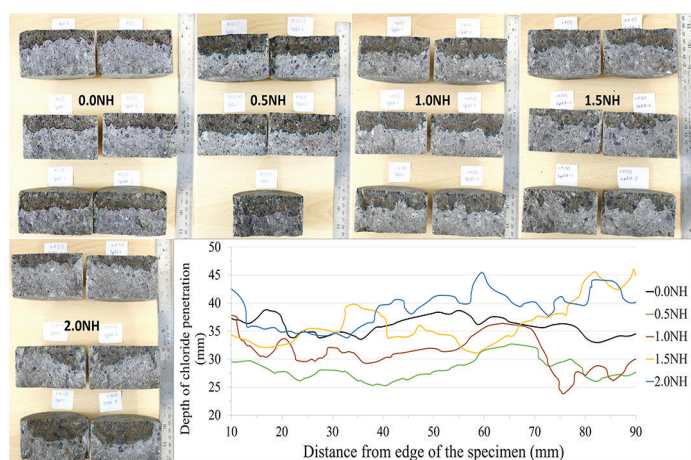


Figure 4: Chloride migration depth for specimens with different nano percentages

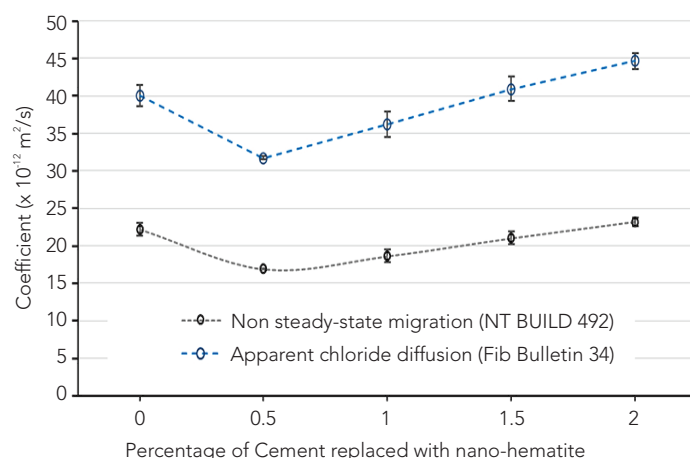


Figure 5: Chloride diffusion coefficients for concrete with nano-hematite

[27] and Fib Bulletin 34 [40], respectively and presented in Figure 5 along with standard error bar.

The apparent chloride diffusion coefficients for 0.5NH and 1.0NH specimens have shown 20.7% and 9.6% lesser chloride ingress in concrete compared to control specimen respectively, whereas, the performance of 1.5NH and 2.0NH specimens are relatively weak. The variation in the performance pattern of chloride ingress in concrete with different proportions of nano-hematite has motivated for further examination through FEG-SEM and EDS mapping analyses to understand the influence of adding  $\text{Fe}_2\text{O}_3$  nanoparticles on the physical properties of concrete.

### 3.4 Pore structure of nano blended concrete

Cumulative pore volume and pore size distribution curves obtained from MIP tests of the concrete with and without synthesised nanoparticles are presented in Figure 6. The cumulative porosity and pore structure of the blended concrete after 28 days of curing are summarised in Table 2. The differential curve shows several pore sizes that are present in the concrete matrix. The corresponding critical pore diameters are obtained from the maximums of the derivative of the

pore distribution curve [41]. However, only the critical pore diameter where mercury enter and percolate the pore system in appreciable quantity has been itemised in Table 2. The volume of intrusion is highest at low intrusion pressure in the control mixture due to the dominating presence of the pores that are larger than one-micron meter. With the replacement of a portion of cement with synthesised nanoparticles, pore sizes substantially reduced by 99.4% and 98.5% respectively for 0.5NH and 1.0NH specimens. Increase in the dosage of nanoparticles has shown the negative effect on the critical pore size, pore volume and thereby the total porosity of the concrete specimen. However, 1.5NH and 2.0NH specimens have shown a significant reduction in the critical pore size compared with the control specimen. Overall, MIP results indicate that the synthesised hematite nanoparticles are beneficial in both decreasing the total connected porosity and refining the pore structure of concrete, where 0.5% replacement being the optimum. Significant reduction in the critical pore diameter and total porosity are the prime reasons behind the enhancement in the chloride resistivity and compressive strength of 0.5NH concrete specimen. Thereby, in the RCMT test, the 0.5NH concrete specimens has shown the highest resistivity for the chloride ion migration and possess the least penetration depth.

Table 2: Pore structure of nano blended concrete

SPECIMEN ID	PORE VOLUME (x 10 <sup>-2</sup> ) IN cc/g (V <sub>p</sub> )	POROSITY (%)	PORE DIAMETER								CRITICAL PORE DIAMETER (nm)
			> = 1μm		1μm-100nm		100nm-10nm		< = 10nm		
			V <sub>p</sub>	%	V <sub>p</sub>	%	V <sub>p</sub>	%	V <sub>p</sub>	%	
0.0NH	9.56	23.01	9.56	100	0.00	0.04	0.00	0.00	0.00	0.0	2792.64
0.5NH	8.68	20.83	0.10	1.13	0.00	0.04	8.58	98.8	0.00	0.0	15.43
1.0NH	8.80	21.17	0.63	7.20	0.25	2.88	7.92	89.9	0.00	0.0	39.52
1.5NH	9.36	22.47	0.33	3.48	4.52	48.3	4.50	48.1	0.02	0.2	115.0
2.0NH	9.66	23.20	1.71	17.8	5.26	54.4	1.88	19.4	0.81	8.4	435.15

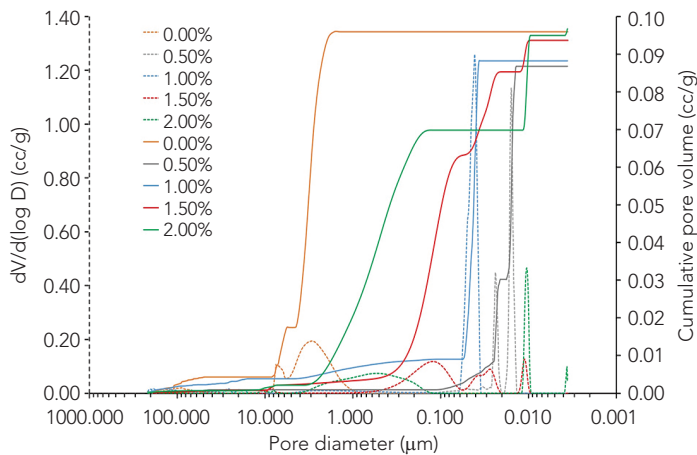


Figure 6: Cumulative pore volume and pore size distribution of nano blended concrete

### 3.5 XRD analysis on concrete with nanoparticles

XRD results were analysed to qualitatively study the mineral composition and understand the effect of synthesised nanoparticles dosage on hydration products. Figure 7 shows the XRD patterns of nano blended concrete at curing age of 28 days. Peaks representing the hydration products are alone highlighted in the diffractograms ignoring the peaks related to aggregates (Silica) present in the concrete matrix. It can be observed from the figure that the main hydration products identified are Calcium Silicate Hydrate phase (C-S-H), Calcium hydroxide  $[\text{Ca}(\text{OH})_2]$ , Calcite ( $\text{CaCO}_3$ ) and Ettringite  $[\text{Ca}_6\text{Al}_2(\text{SO}_4)_3(\text{OH})_{12} \cdot 26\text{H}_2\text{O}]$ .

C-S-H is one of the significant hydration products, as it is a binding compound that imparts compressive strength to the concrete<sup>[30]</sup> due to its high adhesion capacity and high surface area<sup>[42]</sup>. Though it is challenging to identify the C-S-H compound through XRD analysis, researchers in the past<sup>[43,44]</sup> have reported the diffraction peak of the C-S-H because of its semi-amorphous and poorly crystalline nature<sup>[30,42]</sup>. The present XRD analysis shows that the diffraction peak of C-S-H overlaps with that of Calcite at approximately  $29.3^\circ$  ( $2\theta$ ). The semi-amorphous nature of C-S-H is the prime reason behind its overlapping with the strong peak of Calcite in a  $2\theta$  range of  $28^\circ$  to  $30^\circ$ <sup>[45]</sup>. The intensity of peak representing the C-S-H is highest for 1.0NH, indicating that its formation is relatively more compared to other specimens, which is the main reason behind the higher compressive strength of 1.0NH specimen. Test results indicate that the addition of nanoparticles did not result in the formation of any new hydration products. However, nanoparticles were acting as an accelerating agent<sup>[46,47]</sup> to promote the further formation of C-S-H<sup>[48]</sup> till 1% dosage. Well-dispersed nanoparticles act as reaction centers, accelerating cement hydration<sup>[16]</sup> because of their high surface area and chemical reactivity<sup>[23,24]</sup>. Further increase in nano-hematite content attributes to the reduction in the spacing between the

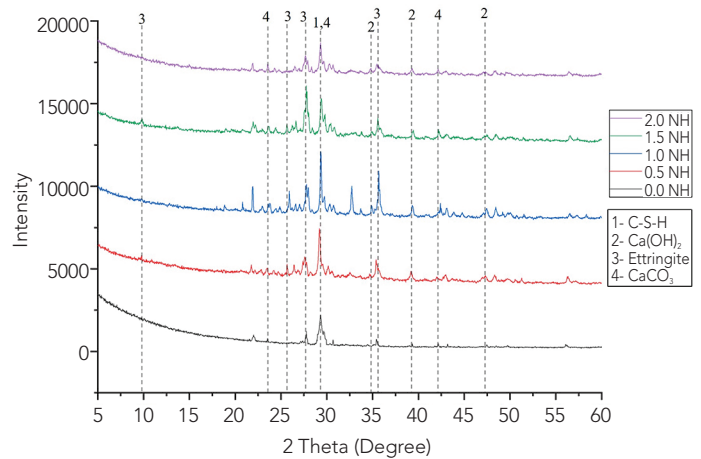


Figure 7: X-Ray diffractograms of the concrete containing nano-hematite

nanoparticles (agglomeration), decreasing their high activity, thereby restricting the growth of C-S-H gel.

### 3.6 Microstructure morphology of ITZ

Interfacial transition zone (ITZ) is the weakest portion of concrete that ease the transport of chloride ions; hence, its microstructure influences the permeability, resistivity and strength characteristics of concrete<sup>[42]</sup>. To understand the effectiveness of nanoparticle blended concrete in improving the ITZ, microstructure morphology has been studied using FEG-SEM analysis for various percentage replacements of cement with synthesised nano-hematite. Specimens, prepared by englobing the representative concrete specimen of  $15 \text{ mm} \times 15 \text{ mm}$  in epoxy resin, were ground, polished and coated with platinum for the FEG-SEM analysis. Specimens were stored in a desiccator containing silica gel and calcium hydroxide pellets to absorb the moisture and carbon dioxide present in the surrounding atmosphere. FEG-SEM micrographs were then taken at different magnification levels (up to  $100000\times$ ) to understand the microstructure morphology of ITZ, as given in Figure 8.

It is clear from the micrographs that wide gaps between aggregate and cement matrix; numerous microcracks were observed in 0.0NH specimens. Whereas, in 0.5NH specimen, the dense and compact microstructure was observed in the ITZ with narrow gaps between the aggregate and cement matrix. At higher magnification levels, the presence of synthesised NRs was identified for the 0.5NH specimen in the vicinity of the aggregates and the narrow gaps between the aggregate and cement matrix were found to be filled. This is the primary reason for the lesser chloride ingress and the better performance of 0.5NH specimens in strength and durability characteristics. It is also observed that, for the specimen with 1 wt.% of nano-hematite, ITZ found to be dense and compact with lesser number of micro-cracks in the cement matrix compared to that of 1.5NH and 2.0NH specimens. Increasing



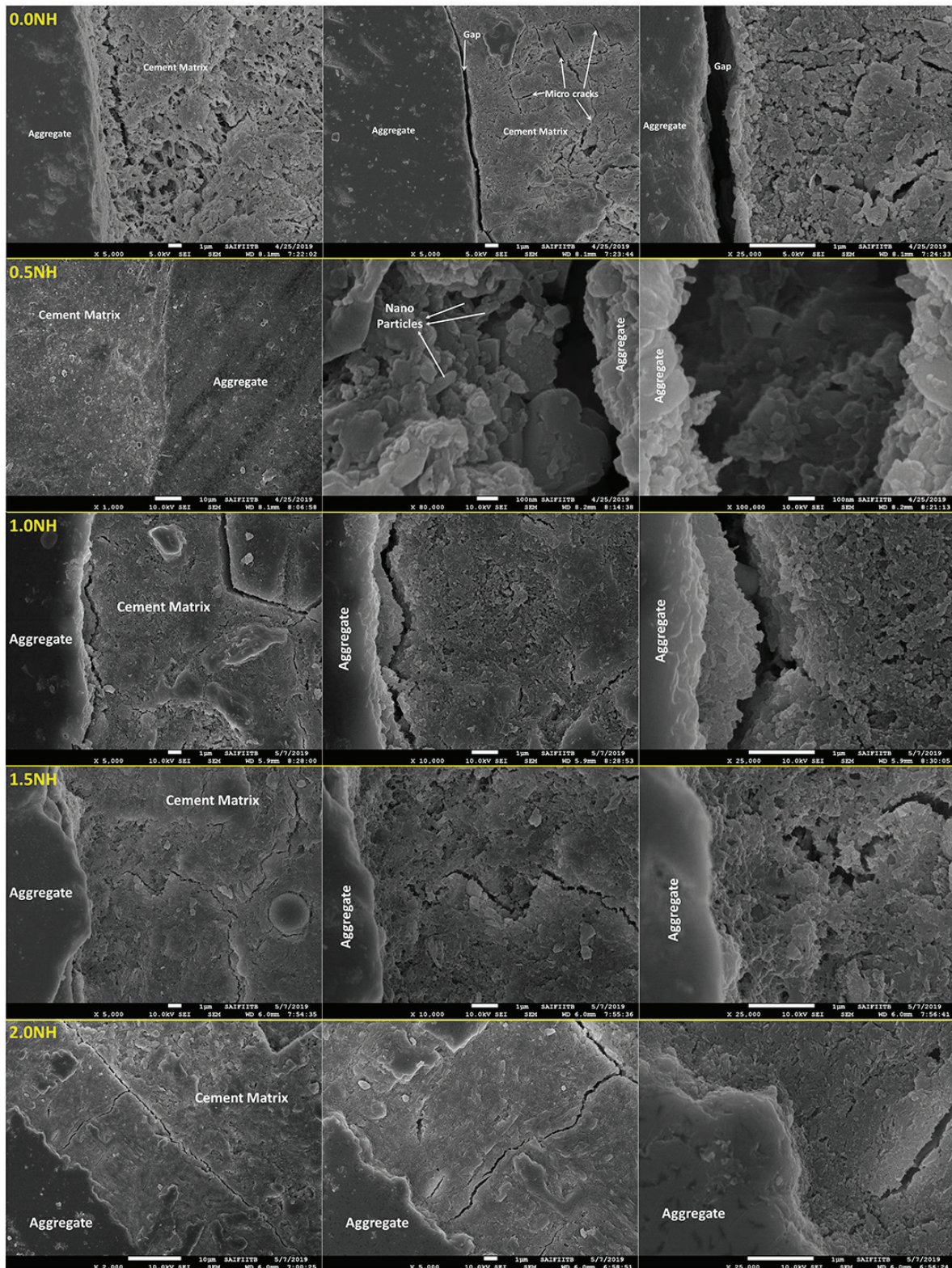


Figure 8: The morphological microstructure of ITZ for different percentages of nano-hematite

the content of nanoparticles will decrease the spacing between the nanoparticles, causing agglomeration. As discussed earlier, agglomeration of nanoparticles reduces the total surface area and restricts their high activity, thereby reducing the further growth of C-S-H gel formation. Thus, a sufficient quantity of

C-S-H is not available to fill the ITZ due to which relatively a greater number of microcracks and voids in concrete blended with a higher dosage of nanoparticles (1.5NH and 2.0NH specimens) were found. Overall, it is observed that synthesised nanoparticles strengthened the ITZ microstructure of concrete.



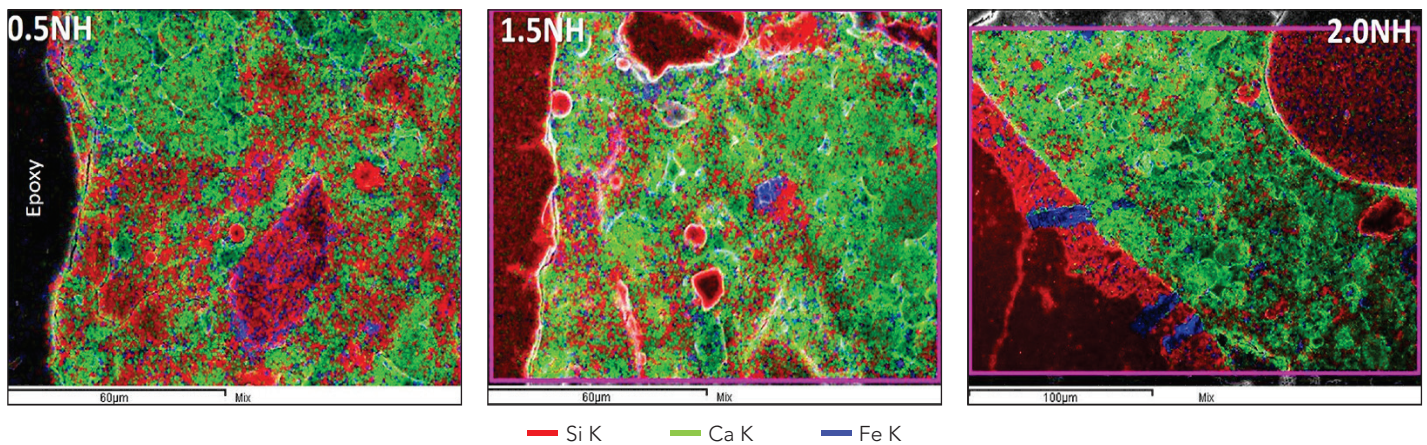


Figure 9: Dispersion and agglomeration of nanoparticles (EDS-Mapping)

The compressive strength and chloride migration tests signify that despite adding relatively more quantity of nanoparticles, 1.5NH and 2.0NH specimens have not performed well, whereas, 0.5NH specimen has shown better performance among all. In order to understand the dispersion of nanoparticles over the cement matrix, which influences their activity and alters the performance of concrete [23], three specimens with different proportions of nano-hematite (0.5NH, 1.5NH and 2.0NH) were considered for elemental mapping analysis using EDS (Figure 9). It is evident from the elemental mapping that nanoparticles are well dispersed filling up the micropores/cracks present in the ITZ with less/no agglomerations in 0.5NH specimen. In contrast, agglomeration of nanoparticles was observed at numerous locations in the specimens containing the dosage of nanoparticles above 1.0wt. %.

## 4. CONCLUSIONS

The present study investigates the microstructural and durability properties of concrete incorporated with synthesised nanoparticles. The results imply that synthesised nanoparticles could effectively be used at low Portland cement replacement. However, it should be noted that despite its positive effect on compressive strength, porosity and chloride resistance of concrete, a reduction in workability should be expected. The salient conclusions of this study are as follows:

- i. Nanoparticles synthesised by adopted hydrothermal procedure resulted in no impurities and morphology was found to be a mixture of nanorods and distorted nanospheres with an average size of 66.8 nm.
- ii. The workability of nano blended concrete decreases with an increase in the dosage of nanoparticles due to high surface area to volume ratio. Concrete specimen with 2 wt. % of cement replacement has shown 63% decrement in slump value compared to control specimen.

- iii. Results indicate that at the age of 28 days, cement replaced by 1 wt. % of nano-hematite shown maximum growth in compressive strength up to 21.8% which is mainly due to the formation of more C-S-H gel and low porosity of hardened concrete.
- iv. The critical pore diameter of nano blended concrete has been substantially reduced from 2.79 µm to 15.43 nm with 0.5% of Portland cement replaced by synthesised nano-hematite. The effectiveness of nano-hematite in improving the pore structure of concretes increases in the order: 0.0NH < 2.0NH < 1.5NH < 1.0NH < 0.5NH.
- v. Rapid chloride migration test results revealed that cement replaced with nano-hematite by 0.5 wt. % and 1.0 wt. % has a positive effect, while 1.5 wt. % and 2.0 wt. % dosages affected their apparent chloride diffusion coefficients.
- vi. Among the tested specimens, 0.5NH specimens have shown the highest electrical resistivity and least chloride migration because of the least total connected porosity and compact microstructure observed during the MIP test and SEM analysis.
- vii. Microstructural analysis revealed that nanoparticles were well dispersed, filling up the micropores and cracks, leading to the strengthening the ITZ of concrete for 0.5NH specimen; whereas, agglomeration of nanoparticles was observed at numerous locations in the concrete specimen with cement replacement above 1 wt. %.

Overall, Portland cement replaced by 0.5 wt. % of synthesised nano-hematite found to be the optimal dosage in terms of its performance in chloride ingress and electrical resistivity characteristics due to the lesser critical pore size, dense microstructure and better distribution of nanoparticles over the concrete.

## ACKNOWLEDGEMENT

Authors thank Industrial Research and Consultancy Centre - IIT Bombay for financially supporting the research work. Authors acknowledge Dr D.N. Singh, Institute Chair Professor, Department of Civil Engineering, IIT Bombay for allowing the authors to avail the Mercury Intrusion Porosimetry facility.

## REFERENCES

- [1] Vanama, R. K., & Ramakrishnan, B. (2020). "Improved degradation relations for the tensile properties of naturally and artificially corroded steel rebars", *Construction and Building Materials*, Vol. 249, pp. 118706-118727. <https://doi.org/10.1016/j.conbuildmat.2020.118706>.
- [2] Real, S., Bogas, J. A., & Ferrer, B. (2017). "Service life of reinforced structural lightweight aggregate concrete under chloride-induced corrosion", *Materials and Structures*, Vol. 50, No. 2, pp. 1-17.
- [3] Chindaprasirt, P., & Rukzon, S. (2015). "Strength and chloride resistance of the blended Portland cement mortar containing rice husk ash and ground river sand", *Materials and structures*, Vol. 48, No. 11, pp. 3771-3777.
- [4] Otieno, M., Golden, G., Alexander, M. G., & Beushausen, H. (2019). "Acceleration of steel corrosion in concrete by cyclic wetting and drying: effect of drying duration and concrete quality", *Materials and Structures*, Vol. 52, No. 2, pp. 1-14.
- [5] Reches, Y. (2018). "Nanoparticles as concrete additives: Review and perspectives", *Construction and Building Materials*, Vol. 175, pp. 483-495.
- [6] Kwalramani, M. A., & Syed, Z. I. (2018). "Application of nanomaterials to enhance microstructure and mechanical properties of concrete", *International Journal of Integrated Engineering*, Vol. 10, No. 2, pp. 98-104.
- [7] Paul, S. C., Van Rooyen, A. S., van Zijl, G. P., & Petrik, L. F. (2018). "Properties of cement-based composites using nanoparticles: A comprehensive review", *Construction and Building Materials*, Vol. 189, pp. 1019-1034.
- [8] Sumesh, M., Alengaram, U. J., Jumaat, M. Z., Mo, K. H., & Alnahhal, M. F. (2017). "Incorporation of nanomaterials in cement composite and geopolymer based paste and mortar—A review", *Construction and Building Materials*, Vol. 148, pp. 62-84.
- [9] Parreño, F. F., Antonio, O. V. M., & Balela, M. D. L. "Investigation of Hematite ( $\alpha$ -Fe<sub>2</sub>O<sub>3</sub>) Nanoparticle Treatment in Mitigating Corrosion in Reinforced Concrete", 15th Asia Pacific Conference for Non-Destructive Testing (APCNDT2017), Singapore, pp. 1-8.
- [10] Nazari, A., & Riahi, S. (2011). "Assessment of the effects of Fe<sub>2</sub>O<sub>3</sub> nanoparticles on water permeability, workability, and setting time of concrete", *Journal of Composite Materials*, Vol. 45, No. 8, pp. 923-930.
- [11] Salemi, N., Behfarnia, K. & Zaree, S. A. (2014). "Effect of nanoparticles on frost durability of concrete", *Asian Journal of Civil Engineering*, Vol. 15, pp. 411-420.
- [12] Fang, Y., Sun, Y., Lu, M., Xing, F., & Li, W. (2018). "Mechanical and Pressure-sensitive Properties of Cement Mortar Containing Nano-Fe<sub>2</sub>O<sub>3</sub>", 4th Annual International Conference on Material Engineering and Application (ICMEA 2017), Atlantis Press, pp. 206-210.
- [13] Nivethitha, D., Srividhya, S., & Dharmar, S. (2016). "Review on mechanical properties of cement mortar enhanced with nanoparticles", *International Journal of Science and Research*, Vol. 5, No. 1, pp. 913-916.
- [14] Shekari, A. H., & Razzaghi, M. S. (2011). "Influence of nano particles on durability and mechanical properties of high performance concrete", *Procedia Engineering*, Vol. 14, pp. 3036-3041.
- [15] Nazari, A., Riahi, S., Riahi, S., Shamekhi, S. F., & Khademno, A. (2010). "Benefits of Fe<sub>2</sub>O<sub>3</sub> nanoparticles in concrete mixing matrix", *Journal of American Science*, Vol. 6, No. 4, pp. 102-106.
- [16] Vipulanandan, C., & Mohammed, A. (2015). "Smart cement modified with iron oxide nanoparticles to enhance the piezoresistive behavior and compressive strength for oil well applications", *Smart Materials and Structures*, Vol. 24, No. 12, 125020.
- [17] IS 269: 2015. *Ordinary Portland Cement- Specification*. Bureau of Indian Standards, New Delhi.
- [18] IS 383: 2016. *Coarse and fine aggregate for concrete – Specification*. Bureau of Indian Standards, New Delhi.
- [19] Bazrafshan, H., Tesieh, Z. A., Dabirnia, S., Toubia, R. S., Manghabati, H., & Nasernejad, B. (2017). "Synthesis of novel  $\alpha$ -Fe<sub>2</sub>O<sub>3</sub> nanorods without surfactant and its electrochemical performance", *Powder Technology*, Vol. 308, pp. 266-272.
- [20] Lassoued, A., Dkhil, B., Gadri, A. & Ammar, S. (2017). "Control of the shape and size of iron oxide ( $\alpha$ -Fe<sub>2</sub>O<sub>3</sub>) nanoparticles synthesised through the chemical precipitation method", *Results in Physics*. Vol. 7, pp. 3007-3015.

- [21] Darezereshki, E. (2011). "One-step synthesis of hematite ( $\alpha$ -Fe<sub>2</sub>O<sub>3</sub>) nano-particles by direct thermal-decomposition of maghemite", *Materials Letters*. Vol. 65, pp. 642-645.
- [22] IS 10262: 2019. *Concrete mix proportioning-guidelines*. Bureau of Indian Standards, New Delhi.
- [23] Liu, X., Feng, P., Shu, X., & Ran, Q. (2020). "Effects of highly dispersed nano-SiO<sub>2</sub> on the microstructure development of cement pastes", *Materials and Structures*, Vol. 53, No. 1, pp. 1-12.
- [24] Kawashima, S., Seo, J. W. T., Corr, D., Hersam, M. C., & Shah, S. P. (2014). "Dispersion of CaCO<sub>3</sub> nanoparticles by sonication and surfactant treatment for application in fly ash-cement systems" *Materials and structures*, Vol. 47, No. 6, pp. 1011-1023.
- [25] ASTM C511. Standard Specification for Mixing Rooms, Moist Cabinets, Moist Rooms, and Water Storage Tanks Used in the Testing of Hydraulic Cements and Concretes. *ASTM Int.* 1-3 (2013).
- [26] IS 516: 2018. *Methods of Tests for Strengthening of Concrete*. Bureau of Indian Standards, New Delhi.
- [27] NT Build, 492. Chloride migration coefficient from non-steady-state migration experiments. *Nordtest method 1-8* (1999)
- [28] Vanama, R. K. & Ramakrishnan, B. "An interface circuit for an accelerated corrosion test apparatus", Indian patent application No. 201921020474, published September 20, 2019.
- [29] Nazari, A. & Riahi, S. (2011). "The effects of SiO<sub>2</sub> nanoparticles on physical and mechanical properties of high strength compacting concrete" *Composites Part B* Vol. 42, pp. 570-578.
- [30] Sun, J., Shen, X., Tan, G., & Tanner, J. E. (2019). "Modification effects of nano-SiO<sub>2</sub> on early compressive strength and hydration characteristics of high-volume fly ash concrete" *Journal of Materials in Civil Engineering*, Vol. 31, No. 6, pp. 04019057.
- [31] Supit, S. W. M., & Shaikh, F. U. A. (2015). Durability properties of high volume fly ash concrete containing nano-silica. *Materials and structures*, Vol. 48, No. 8, pp. 2431-2445.
- [32] Kumar, R., & Bhattacharjee, B. (2004). "Assessment of permeation quality of concrete through mercury intrusion porosimetry" *Cement and concrete research*, Vol. 34, No. 2, pp. 321-328.
- [33] Kumar, R., & Bhattacharjee, B. (2003). "Study on some factors affecting the results in the use of MIP method in concrete research" *Cement and Concrete Research*, Vol. 33, No. 3, pp. 417-424.
- [34] Washburn, E. W. (1921). "Note on a method of determining the distribution of pore sizes in a porous material", *Proceedings of the National academy of Sciences of the United States of America*, Vol. 7, No. 4, 115.
- [35] Madandoust, R., Mohseni, E., Mousavi, S. Y., & Namnevis, M. (2015). "An experimental investigation on the durability of self-compacting mortar containing nano-SiO<sub>2</sub>, nano-Fe<sub>2</sub>O<sub>3</sub> and nano-CuO" *Construction and Building Materials*, Vol. 86, pp. 44-50.
- [36] Jalal, M., Mansouri, E., Sharifipour, M., & Pouladkhan, A. R. (2012). "Mechanical, rheological, durability and microstructural properties of high performance self-compacting concrete containing SiO<sub>2</sub> micro and nanoparticles" *Materials & Design*, Vol. 34, pp. 389-400.
- [37] McCarter, W. J., Starrs, G., & Chrisp, T. M. (2000). "Electrical conductivity, diffusion, and permeability of Portland cement-based mortars", *Cement and Concrete Research*, Vol. 30, No. 9, pp. 1395-1400.
- [38] Wei, X., Xiao, L., & Li, Z. (2008). "Electrical measurement to assess hydration process and the porosity formation", *Journal of Wuhan University of Technology-Mater. Sci. Ed.*, Vol. 23, No. 5, pp. 761-766.
- [39] Zuo, Y., Zi, J., & Wei, X. (2014). "Hydration of cement with retarder characterized via electrical resistivity measurements and computer simulation", *Construction and building materials*, Vol. 53, pp. 411-418.
- [40] FibBulletin 34. *Model Code for Service Life Design*. International Federation for Structural Concrete, 2006.
- [41] Nokken, M. R., & Hooton, R. D. (2008). "Using pore parameters to estimate permeability or conductivity of concrete", *Materials and Structures*, Vol. 41, No. 1.
- [42] Mehta, P. K. & Monteiro, P. J. M. M. *Concrete: Microstructure, Properties, and Materials, Fourth Edition*. (McGraw-Hill Education, 2014).
- [43] Akturk, B., Nayak, S., Das, S., & Kizilkanat, A. B. (2019). "Microstructure and Strength Development of Sodium Carbonate-Activated Blast Furnace Slags", *Journal of Materials in Civil Engineering*, Vol. 31, No. 11, pp. 04019283.
- [44] Kore, S. D., & Vyas, A. K. (2016). "Impact of marble waste as coarse aggregate on properties of lean cement concrete", *Case Studies in Construction Materials*, Vol. 4, pp. 85-92.



- [45] Gu, K., Jin, F., Al-tabbaa, A., Shi, B. & Liu, J. (2014). "Mechanical and hydration properties of ground granulated blast furnace slag pastes activated with MgO – CaO mixtures", *Construction and Building Materials*, Vol. 69, pp. 101-108.
- [46] Nazari, A., & Riahi, S. (2011). "The effects of SiO<sub>2</sub> nanoparticles on physical and mechanical properties of high strength compacting concrete", *Composites Part B: Engineering*, Vol. 42, No. 3, pp. 570-578.
- [47] Legrand, C., & Wirquin, E. (1994). "Study of the strength of very young concrete as a function of the amount of hydrates formed—influence of superplasticizer", *Materials and Structures*, Vol. 27, No. 2, pp. 106-109.
- [48] Khoshakhlagh, A., Nazari, A., & Khalaj, G. (2012). "Effects of Fe<sub>2</sub>O<sub>3</sub> nanoparticles on water permeability and strength assessments of high strength self-compacting concrete", *Journal of Materials Science & Technology*, Vol. 28, No. 1, pp. 73-82.



**RAGHAVA KUMAR VANAMA** holds a master's degree in Structural Engineering from Visvesvaraya National Institute of Technology (VNIT) Nagpur and is pursuing his Ph.D. at the Department of Civil Engineering, Indian Institute of Technology (IIT) Bombay. He worked as a Project Scientist at the National Institute of Ocean Technology (NIOT), Chennai, on analysis, design and implementation of various offshore and onshore marine structures. His research interests include monitoring and mitigating chloride/carbonation-induced corrosion in reinforced concrete structures, corrosion mitigative coatings, durable concrete, non-destructive testing, repair and rehabilitation of marine structures. Email: vanama.raghavakumar@gmail.com



**HARINEE ADDEPALLI** holds a bachelor's degree in Nano Science and Technology from Anna University. She interned at Indian Institute of Technology (IIT) Bombay and Henkel Adhesives Technologies India Private Limited. Her research interests include nanoparticle synthesis, corrosion mitigative coatings, biological application of nanoparticles and nanotechnology in coatings. Email: harineetweet@gmail.com



**BALAJI RAMAKRISHNAN** is an Associate Professor in the Department of Civil Engineering at Indian Institute of Technology (IIT) Bombay. He received his master's and Ph.D. Degrees in Ocean Engineering from Indian Institute of Technology (IIT) Madras. Earlier, he was an Assistant Professor at the Department of Civil Engineering, NIT Calicut and worked as a senior coastal engineer at M/s Sogreah Gulf FZCO. He has authored/co-authored several journal articles, book chapters and national/international conference proceedings. His research interests include repair and rehabilitation of marine reinforced concrete structures, understanding the dynamics of waves, tides, currents & sediments, application of Remote Sensing in coastal engineering. Email: rbalaji@iitb.ac.in

**Cite this article:** Vanama, R.K., Addepalli, H., and Balaji, R., (2021). "Optimal dosage of Fe<sub>2</sub>O<sub>3</sub> nanoparticles to enhance chloride resistance and microstructural properties of concrete- A comprehensive study", *The Indian Concrete Journal*, Vol. 95, No. 4, pp. 17-28.

# PERFORMANCE OF ORGANIC AND INORGANIC FUNCTIONAL GROUPS AS CORROSION INHIBITORS IN CONCRETE EXPERIENCING EXTREME CORROSIVE ENVIRONMENT

HIMANSHU GULERIA,  
PURNIMA,  
ASHISH KUMAR TIWARI,  
SHWETA GOYAL\*

## Abstract

Reinforcement corrosion is the major durability issue causing premature failure of reinforced concrete structures. Ingress of chloride and atmospheric CO<sub>2</sub> are two important phenomena promoting the corrosion, but combined effect of these two causes even more severe damage than individual environment. The corrosion inhibition mechanism of various compounds depends upon the presence of functional group in their molecular structure. The present study deals with determination of the inhibition efficiency of organic and inorganic based compounds in combined chloride and carbonated environment. The aggressive environment was achieved by subjecting specimen to alternate wetting-drying-carbonation cycles. Specimen was wetted by ponding in 5% NaCl solution followed by air drying and exposed to carbonation by using environment chamber. The results show that compound containing organic functional group was able to reduce corrosion rate in combined environment, while inorganic inhibitor was unable to perform in aggressive conditions. Chloride and carbonation profile also shows that organic functional group-based inhibitor blocks the pores and resists the movement of aggressive chloride ions and carbonation front.

**Keywords:** Carbonation, Chloride, Corrosion inhibitors, Half-cell potential (HCP), Linear polarization resistance, Reinforced concrete.

## 1. INTRODUCTION

Corrosion of reinforced concrete (RC) structure is the major durability issue for infrastructure, such as offshore and harbour structure, pavement and bridges. The methodical increase of pollutants in the environment has led to inflation in chloride ions and carbon dioxide (CO<sub>2</sub>) leading to corrosion process which is a major concern for reinforcement in concrete.

For a better representation of in-service modern concrete itself, characterizing the realistic exposed deteriorating environments is however more challenging. Most RC structures are experiencing multi-deteriorating actions simultaneously over their entire service life; the combination of them may be even more detrimental than any single deterioration process alone. For instance, when chloride attack is accompanied with carbonation under wetting-drying cycles, it may even further increase the risk of corrosion in RC structures. Recently, there are several studies regarding the influence of carbonation on chloride penetration in concrete. For instance, Tumidajski and Chan (1996)<sup>[1]</sup> found that carbonation has a minor effect on the chloride diffusivity of ordinary portland cement-based concrete, but increases the chloride diffusivity for concrete with blast-furnace slag. However, Lee *et al.* (2013)<sup>[2]</sup> found that the ratio of water-soluble chloride (i.e. free chlorides) to the acid-soluble chloride (total chlorides) content is higher for the case of accelerated carbonation than that of natural air exposure. Hailong *et al.* (2016)<sup>[3]</sup> also observed that with the increase in the carbonation front, both free and total chloride content decreases.

To have longer and durable RC life, some preventive measures against the corrosion should be taken. Some of these methods includes: design as per standard codes, protective coating, use of sealant, use of non-corrosive steel and corrosion inhibitors. Among all the available preventive measures, inhibitors seem to be the most significant preventive measure in terms of usage, economy, easy handling and overall effect on durability of concrete structures<sup>[4-6]</sup>. Inhibitor is defined as a substance made up of chemicals which decrease the rate of corrosion when present at suitable concentration in system without affecting the concentration of any other corrosion agent<sup>[7,8]</sup>. Inhibitors can be either used as admixed or migratory in concrete system. For fresh concrete, admixed inhibitors have been used since 1970s whereas; in repair work migratory corrosion inhibitors have come

\*Corresponding author : Shweta Goyal, Email: shweta@thapar.edu

in existence only past few decades. They are characterized as inorganic and organic corrosion inhibitors on the basis of their functional groups. Generally, inorganic inhibitors have either cathodic or anodic actions. The inorganic compounds which are based upon calcium nitrite, sodium nitrite, sodium benzoate, sodium monofluorophosphate (MFP) and sodium chromate are used as admixed inhibitors<sup>[9]</sup>.

Organic inhibitors occasionally act as cathodic, anodic or together, as cathodic and anodic inhibitors, act through a process of surface adsorption and form a protective film over the surface. Organic inhibitors can be used as both admixed corrosion inhibitors (ACI) and migratory corrosion inhibitors (MCI)<sup>[9-16]</sup>. Both, ACI and MCI are able to create thin passive layer on steel surface. Organic inhibitors build up a protective hydrophobic film by molecular adsorption on the metal surface enacting as a barrier against dissolution of the metal. As a secondary protection mechanism, organic inhibitors tend to block the pores of the concrete matrix protecting the steel bars from the aggressive ions<sup>[17-20]</sup>. A certain threshold concentration of the inhibitor always needs to be present at the steel surface to assure effective inhibition<sup>[21]</sup>. Most of the previous studies on the use of generic admixed inhibitors have used initial concentration of 1% wt. of cement<sup>[22-23]</sup>. So, in the present study, same concentration was adopted.

In the present study, two inhibitors on the basis of their functional groups (organic and inorganic) were selected to find their efficiency in Ordinary Portland Cement (OPC) concrete subjected to combined chloride and carbonated environment. The objective of this investigation was to compare the organic and inorganic CI in combined corrosive environment. The assessment of corrosion process was carried out via non-destructive testing, such as Half Cell Potential (HCP) and Linear Polarization Resistance (LPR) on specimens that were exposed to most aggressive environment. Carbonation and chloride profiles were also recorded to study the effectiveness of ACI.

## 2. EXPERIMENTAL PROCEDURE

### 2.1 Materials used in the study

In the present study, OPC conforming to IS: 8112- 1989 (BIS, 2013)<sup>[24]</sup> was used and physical properties are presented in Table 1. The coarse aggregate used was crushed gravel with nominal maximum size of 20 mm. Locally available river sand conforming to grading zone II as per IS: 383 (2002)<sup>[25]</sup> was used as fine aggregate. The properties of fine aggregates and coarse aggregates are shown in Table 2 and Table 3. The main focus of study is to evaluate the effect of the presence of type of functional group in reducing combined rate of corrosion. It was observed from the literature that inorganic compounds were more effective for chloride induced corrosion; while for carbonation induced corrosion, organic-based corrosion inhibitors worked more efficiently<sup>[26-30]</sup>. The presence of these compounds still needs to be tested in combined exposure

Table 1: Physical properties of OPC

PARAMETER	OBTAINED VALUES	STANDARD VALUES (As per IS 8112:1989)
Specific gravity	3.1	-
Standard consistency	26 %	30 %
Initial setting time	123 minutes	30 minutes (Minimum)
Final setting time	270 minutes	600 minutes (Maximum)
Fineness	255 m <sup>2</sup> /kg	225 m <sup>2</sup> /kg (Minimum)

Table 2: Physical properties of fine aggregates

PARAMETER	OBTAINED VALUES	PERMISSIBLE VALUES
Properties	Results obtained	Permissible Values
Grading Zone	Zone II	-
Specific gravity	2.64	2.65 to 2.67
Water absorption (%)	0.87	0.3-2.5%
Fineness modulus	3.02	2.2-3.2

Table 3: Physical properties of coarse aggregates

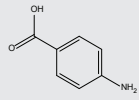
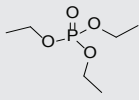
PROPERTIES	10 mm	20 mm	PERMISSIBLE VALUES
Specific gravity	2.84	2.82	2.5 to 3.0
Water absorption (%)	0.65	0.53	Shall not be >2%
Fineness modulus	6.24	6.95	3.3-8

environment. For this purpose, two CI on the basis of their functional group i.e., 4-Aminobenzoic acid (AB) consisting amine group (organic) and Triethylphosphate (TEP) consist phosphate (inorganic) were selected. The physical properties of AB and TEP CI are shown in Table 4. The nomenclature assigned to various control and inhibitor applied specimens are given in Table 5. For mix proportion, w/c ratio of 0.44 was used and quantity of ingredients used is shown in Table 6.

### 2.2 Specimen preparation

The effect of AB and TEP were studied on the four properties of resultant concrete viz. HCP, corrosion current density,

Table 4: Physical and Chemical properties of corrosion inhibitors

CHEMICAL NAME AND FORMULA	4-AMINO BENZOIC ACID (C <sub>7</sub> H <sub>7</sub> NO <sub>2</sub> )	TRIETHYLPHOSPHATE (C <sub>6</sub> H <sub>15</sub> O <sub>4</sub> P)
Molecular structure		
Molar Mass	137.14 g/mol	182.15 g/mol
Physical State	Powder	Liquid
Appearance	White-Grey	Colour less
Density	1.374 g/cc	1.072 g/cc
Melting Point	188 °C	-56.5 °C

**Table 5: Nomenclature assigned to concrete specimens**

CEMENT TYPE	ADMIXED CHEMICAL	NOMENCLATURE
OPC	-	OC
OPC	4-Aminobenzoic acid	OA
OPC	Triethylphosphate	OT

**Table 6: Mix Proportions**

MATERIAL	QUANTITY (kg/m <sup>3</sup> )
Cement	410
Fine Aggregates	572.4
Coarse Aggregate (20mm)	836.34
Coarse Aggregate (10mm)	360.4
Water	180

carbonation depth and chloride concentration. Former two properties, indicates their corrosion inhibition efficiency, while later two gives an indication of pore blocking effect. For measurement of first two properties, prism specimens of size 300 × 300 × 150 mm were used. Three Thermo Mechanically Treated (TMT) bars conforming to IS: 1786-1985<sup>[31]</sup> were embedded in the specimen and were prepared in accordance with the ASTM G109<sup>[32]</sup>. One rebar was embedded at the top with a clear cover of 15mm and other two were placed at bottom with clear cover of 25mm as shown in Figure 1. For other two properties, concrete cubes of size 100 mm were used. For uni-dimensional penetration of carbon dioxide and chloride ion; only one face of cube remained exposed while other faces were sealed by applying epoxy on the surfaces of cube. Corrosion inhibitors were added by 1% weight of cement as an admixture in concrete during casting of specimens. All the specimens were cast in triplicate in order to ensure precision.

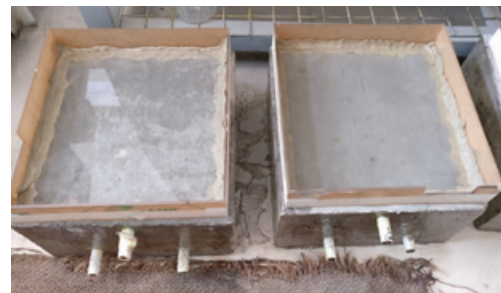
## 2.3 Exposure Condition

All the specimens were demoulded after 24 hr and water cured for 7 days at temperature of 27 ± 2°C and RH of 100%. Subsequently the specimens were kept in the laboratory environment for next 7 days with RH between 60-80%. Before subjected to combined environment, all the specimens were preconditioned in order to achieve even distribution of

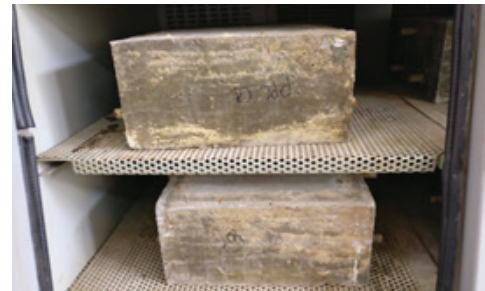
moisture. This was done by keeping the specimen in closed chamber at 30 ± 2°C and RH of 60-70% for 15 days. After preconditioning, specimens were subjected to total number of 8 exposure cycles. Each exposure cycle was consisting of 7-day chloride ponding (5% NaCl solution) followed by 2 day of air drying and 7-day carbonation exposure respectively. To ensure one dimensional penetration of chlorides, a plexiglass of size 280 × 280 × 70mm was installed on the top [as shown in Figure 2(a)]. The carbonation chamber which was programmed to a CO<sub>2</sub> concentration of 5%, temperature of 28 ± 5 °C, and 70 ± 5% RH [as shown in Figure 2(b)].

## 2.4 Electrochemical measurements

To monitor the corrosion rate in RC specimens, different non-destructive techniques have been utilised, such as Half Cell Potential (HCP) and Linear Polarization Resistance (LPR). HCP is one of the most utilised procedures which predicts the probability of corrosion and is governed by ASTM C876<sup>[33]</sup> standards. HCP measurements were performed with ACM field



(a) Specimen subjected to chloride ponding



(b) Specimen exposed to carbonated environment in environment chamber

Figure 2: Exposure of RC specimens

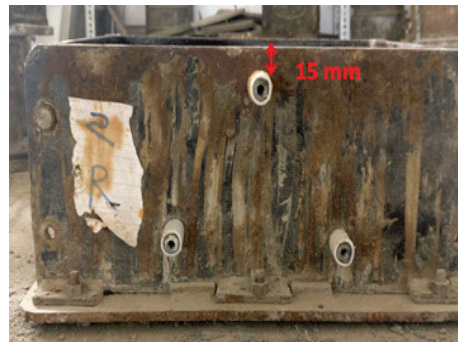
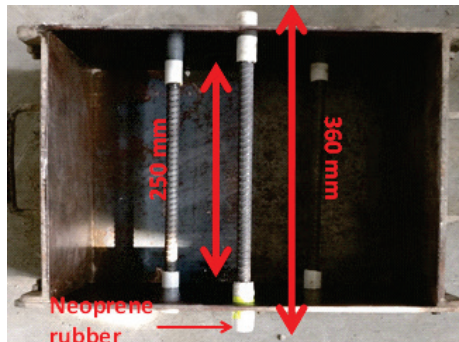


Figure 1: Specimen preparation for accelerated corrosion test



machine (serial 1463) using saturated calomel electrode as reference electrode. The measurements were taken parallel to the rebar at five points and the average value was considered as the final HCP value of the specimens. The LPR measurement was done using ACM field machine provided with guard ring for restraint current on prismatic specimens. Guard ring was placed over the concrete top face parallel to the rebar line as shown in Figure 3.

The LPR test (non destructive type) was performed on RC specimen by applying over potential of  $\pm 25\text{mV}$  at a sweep rate of  $0.167\text{mV/sec}$  in order to avoid the casting of multiple specimens. However, potentiodynamic scan (PDP) is preferred over LPR in order to obtain the passivating current density, especially in case of organic inhibitors. The HCP and LPR tests were performed after completion of each exposure cycle.

## 2.5 Free chloride Content

The chloride concentration in concrete was measured at the end of 4<sup>th</sup> and 8<sup>th</sup> exposure cycle. The steps involved for determining chloride concentration are shown in Figure 4. For finding out chloride concentration the powdered sample powder from cubes were obtained by drilling the cubes at 10 mm, 20 mm, 30 mm, 40 mm and 50 mm depth from the exposed surface. Samples from six different locations were collected from each concrete cube and kept in air tight packets. For the determination of free chloride content, 3 g of concrete powder was transferred to a 100-mL beaker and 50 mL of distilled water was added. The sample was heated gently and thoroughly mixed by a stirrer. The solution was then cooled and filtered using Whatman No. 1 filter paper and the free chloride content was then determined by titrating against  $0.1\text{M AgNO}_3$  solution [34-35]. The steps involved in determination of chloride concentration are shown in Figure 4.

## 2.6 Carbonation depth

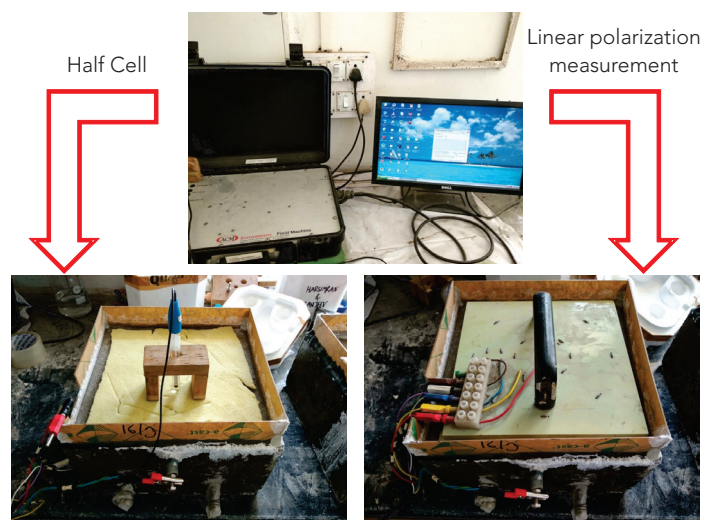


Figure 3: Test setup for electrochemical corrosion measurement

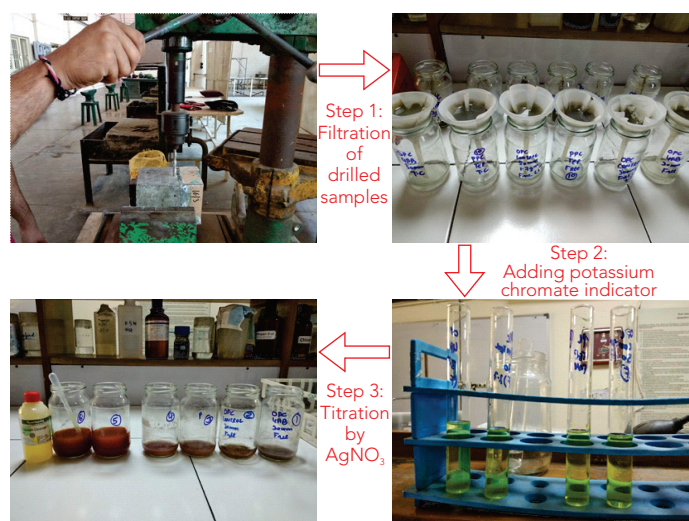


Figure 4: Chloride concentration determination by titration method

The carbonation depth in concrete was measured for each sample (i.e., control and inhibitor admixed) after 4<sup>th</sup> and 8<sup>th</sup> cycle. The depth of carbonation was determined by spraying phenolphthalein solution on freshly broken specimen. Given non-carbonated portion indicated by purple colour and carbonated zone is uncoloured. Depth of carbonated part was measured using vernier calliper of least count  $0.01\text{mm}$  from the exposed side of the cube by averaging 10 different points along the edge of broken surface. The procedure for measuring carbonation depth is shown in Figure 5.

## 3. RESULTS

### 3.1 Half-cell potential measurement

Figure 6 reveals the HCP values for OPC control as well as inhibitor admixed specimens exposed to combined aggressive environment. HCP values were measured after every exposure cycle.

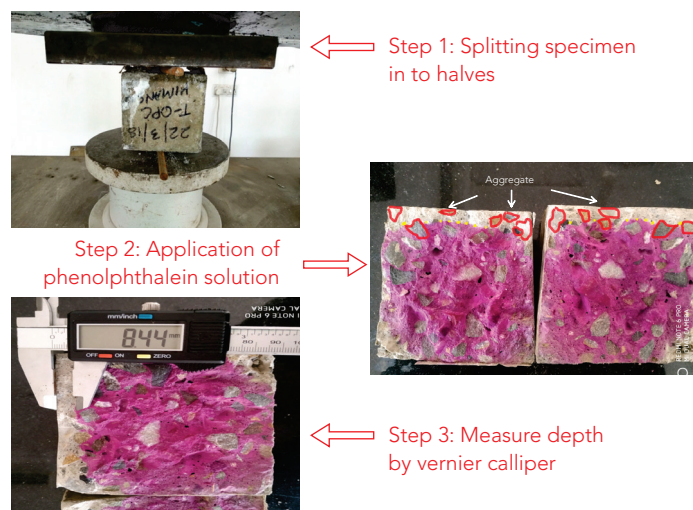


Figure 5: Carbonation depth measurement

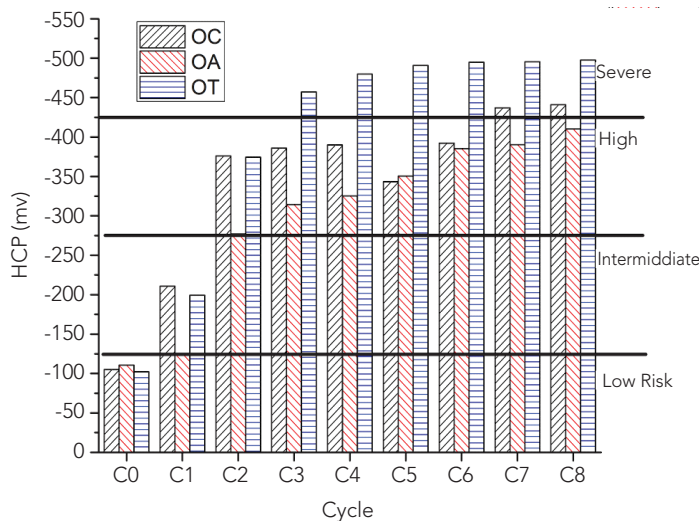


Figure 6: HCP measurements during the consequent exposure cycles

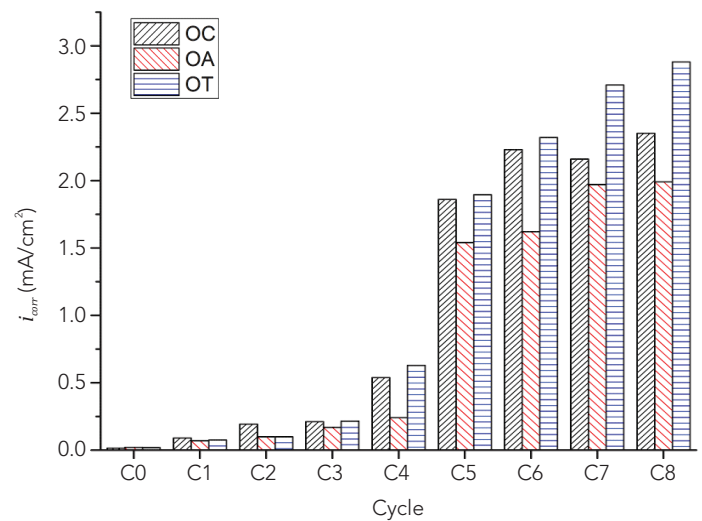


Figure 7: Corrosion current density measurements during the consequent exposure cycles

Before exposure cycle, control and admixed specimens were in passive state and the probability of corrosion was less than 10% that means lies on low-risk zone as shown in Figure 6. After 1<sup>st</sup> exposure cycle control and OT enter into intermediate zone but OA shows some resistance to potential increment. With increase in cycle, decrease in pH of concrete pore solution and simultaneous penetration of chloride ions cause destabilisation of passive layer of steel surface, which initiates the corrosion propagation stage. After 3<sup>rd</sup> exposure cycle, control as well as inhibitor admixed specimen showing higher risk of corrosion in OPC throughout the end of testing duration. In comparison to OC and OA, OT moves rapidly towards the severe corrosion region indicating higher rate of corrosion. It can be therefore stated that OT have higher probability of corrosion than OC and OA.

The HCP values clearly indicate that among the used ACI, TEP failed to retard corrosion and AB has some potential to fight against the combined exposure.

### 3.2 Linear Polarization Resistance

Figure 7 shows the corrosion current density of OPC specimen subjected to combined exposure.

In Figure 7, the behaviour over time is shown for the control as well inhibitor admixed specimen as that were exposed to combine environment. Figure shows that the corrosion intensity values increases with increase in the exposure duration. Initially, the specimens remained in negligible corrosion region as the rebars were in a passive state before the exposure. After the 2<sup>nd</sup> cycle of exposure, the  $i_{corr}$  for all the specimens enter into low corrosion zone. With the continuous exposure, the current density values shifted from moderate to high corrosion region after 5<sup>th</sup> exposure cycle. The specimens subjected to combined aggressive environment (carbonation after chloride ponding) may have led to the solubility of some carbonated species

resulting to the increase in the porosity of concrete. Due to increased porosity, there may have developed a pathway for the entry of free chlorides towards the steel bars and initiate corrosion. The value of  $i_{corr}$  for the OC specimen has been raised from 0.015 to 2.35  $\mu\text{A}/\text{cm}^2$ , while that for the specimen OA have the current density values lowered as compared to OC. At the 8<sup>th</sup> cycle, the value of the OC is 2.35  $\mu\text{A}/\text{cm}^2$  whereas that for the OA is 1.99  $\mu\text{A}/\text{cm}^2$ . This clearly indicates that the inhibitor has helped inhibit the corrosion process in the concrete. The current density values obtained for OT are higher than the un-inhibited specimens which indicate that this inhibitor has a detrimental effect on the concrete properties. Overall, it can be assessed that AB has helped inhibit the concrete specimens from corrosion.

### 3.3 Chloride concentration

Figure 8 and Figure 9 depict the chloride concentration of uninhibited and inhibitor admixed specimens after 4<sup>th</sup> and 8<sup>th</sup> cycle of exposure at different depths.

It can be seen that the free chloride content increases at each location with increasing number of cycles. The chloride concentration of control OC was higher than OA but at deeper depth (i.e. at 40 and 50 mm), the chloride concentration of OT specimen was higher than OC. After the 8<sup>th</sup> exposure cycle, the chloride concentration of OT surpasses the uninhibited specimen even at lowers depth, while chloride concentration of OA remains on lower side at all testing depth. This states that TEP failed to reduce the penetration of chloride and AB restricts the movement by blocking the concrete pores. These results are in accordance with the current density values, especially for TEP.

This illustrates that AB when used as an admixture blocks the pores of the concrete, abandoning the ingress of the chloride ions, which eventually helps in suppressing the corrosion process. TEP did not perform as a good inhibitor. It rather

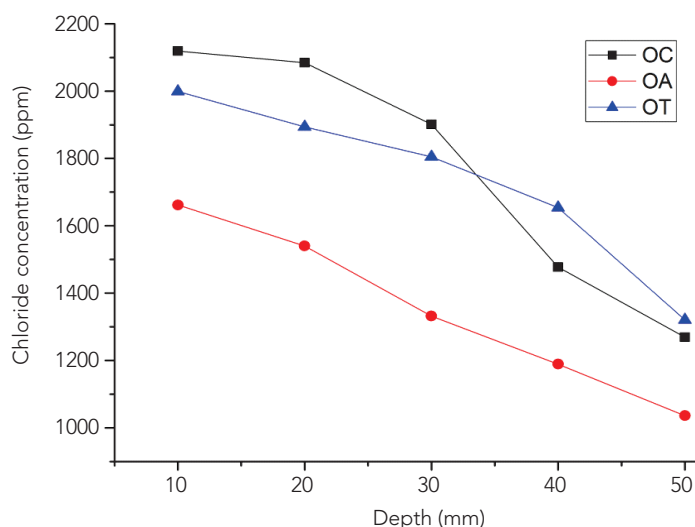


Figure 8: Chloride concentrations at various depths after 4<sup>th</sup> cycle

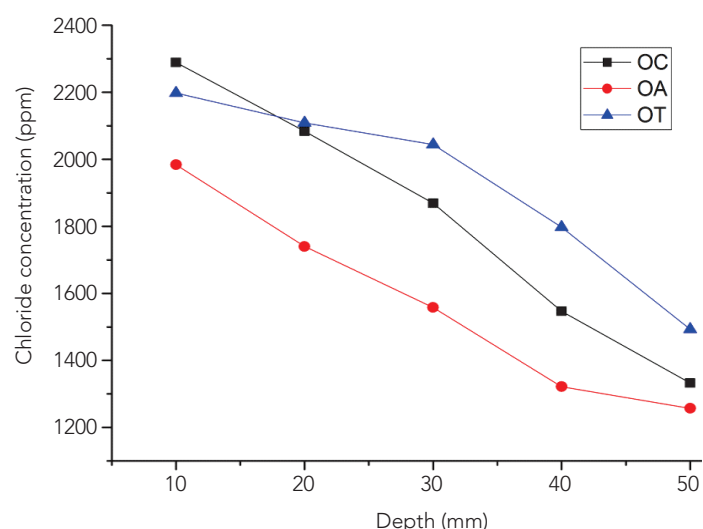


Figure 9: Chloride concentrations at various depths after 8<sup>th</sup> cycle

helped the chloride ions to penetrate because the values of chloride concentration in this case are higher than the uninhibited specimens.

Figure 10 portrays the carbonation depths in mm after the 4<sup>th</sup> and 8<sup>th</sup> cycle of concrete specimens inhibited with the initially specified corrosion inhibitors. At the 4<sup>th</sup> cycle, the values of the carbonation depths were 3.27mm, 3.19mm and 3.39mm for the control, AB and TEP respectively, while after the 8<sup>th</sup> cycle, the values were 6.67mm, 5.02mm and 6.48mm for the control, AB and TEP respectively. These results are in agreement with the chloride profiles depicting that AB acts as a pore blocker and TEP is unable to perform.

## 4. DISCUSSION

The results of the HCP, LPR, chloride and carbonation inspection are correlated, and this gives good confidence on the results. Organic inhibitors perform well in both chloride and carbonated

environment. Benzotriazole and its derivatives are the organic inhibitors, when admixed as an inhibitor performed well in chlorides exposure condition<sup>[36-38]</sup> monitored some compounds up to 400 days in carbonated environment, but only two (the sodium salts of benzoic acid and, particularly, 2-amino benzoic acid) exhibited some inhibitive effect towards the rebar

Performance of AB as an inhibitor can be due to fact that it contains multi-functional organic group whereas, TEP is single functional group inhibitor. Multi-functional organic inhibitors are considered as most effective inhibitors compared to single functional group inhibitor<sup>[39]</sup>. ABA contains amines and fatty acid esters which results into two-fold mechanism. First, they block chloride ions due to chemical structure. Then they form coating on rebar surface as esters reacts in alkali medium and forms alcohols and carboxylic ions which then reacts with calcium ions. Also, fatty acid lined and chained up the non-polar groups on rebars to form mechanical barrier for destructive elements for corrosion like moisture, chloride ions and oxygen. Another reason of TEP not performed as AB, due to chelating effect. Multi-functional groups as an inhibitor forms stable compound which is soluble in water by reacting with metal ions and known as chelating agents. The inefficiency of TEP is might be due to under dosage present in concrete.

## 5. CONCLUSION

The major conclusions drawn from the experimental work are as under:

1. HCP values indicate that AB was able to inhibit the corrosion process when used as an admixture, while TEP fails to perform in combined environment.
2. Similar with HCP, reduction in corrosion current density was observed with OA. On the other side, TEP was not able to reduce the corrosion rate that remained on higher side throughout the exposure duration. Thus, in a combined

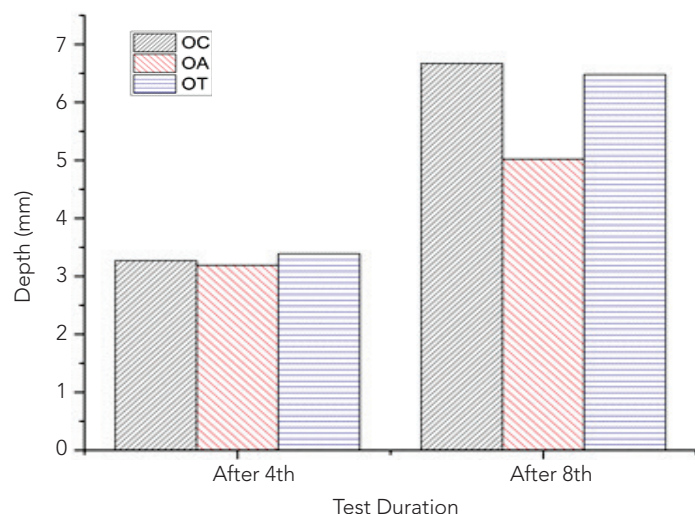


Figure 10: Carbonation Depth after 4<sup>th</sup> and 8<sup>th</sup> exposure cycle



chloride and carbonated exposure, organic inhibitor reduces the corrosion rate, while inorganic inhibitor fails to do so.

3. Chloride and carbonation profile suggest that, AB acts as a pore blocker whereas TEP fails to resist the movement of aggressive ions which leading to corrosion of embedded steel rebar.

## 6. FUTURE SCOPE

The ability of an RC structure to withstand aggressive environmental actions, while at same time able to maintain its performance well above a minimum acceptable level is defined as 'durability'. Effective service life of an RC structure is defined as the time period for which the structure, or a structural element, can be used for its indented purpose without the need for maintenance. Deterioration of concrete structures concludes that 50% of all cases of deterioration considered were caused by corrosion of reinforcement, from chloride penetration or carbonation<sup>[40]</sup>, emphasis should be paid on utilizing service-life estimation tools (SLT) on such types of deterioration processes as they can be vital aids. After all, the prospect that a structure is durable can only be accessed through tools simulating the deterioration processes to which the structure is likely to be subjected.

Service Life Modelling (SLM) is intended to allow quantification of the design service life of structures, for purposes of economic optimisation, operational efficiency, and sustained structural and aesthetic performance. One of the principal challenges in developing a mathematical model for service life prediction is that many parameters, including material characteristics, climatic environment, and construction method, will all affect service life. The service life of a reinforced concrete structure can be divided into two stages, the initiation period and the propagation period. In service life estimation, it is common to conservatively assume the service life end when corrosion initiates.

So far, various models have been proposed, such as empirical models, statistical models, numerical models and simulation models. Most models cover either service life prediction of structure subjected to chloride induced corrosion<sup>[41-45]</sup> or carbonation induced corrosion<sup>[46-47]</sup>. But these models cannot be valid for combined (chloride and carbonation ingress) environment due to various uncertainty in data.

The above study concludes that organic inhibitors able to restrict the chloride and carbon-dioxide penetration in combined environmental exposure. This can be related with the increase in corrosion initiation period and increment in service life of reinforced structure subjected to real environmental exposure of RC structure. In order to contribute with the service life prediction of the structures when inserted in combined saline and CO<sub>2</sub> environments with admixed inhibitor, a mathematical model need to be developed.

## 7. ACKNOWLEDGEMENT

The authors gratefully acknowledge the financial support provided by the Atomic Energy Regulatory Board under Committee for Safety Research Programmes (Sanction No. AERB/CSRP/73/02/19). The authors also acknowledge Dr. Vijay Luxami (Associate professor, School of Chemistry and Biochemistry, TIET) for providing the helpful suggestion for this research.

## REFERENCES

- [1] Tumidajski, P. J., & Chan, G. W. (1996). "Effect of sulfate and carbon dioxide on chloride diffusivity", *Cement and Concrete Research*, Vol. 26, No. 4, pp. 551-556.
- [2] Lee, M. K., Jung, S. H., & Oh, B. H. (2014). "Effects of carbonation on chloride penetration in concrete". *ACI Materials Journal*, V. 110, No. 5, pp. 559-566.
- [3] Ye, H., Jin, X., Fu, C., Jin, N., Xu, Y., & Huang, T. (2016). "Chloride penetration in concrete exposed to cyclic drying-wetting and carbonation". *Construction and Building Materials*, Vol. 112, pp. 457-463.
- [4] Al-Otaibi, M. S., Al-Mayouf, A. M., Khan, M., Mousa, A. A., Al-Mazroa, S. A., & Alkhathlan, H. Z. (2014). "Corrosion inhibitory action of some plant extracts on the corrosion of mild steel in acidic media". *Arabian Journal of Chemistry*, Vol. 7, No. 3, pp. 340-346.
- [5] Obot, I. B., Obi-Egbedi, N. O., & Umoren, S. A. (2009). Antifungal drugs as corrosion inhibitors for aluminium in 0.1 M HCl. *Corrosion Science*, Vol. 51, No. 8, pp. 1868-1875.
- [6] Królikowski, A., & Kuziak, J. (2011). "Impedance study on calcium nitrite as a penetrating corrosion inhibitor for steel in concrete". *Electrochimica Acta*, Vol. 56, No. 23, pp. 7845-7853.
- [7] Popov, B. N. (2015). "Corrosion engineering: principles and solved problems". Elsevier.
- [8] Raja, P. B., Ismail, M., Ghoreishiamiri, S., Mirza, J., Ismail, M. C., Kakooei, S., & Rahim, A. A. (2016). "Reviews on corrosion inhibitors: a short view". *Chemical Engineering Communications*, Vol. 203, No. 9, pp. 1145-1156.
- [9] Ormellese, M., Lazzari, L., Goidanich, S., Fumagalli, G., & Brenna, A. (2009). "A study of organic substances as inhibitors for chloride-induced corrosion in concrete". *Corrosion Science*, Vol. 51, No. 12, pp. 2959-2968.
- [10] Malik, A. U., Andijani, I., Al-Moaili, F., & Ozair, G. (2004). "Studies on the performance of migratory corrosion inhibitors in protection of rebar concrete in Gulf seawater environment". *Cement and concrete composites*, Vol. 26, No. 3, pp. 235-242.
- [11] Fedrizzi, L., Azzolini, F., & Bonora, P. L. (2005). "The use of migrating corrosion inhibitors to repair motorways' concrete structures contaminated by chlorides". *Cement and Concrete Research*, Vol. 35, No. 3, pp. 551-561.
- [12] Jamil, H. E., Shri, A., Boulif, R., Bastos, C., Montemor, M. F., & Ferreira, M. G. S. (2004). "Electrochemical behaviour of

- amino alcohol-based inhibitors used to control corrosion of reinforcing steel". *Electrochimica acta*, Vol. 49, No. 17-18, pp. 2753-2760.
- [13] Holloway, L., Nairn, K., & Forsyth, M. (2004). "Concentration monitoring and performance of a migratory corrosion inhibitor in steel-reinforced concrete". *Cement and concrete research*, Vol.34, No. 8, pp. 1435-1440.
- [14] Rakanta, E., Zafeiropoulou, T., &Batis, G. (2013). "Corrosion protection of steel with DMEA-based organic inhibitor". *Construction and Building Materials*, Vol. 44, pp. 507-513.
- [15] Gaidis, J. M. (2004). "Chemistry of corrosion inhibitors. *Cement and Concrete Composites*", Vol. 26, No. 3, pp. 181-189.
- [16] Ormellesse, M., Bolzoni, F., Perez, E. R., &Goidanich, S. (2007). "Migrating Corrosion Inhibitors for Reinforced Concrete Structures". In *Int. Conf. Corrosion/07, NACE*, pp. 1-16.
- [17] Vyrides, E. Rakanta, T. Zafeiropoulou and G. Batis. (2013) "Efficiency of Amino Alcohols as Corrosion Inhibitors in Reinforced Concrete". *Open Journal of Civil Engineering*, Vol. 3, No. 2A, pp. 1-8.
- [18] Gaidis M. J. (2004). "Chemistry of corrosion inhibitors". *Cement and Concrete Composites*. Vol. 26, No. 3, pp. 181-189.
- [19] Yohai, L., Valcarce, M. B., &Vázquez, M. (2016). "Testing phosphate ions as corrosion inhibitors for construction steel in mortars". *ElectrochimicaActa*, Vol. 202, pp. 316-324.
- [20] Söylev, T. A., & Richardson, M. G. (2008). "Corrosion inhibitors for steel in concrete: State-of-the-art report". *Construction and Building Materials*, Vol. 22, No. 4, pp. 609-622.
- [21] Söylev, T.A., McNally, C., &Richardson, M. (2007). "Effectiveness of amino alcohol-based surface-applied corrosion inhibitors in chloride-contaminated concrete". *Cement and concrete research*, Vol. 37, No. 6, pp. 972-977.
- [22] Saraswathy, V., Muralidharan, S., Kalyanasundaram, R. M., Thangavel, K., &Srinivasan, S. (2001). "Evaluation of a composite corrosion-inhibiting admixture and its performance in concrete under macrocell corrosion conditions". *Cement and Concrete Research*, Vol. 31, No. 5, pp. 789-794.
- [23] Trabanelli, G., Monticelli, C., Grassi, V., &Frignani, A. (2005). "Electrochemical study on inhibitors of rebar corrosion in carbonated concrete". *Cement and Concrete Research*, Vol. 35, No. 9, pp. 1804-1813.
- [24] IS 8112- 1989. (Reconfirmed 2013). "Specification for 43 Grade Ordinary Portland Cement." Bureau of Indian Standards, New Delhi, India.
- [25] IS 383-1970. (Reconfirmed 2002) "Specification for Coarse and Fine Aggregates from Natural sources for concrete". Bureau of Indian Standards, New Delhi, India.
- [26] Heiyantuduwa, R., Alexander, M. G., &Mackechnie, J. R. (2006). "Performance of a penetrating corrosion inhibitor in concrete affected by carbonation-induced corrosion". *Journal of materials in civil engineering*, Vol. 18, No. 6, pp. 842-850.
- [27] Monticelli, C., Frignani, A., Balbo, A., &Zucchi, F. (2011). "Influence of two specific inhibitors on steel corrosion in a synthetic solution simulating a carbonated concrete with chlorides". *Materials and Corrosion*, Vol. 62, No. 2, pp. 178-186.
- [28] Nmai, C. K. (2004). "Multi-functional organic corrosion inhibitor". *Cement and Concrete Composites*, Vol. 26, No. 3, pp. 199-207.
- [29] Montemor, M. F., Cunha, M. P., Ferreira, M. G., & Simões, A. M. (2002). "Corrosion behaviour of rebars in fly ash mortar exposed to carbon dioxide and chlorides". *Cement and Concrete Composites*, Vol. 24, No. 1, pp. 45-53.
- [30] Jamil, H. E., Shrir, A., Boulif, R., Bastos, C., Montemor, M. F., & Ferreira, M. G. S. (2004). "Electrochemical behaviour of amino alcohol-based inhibitors used to control corrosion of reinforcing steel". *Electrochimica acta*, Vol. 49, No.17-18, pp. 2753-2760.
- [31] IS 1786- 1985. (Reconfirmed 2004). "Indian Standard Specification for High Strength Deformed Steel Bars and Wires for Concrete Reinforcement." Bureau of Indian Standards, New Delhi, India.
- [32] ASTM G 109 -99a. (Reapproved 2005). "Standard test method for determining the effects of chemical admixtures on the corrosion of embedded steel reinforcement in concrete exposed to chloride environments." *American Society of Testing and Materials*, Philadelphia.
- [33] ASTM C 876-91. (Reapproved 1999). "Standard Test Method for Half-cell Potentials of Uncoated Reinforcing Steel in Concrete." *American Society of Testing and Materials*, Philadelphia.
- [34] Kapat, C., Pradhan, B., &Bhattacharjee, B. (2006). "Potentiostatic study of reinforcing steel in chloride contaminated concrete powder solution extracts". *Corrosion science*, Vol. 48,No. 7, pp. 1757-1769.
- [35] Pradhan, B., & Bhattacharjee, B. (2009). Half-cell potential as an indicator of chloride-induced rebar corrosion initiation in RC. *Journal of Materials in Civil Engineering*, Vol. 21,No. 10, pp. 543-552.
- [36] Sheban, M., Abu-Dalo, M., Ababneh, A. and Andreescu, S., (2007). "Effect of benzotriazole derivatives on the corrosion of steel in simulated concrete pore solutions". *Anti-Corrosion Methods and Materials*, Vol. 54, No. 3, pp.135-147.
- [37] Ababneh, Ayman N., Mashal A. Sheban, and Muna A. Abu-Dalo. (2012). "Effectiveness of Benzotriazole as Corrosion Protection Material for Steel Reinforcement in Concrete." *Journal of Materials in Civil Engineering*, Vol. 24, No. 2, pp. 141-51.
- [38] Trabanelli, G., C. Monticelli, V. Grassi, and A. Frignani. (2005). "Electrochemical Study on Inhibitors of Rebar Corrosion in Carbonated Concrete." *Cement and Concrete Research*, Vol. 35, No. 9, pp. 1804-13.
- [39] Nmai, Charles K. (2004). "Multi-Functional Organic Corrosion Inhibitor." *Cement and Concrete Composites*, Vol. 26, No. 3, pp. 199-207.

- [40] Di Prisco, M., Colombo, M., & Dozio, D. (2013). "Fibre-reinforced concrete in fib Model Code 2010: principles, models and test validation". *Structural Concrete*, Vol. 14, No. 4, pp. 342-361.
- [41] Liang, M.T., Wang, K.L., Liang, C.H. (1999), "Service life prediction of reinforced concrete structures", *Cem. Concr. Res.* Vol. 29, pp 1411-1418.
- [42] Andrade, J. J. O., Possan, E., & Dal Molin, D. C. C. (2017). "Considerations about the service life prediction of reinforced concrete structures inserted in chloride environments". *Journal of Building Pathology and Rehabilitation*, Vol. 2, No. 1, pp 1-8.
- [43] Kamde, D. K., & Pillai, R. G. (2021). "Corrosion initiation mechanisms and service life estimation of concrete systems with fusion-bonded-epoxy (FBE) coated steel exposed to chlorides". *Construction and Building Materials*, Vol. 277, 122314.
- [44] Pillai, R. G., Gettu, R., Santhanam, M., Rengaraju, S., Dhandapani, Y., Rathnarajan, S., & Basavaraj, A. S. (2019). "Service life and life cycle assessment of reinforced concrete systems with limestone calcined clay cement (LC3)". *Cement and Concrete Research*, Vol. 118, pp 111-119.
- [45] Belgacem, M.E., Neves, R., Talah A. (2020). "Service life design for carbonation-induced corrosion based on air-permeability requirements", *Construction and Building Materials*. Vol. 261.
- [46] Liu, Peng, Zhiwu Yu, and Ying Chen. (2020). "Carbonation Depth Model and Carbonated Acceleration Rate of Concrete under Different Environment." *Cement and Concrete Composites* Vol. 114 (June): 103736.
- [47] Cho, H. C., Ju, H., Oh, J. Y., Lee, K. J., Hahm, K. W., & Kim, K. S. (2016). "Estimation of concrete carbonation depth considering multiple influencing factors on the deterioration of durability for reinforced concrete structures". *Advances in Materials Science and Engineering*, Vol. 2016.



**HIMANSHU GULERIA** holds M.Tech degree in Structural Engineering from Thapar Institute of Engineering and Technology, Patiala. His area of interest includes corrosion evaluation and protection of RC structure against corrosion. Email: himanshuguleria13@gmail.com



**PURNIMA** holds a B.Tech degree in Civil Engineering from Punjabi University, Patiala and M.Tech Degree in Structural Engineering from Thapar Institute of Engineering and Technology, Patiala. Currently, she is Ph.D. student in the civil engineering department at Thapar Institute of Engineering and Technology, Patiala, India. Her research interest includes corrosion evaluation, study of generic compounds as repair strategy in reinforced concrete structure. Email: dograpurnima07@gmail.com



**ASHISH KUMAR TIWARI** is Ph.D. student in the civil engineering department at Thapar Institute of Engineering and Technology, Patiala, India. He holds a B.Tech Degree in Civil Engineering from Kurukshetra University, Kurukshetra and M.Tech degree in Structural Engineering from Jaypee University, Solan. His research interest includes corrosion evaluation and protection in RC structures, study of functional groups as corrosion inhibitors. Email: tiwariashish841@gmail.com



**SHWETA GOYAL** is working as Associate Professor in the Department of Civil Engineering, Thapar Institute of Engineering and Technology, Patiala, Punjab. Her areas of research include development of microbial concrete, corrosion evaluation and protection in RC structures, development of accelerated carbonation procedure for precast concrete and research oriented towards sustainability of concrete. She has more than 50 publications to her credit out of which 30 are SCI indexed. She has undertaken research projects worth three crores funded by various government agencies. Email: shweta@thapar.edu

**Cite this article:** Guleria, H., Purnima, Tiwari, A. K., and Goyal, S., (2021). "performance of organic and inorganic functional groups as corrosion inhibitors in concrete experiencing extreme corrosive environment", *The Indian Concrete Journal*, Vol. 95, No. 4, pp. 29-37.



# CORROSION INHIBITING ADMIXTURE FOR CORROSION PREVENTION IN SMALL SCALE REINFORCED CONCRETE STRUCTURES

S. SHAFEER AHAMED,  
J. SHERIN MARIYA,  
V. ROOPA,  
M.S. HAJI SHEIK MOHAMMED\*

## Abstract

This study analyses the influence of commercially available mixed inhibitor [sodium nitrite based water reducing and corrosion inhibiting admixture (WSNI)] and bipolar inhibitor [dual mechanism corrosion inhibiting admixture (BPI)] on the strength and durability performance of Portland Pozzolana Cement (PPC) and Portland Slag Cement (PSC) mortar. The strength (compressive, split tensile, flexural, and shear) and durability (water absorption, water sorptivity, chloride ion penetration and accelerated corrosion) tests were conducted on Portland Pozzolana Cement Mortar (PCM) and Portland Slag Cement Mortar (SLCM) with and without inhibitor as per the relevant standards. The mortar mix of 1:3 with workability 75 - 90% in flow test with inhibitor admixing at 1, 2 and 5% by weight of cement were adopted in all the tests. It is found to be that inhibitor incorporation did not influence the fresh mortar properties but had resulted in appreciable reduction of the water cement ratio. The addition of WSNI and BPI significantly increases the compressive strength at early ages but marginal improvement at 28 day. There is a significant improvement in flexural and shear strength (up to 30%) for inhibitor admixed mortar in certain dosages. Appreciable reduction in water absorption and chloride ion penetration; and improved tolerable limit for chlorides were also noticed for inhibitor admixed PCM and SLCM specimens. The addition of mixed inhibitor and bipolar inhibitor at 2% is recommended for use in small sector construction projects for enhanced corrosion prevention in Reinforced Concrete (RC) structures.

**Keywords:** Accelerated corrosion, Bipolar inhibitor, Durability, Mixed inhibitor, Tolerable limit for chlorides.

## I. INTRODUCTION

Premature corrosion related distress in reinforced concrete (RC) structures and subsequent rehabilitation causes huge expenditure to the exchequer. In addition, this indirectly causes depletion of the natural resources such as water, sand and

limestone at inappropriate level (in terms of consumption of these materials for reconstruction / rehabilitation works) and also leads to emission of green gases ( $\text{CO}_2$ )<sup>[1]</sup>. This scenario is very much avoidable by implementation of appropriate corrosion prevention strategies; adopting good construction practices; quality construction materials; skilled manpower, etc., during construction. Out of many causes, negligence to the adoption of technologies / systems for corrosion prevention in steel reinforcement bars surmounts a vital reason for premature distress in RC structures.

The major causes of corrosion in RC structures are chloride ingress and carbonation. The source of chlorides may be from concrete ingredient materials (cement, supplementary cementitious materials (SCM), fine aggregate, coarse aggregate, water, and chemical admixtures), ground water, coastal environment etc. The carbonation is mainly caused by the increasing levels of  $\text{CO}_2$  emission in the atmosphere<sup>[1]</sup>. Incorporation of corrosion inhibitor in concrete is one of the effective method of corrosion prevention in RC structures in lieu of concrete coating, anticorrosive coating to steel bars, sacrificial anode cathodic protection etc.<sup>[2,3]</sup> The commercially available corrosion inhibitors for corrosion prevention in RC structures include anodic, cathodic, mixed, bipolar and vapour phase inhibitors<sup>[4,5]</sup>.

The corrosion inhibitors reduces the corrosion rate by controlling the anodic and / or cathodic reaction on the steel rebar surface. The anodic and cathodic inhibitors reduce the respective electrochemical reactions. Mixed inhibitors control both anodic and cathodic reaction. Bipolar inhibitors enhance the microstructure of the concrete by acting as pore blockers in addition to controlling the electrochemical reactions<sup>[5]</sup>. Whereas vapour phase inhibitors works on diffusion mechanism and controls the electrochemical reactions on the rebar surface. The addition of corrosion inhibitors in newly manufactured concrete pose no additional labour cost except strict supervision at site to enforce usage of adequate dosage considering the environmental conditions. Calcium nitrite is the commonly used

anodic inhibitor and extensive study has been carried out by many researchers to prove its efficacy in terms of strength and durability enhancement to RC [6,7]. Scant research studies were only carried out in sodium nitrite based inhibitors for use in inland and offshore conditions [8-10].

In recent years, bipolar and vapour phase inhibitors are gaining momentum for prevention / protection of steel reinforcement bars from corrosion [11]. It has also been reported that the inhibitor admixed concrete performs better in cementitious systems with a lower water cement ratio (0.4 instead of 0.5) [12]. Whereas in small scale construction projects, higher water cement ratio (0.50 and above) is generally adopted to maintain the desired workability of concrete. So there is need for a corrosion inhibitor which offers inhibition against corrosion and at the same time reduces the water-cement ratio without compromising workability. Nowadays Portland Pozzolana Cement (PPC) is extensively used in construction. Portland Slag Cement (PSC) is recommended in the recent times because of its sustainability aspects (in terms of waste management and reduction in CO<sub>2</sub> emission) and beneficial effects on strength and durability of concrete [13, 14].

This study analyses the influence of commercially available mixed inhibitor [sodium nitrite based water reducing and corrosion inhibiting admixture (WSNI)] and bipolar inhibitor [dual mechanism corrosion inhibiting admixture (BPI)] on strength and durability performance of Portland Pozzolana Cement Mortar (PCM) and Portland Slag Cement Mortar (SLCM).

**Table 1: Physical properties of mortar ingredient materials and corrosion inhibitors**

CEMENT		
PROPERTY	PPC <sup>[15]</sup>	PSC <sup>[16]</sup>
Blaine Fineness (m²/kg)*	340-360	360-370
Specific gravity <sup>[19]</sup>	2.69	2.80
Fine Aggregate (Standard Sand) <sup>[17]</sup>		
Specific gravity <sup>[20]</sup>	2.71	
Water absorption (%) <sup>[20]</sup>	0.80	
Bulk density (kN/m³) <sup>[20]</sup>	17.60	
Fineness Modulus <sup>[21]</sup>	2.87	
Grading zone <sup>[22]</sup>	Zone – III	
Corrosion Inhibiting Admixture		
	BPI	WSNI
pH	11.58	12.65
Specific Gravity <sup>[23]</sup>	1.182	1.105
Colour	Pale white	Dark Brown

\*Manufacturer's data

## 2. MATERIALS AND MORTAR MIX

The two types of cement employed in the study are PPC with 25 - 30% fly ash [15] and PSC with 45 - 50% slag [16]. The standard sand conforming to BIS 650:1991 [17] (fine aggregate) and potable water were used for the preparation of mortar mix in the ratio 1:3. The fine aggregate was prepared by mixing equal quantities of standard sand Grade I, II and III by weight. Commercially available branded Fe550 grade TMT rebar was used in the accelerated corrosion test. The WSNI and BPI was introduced at 1, 2 and 5% by weight of cement [8,9,18]. Water cement ratio of various mixes was arrived using trial and error method for a target workability of 75 - 90% in the mini flow test. Totally fourteen different combinations of mortar mixes were prepared and tested by varying the type of cement, inhibitor and dosage. The physical properties of mortar ingredient materials and corrosion inhibitors used in the study are given in Table 1.

Table 2 gives the initial and final setting time of PPC and PSC cement with the addition of different dosages of inhibitors. The final setting time of BPI admixed PPC and PSC at 5% dosage level is 350 min and 420 min respectively. Irrespective of the type of cement, the addition of BPI at the higher dosages delays the final setting time and consumes 1.75 times more duration. The final setting of PSC and PPC cement decreases with the increase in dosage of WSNI from 2% to 5%. Irrespective of the type of inhibitor added, the final setting time of PSC is increased except at 5% WSNI. This may be due to the reduced heat of hydration at early ages [13]. It can be concluded that the observed initial and final setting time values are in line with the respective codal

**Table 2: Initial and Final Setting time of Cement**

TYPE OF CEMENT	TYPE OF CORROSION INHIBITOR & DOSAGE	INITIAL SETTING TIME [24] (Min)	FINAL SETTING TIME [24] (Min)
PPC	WSNI	0%	150
		1%	195
		2%	118
		5%	210
	BPI	1%	120
		2%	270
		5%	150
		5%	225
PSC	WSNI	0%	144
		1%	240
		2%	140
		5%	260
	BPI	1%	140
		2%	300
		5%	80
		5%	195
	BPI	1%	154
		2%	234
		2%	160
		5%	250
		5%	210
			420

**Table 3: Details of w/c ratio and workability of mortar mix**

TYPE OF MIX	WORKABILITY [% FLOW]	W/C RATIO	SPECIMEN DESIGNATION
PCM	82	0.55	PCON
PCM+1% WSNI	87	0.50	PS1
PCM+2% WSNI	79	0.45	PS2
PCM+5% WSNI	86	0.40	PS5
PCM+1% BPI	80	0.50	PB1
PCM+2% BPI	89	0.45	PB2
PCM+5% BPI	85	0.45	PB5
SLCM	80	0.50	SCON
SLCM+1% WSNI	81	0.50	SS1
SLCM+2% WSNI	89	0.47	SS2
SLCM+5% WSNI	82	0.45	SS5
SLCM+1% BPI	87	0.40	SB1
SLCM+2% BPI	76	0.40	SB2
SLCM+5% BPI	81	0.40	SB5

provisions<sup>[15, 16]</sup>, irrespective of varying the inhibitor dosage from 1 - 5%.

Table 3 gives the water cement ratio and workability of mortar mixes used in the study for the desired workability. The addition of WSNI at 1 - 5% reduced the water cement ratio up to 0.10 and 0.05 for both PCM and SLCM mixes respectively and exhibited the water reducing property of the WSNI<sup>[8]</sup>. In case of BPI, gradual reduction in water cement ratio was observed upon increasing the dosage for PCM upto 0.10. Whereas, the SLCM exhibited a reduction in water cement ratio of 0.10 regardless

of the dosage. It can be inferred that addition of corrosion inhibiting admixture at higher dosages (i.e., 2 - 5%) appreciably reduced the water cement ratio irrespective of type for the desired workability of 75 - 90% in the mini flow test.

It can be concluded that WSNI exhibits reduced water cement ratio for the target workability (for mortar) irrespective of type of cement and inhibitor dosage employed in the study. This may be due to the presence of water reducing agent in the WSNI. Whereas BPI also offered reduced water cement ratio (for mortar) in all the tested dosages which need further study to understand the mechanism. Holistically, irrespective of the type of inhibitor and dosage levels, the observed setting time values are well within time limit proposed by the respective codes<sup>[15, 16]</sup>.

### 3. EXPERIMENTAL INVESTIGATION

The experimental investigation analyses the strength and durability properties of WSNI and BPI admixed PPC and PSC mortar. The strength parameters studied include compressive, tensile, flexure and shear strength. The cube specimens of 70.6 mm were cast and subjected to compressive strength test<sup>[25]</sup> using 500kN compression testing machine (CTM) at the age of 7, 14, and 28 days. In case of SLCM specimens, 56 day compressive strength was also studied considering the reduced rate of hydration<sup>[13]</sup>. Cylinder specimens of 150 mm diameter and 300 mm height were subjected to split tensile strength<sup>[26]</sup> using 150 ton capacity CTM at the age of 28 day. The flexural strength test<sup>[27]</sup> was carried out using a 2 ton capacity Universal Testing Machine (UTM) on mortar specimens of size 160 × 40 × 40 mm.

Figure 1 depicts the flexural strength test set-up. The undamaged prism specimens obtained after the flexural strength test were used to find the shear strength. The specimen of size 60 × 40 × 40 mm was placed over the 'C' type arrangement (40 × 40 × 40 mm) as shown in figure 2 and



Figure 1: Flexural strength test in progress



Figure 2: Shear strength test in progress



subjected to the shear test in a 2 ton UTM. The load was applied gradually without creating shock until failure of the specimen. The shear strength was calculated using the formula:

$$\text{Shear stress} = \frac{P}{2ab} \text{ (N/mm}^2\text{)}$$

Where,

- $P$  – Maximum load in N
- $a$  – Breadth of the specimen in mm
- $b$  – Depth of the specimen in mm

The durability parameters studied include water absorption, water sorptivity, chloride penetration and resistance to accelerated corrosion. Water absorption test was carried out on 100 mm mortar cubes at 28 day age as per procedure outlined in ASTM C 642-06<sup>[28]</sup>. Water sorptivity test<sup>[29]</sup> was conducted on disc type mortar specimens of size 100 mm dia. and 50 mm thickness at the age of 28 days<sup>[29,30]</sup>. Figure 3 shows the specimens under sorptivity test. Chloride ion penetration test<sup>[31,8]</sup> was performed on cube specimens of size 70 mm and cured for 28 days. After curing period, polymer based waterproof coating was applied on all the four sides of specimen except top and bottom surface. The specimens were then immersed in 3% sodium chloride (NaCl) solution for 20 days and split open into two vertical halves. The indicator solution comprising of 0.1 N silver nitrate and 0.1% sodium fluorescein was sprayed along the broken cross sectional area. The area intruded by the chlorides turned to white colour. However, the unaffected area maintained the original colour as depicted in figure 4. The depth of chloride penetration was measured radially at 8 locations along the periphery and the average value is considered<sup>[8]</sup>.

To find the resistance against accelerated chloride penetration of WSNi and BPI admixed mortar, Accelerated Corrosion Test (ACT) was conducted on lollipop specimens as outlined in Dyana et al.<sup>[32]</sup>. The size of the specimen was 50 mm diameter and 110 mm height mortar cylinder with a conical end on one side

as shown in figure 5. The working electrode was 8 mm diameter TMT rebar of exposed length 90 mm, which was made rust-free using sonication process followed by air drying and introduction of electrical connection (by drilling & threading at the top end) using 3 mm diameter stainless steel rod. The intersection of working electrode and stainless rod was capped with heat-shrink tube to avoid pitting corrosion. The nichrome mesh was used as the counter electrode and 3% NaCl solution as electrolyte. The specimen was kept inside the non-conducting transparent acrylic container (as shown in figure 5) and impressed with 2V potential for the first 24 hours, then increased to 4V until failure of specimens.

The current development during the test period was monitored using a high impedance multimeter. The time for initiation of first crack which indicates the failure of specimens and the corresponding maximum current values were also observed and reported. Time factor is the ratio between time to cracking for control and inhibitor admixed mortar specimens. The EIS plot was taken before and after the test to confirm the failure of specimens and to understand the impedance behavior. The mortar samples adjacent to crack region was collected carefully and the chloride levels in percentage of binder was arrived using silver nitrate titration method which is the tolerable limit for crack initiation. The working electrode (rebar) was also removed with care to visually assess the corrosion resistance behavior exhibited by different inhibitor admixed systems. Figure 6 shows the view of accelerated corrosion test.

In all the tests, in each category i.e., type of cement, type of inhibitor and dosage level (0, 1, 2 and 5%), 3 specimens were cast and tested to arrive at results, discussion, and further conclusions (except ACT). In case of ACT, two specimens in each category were tested. In total, 378 specimens were cast and tested to assess the strength and durability performance of WSNi and BPI admixed cement mortar.

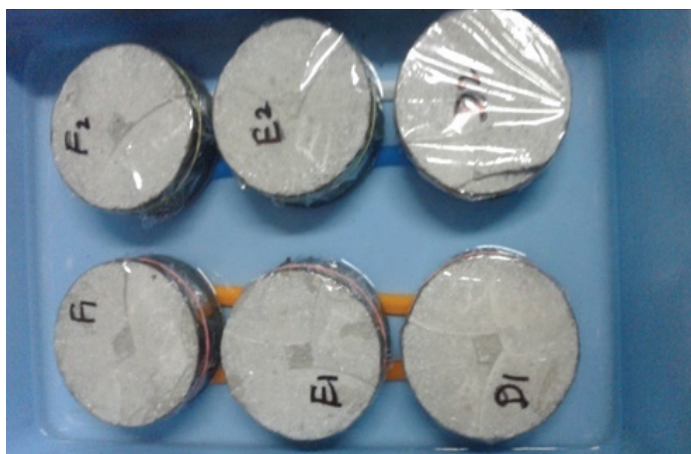


Figure 3: Specimens in sorptivity test

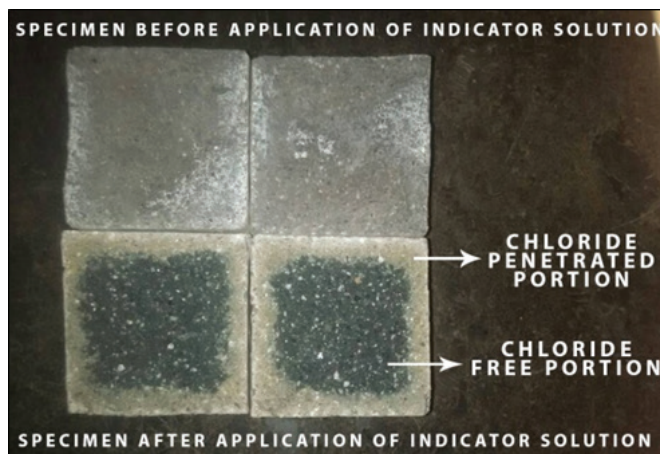


Figure 4: Specimens before and after chloride penetration test

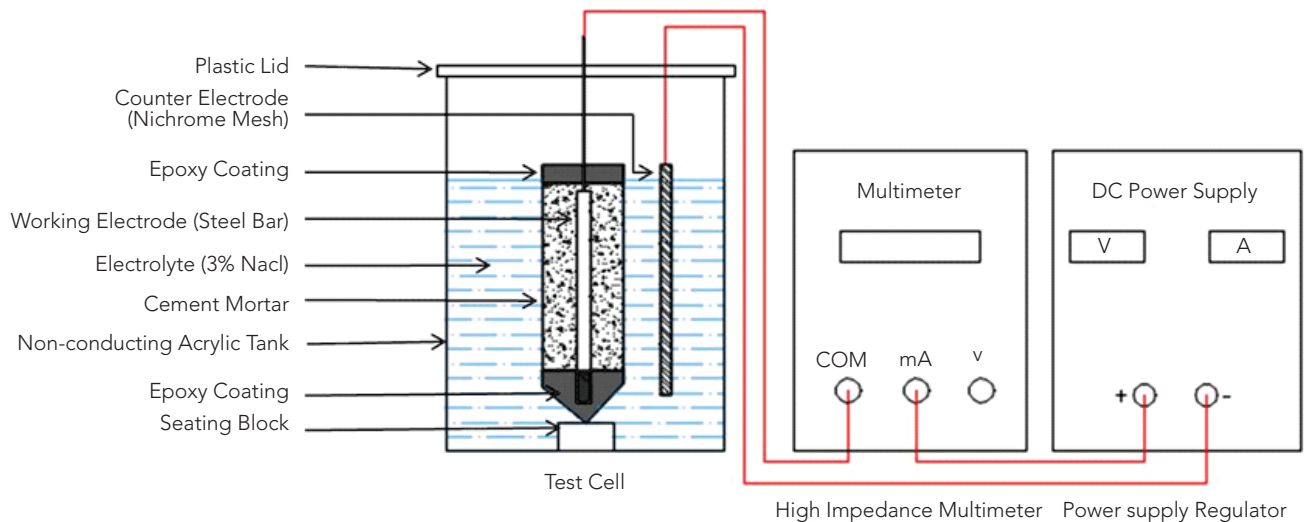


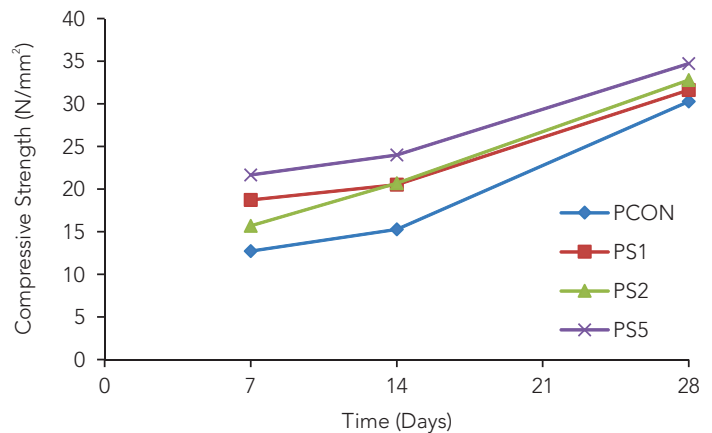
Figure 5: Schematic of accelerated corrosion test set-up



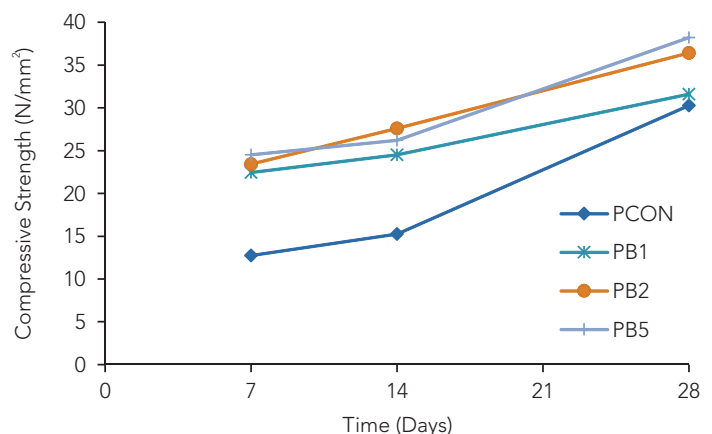
Figure 6: View of accelerated corrosion test in progress

## 4. RESULTS AND DISCUSSION

Figure 7a shows the compressive strength of WSNI admixed and control PCM specimens at the age of 7, 14 and 28 days. It can be noticed that the compressive strength of WSNI admixed mortar exhibited an increasing trend regardless of the dosage of inhibitor addition and age of test when compared to control mortar (PCON). The 7 day compressive strength of PS1, PS2 and PS5 specimens showed an increase of the order of 47, 23 and 70% respectively in comparison to inhibitor free specimens (PCON). The 14 day compressive strength of PCM specimens ranged from 15 N/mm<sup>2</sup> to 24 N/mm<sup>2</sup> and the increase in compressive strength was between 34 - 57% for WSNI admixed specimens [8,33]. The 28 day compressive strength of PS1, PS2 and PS5 specimens were 5, 8 and 15% more than the PCON and the increase was marginal. It can be observed that the addition of WSNI significantly enhanced the early age strength (7 day and 14 day) whereas the increase in strength at the age of 28 days was only marginal.



a. WSNI



b. BPI

Figure 7: Compressive strength of PCM specimens with various dosages of WSNI and BPI

Figure 7b shows the compressive strength of BPI admixed and control PCM specimens at the age of 7, 14 and 28 days. It can be observed that addition of BPI inhibitor at dosage levels of 1,

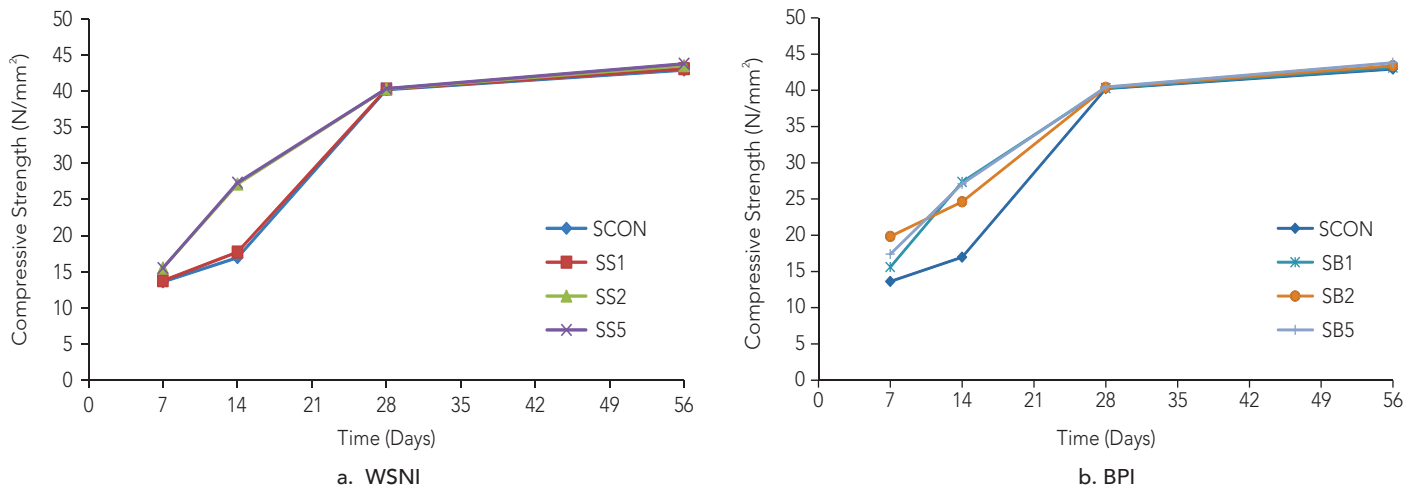


Figure 8: Compressive strength of SLCM specimens with various dosages of WSNI and BPI

2 and 5% significantly increased the 7 day compressive strength in the order of 76 to 92% when compared to control PCM mortar. The 14 days compressive strength test results exhibited a similar trend with improvement in the order of 60 to 80% when compared to the PCON specimens. However PB1 specimen showed only a 5% increase in 28 day compressive strength, whereas PB2 and PB5 specimens significantly increased the compressive strength in the order of 17 and 26% respectively in comparison to PCON. It can be concluded that incorporation of WSNI and BPI helped in achieving higher early strength without affecting the strength gain at 28 days as compared to inhibitor free PCM specimens (PCON).

Figure 8a shows the compressive strength of WSNI admixed slag cement mortar specimens at 7, 14, 28 and 56 days. It can be noticed that WSNI at 2 and 5% dosage increased the 7 day strength by 14% when compared to SCON; whereas addition of 1% inhibitor did not change the compressive strength value at 7 days. The 14 day compressive strength results exhibited a slight increase at 1% inhibitor addition and significant increase

at 2 and 5% of WSNI. The strength at 28 and 56 days revealed that the addition of WSNI Inhibitor did not vary the compressive strength values irrespective of inhibitor dosage and was similar to that of SCON.

Figure 8b shows the compressive strength of BPI admixed slag cement mortar specimens at 7, 14, 28 and 56 days. It can be inferred that in case of SB1, SB2 and SB5 specimens, the 7 day compressive strength increased by 14, 45 and 27% respectively. However the compressive strength developed at 14 days revealed an increase in the order of 45 to 60% as compared to control slag cement mortar (SCON). The 28 and 56 day compressive strength values revealed that there was no change due to addition of BPI in cement mortar irrespective of dosage levels. The slag cement when admixed with both the inhibitors showed appreciable increase in the early strength development, but the 28 and 56 days strength was similar to the control slag cement specimens<sup>[34]</sup>.

Figure 9a displays the split tensile strength for specimens with

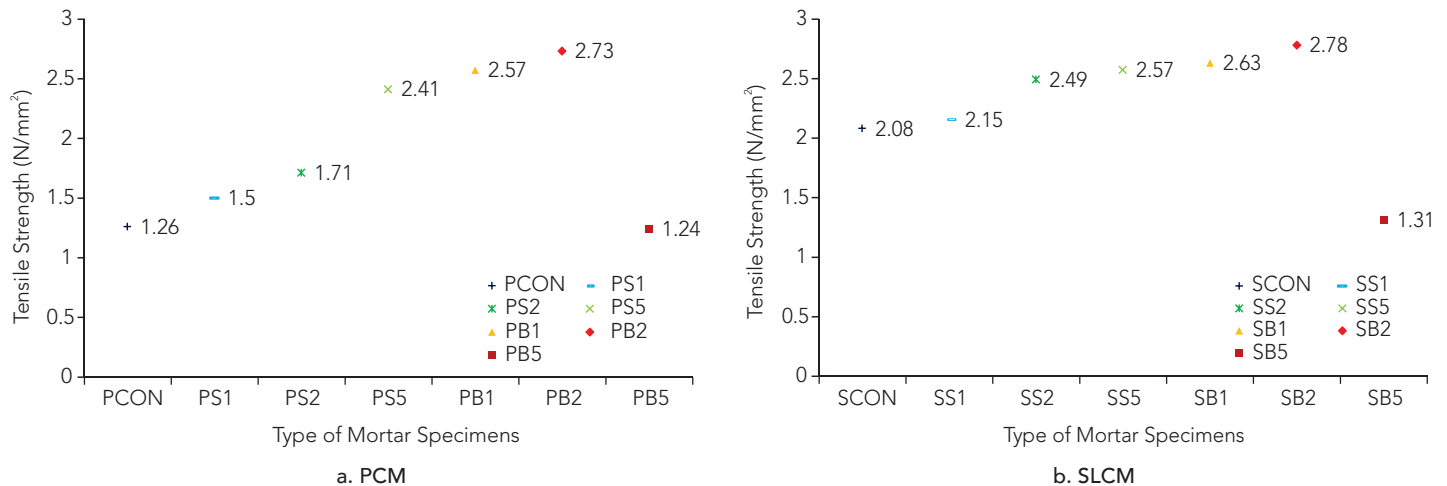


Figure 9: Tensile strength of PCM and SLCM specimens with different dosage of inhibitors



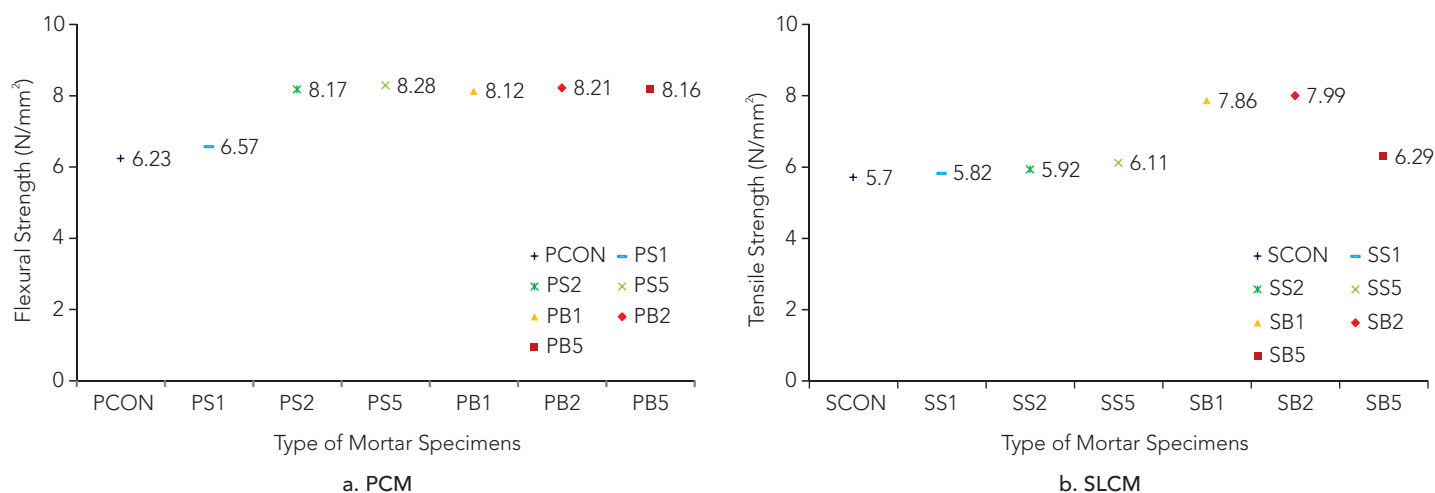


Figure 10: Flexural strength of PCM and SLCM specimens with different dosage of inhibitors

and without corrosion inhibitors in PCM. The addition of WSNI and BPI in PCM increased the split tensile strength in all the tested dosage levels. Addition of WSNI at 1, 2 and 5% increased the tensile strength by 20, 35 and 90% respectively as compared to PCON<sup>[6]</sup>. Upon addition of 1 and 2% BPI inhibitor, the tensile strength increased by 2 times as that of control mortar. Addition of 5% did not influence the tensile strength positively and the values were similar to that of PCON.

Figure 9b shows the effect of corrosion inhibitors on split tensile strength of SLCM at different dosages. It can be noticed that the split tensile strength of SCON was higher than the PCON by 65%. Addition of WSNI at dosage levels of 2 and 5% increased the tensile strength by 19 and 24% respectively. WSNI at 1% addition did not show any appreciable improvement in tensile strength. The tensile strength was increased by 26, 34% and reduced by 37% when the BPI was added at dosage levels of 1, 2 and 5% respectively.

It can be concluded that SLCM offered higher tensile strength values as compared to PCM. This increase in splitting tensile strength values for both WSNI and BPI admixed mortar specimens (except PB5 and SB5) may be due to the good workability offered by WSNI and BPI at reduced water cement ratio when compared to control specimens. The reduction in tensile strength for SB5 specimens needs further study.

Figure 10a shows the effect of inhibitors on flexural strength of PCM specimens. It can be noticed that flexural strength of PCON is 6.23 MPa which is marginally less than the PS1 specimen. However the flexural strength of PS2 and PS5 specimens were 8.17 N/mm<sup>2</sup> and 8.28 N/mm<sup>2</sup> and the inhibitor addition had increased the flexural strength by 30% - 33% as compared to PCON. The flexural strength of BPI inhibitor specimens at all the dosage levels was around 8.1 N/mm<sup>2</sup> which is 30% more than the PCON.

Figure 10b shows the effect of inhibitors on flexural strength of SLCM. The flexural strength of SCON was 8% less than that of PCON and the value was 5.70 MPa. Regardless of the dosage level addition of WSNI, flexural strength was slightly increased by 2 - 7% when compared to SCON; whereas BPI inhibitor addition at 1, 2 and 5% dosage increased the flexural strength at 38, 40 and 10% respectively compared to control slag cement mortar.

It can be deduced that the addition of WSNI and BPI in PCM had increased the flexural strength in the range of 8 - 33%. The addition of WSNI in SLCM marginally improved the flexural strength in the range of 2 - 7%; whereas BPI addition significantly improved the flexural strength up to 40% at higher dosages (2%, 5%) and marginally at 10% in lower dosage (1%). The increase in flexural strength for inhibitor admixed mortar specimens may be due to the improved workability in the fresh state at relatively low water cement ratio and subsequent well formation of micro structure in the mortar matrix<sup>[8]</sup>.

Figure 11a displays the effect of inhibitors on shear strength of PCM. It can be noticed that irrespective of the dosage level of addition, WSNI and BPI improved the shear strength of mortar mix. The shear strength of PS1, PS2 and PS5 specimens were 25, 29 and 33% respectively higher than that of PCON. At 1, 2 and 5% dosage level of addition, the BPI significantly increased the shear strength of PCM in the range of 28 - 32%.

Figure 11b shows the shear strength of control and inhibitor admixed slag cement mortar. It can be seen that the shear strength of SCON was 2.72 MPa which was 30% more than PCON. The shear strength of slag cement mortar with Inhibitor showed only a slight increase in the range of 1 to 5% irrespective of the type of inhibitor added to the slag cement mortar. It can be concluded that the shear strength of PCM increased significantly with the addition of both WSNI and BPI in the range of 25 - 32%; whereas the addition of inhibitors in slag cement mortar increased the shear strength only marginally.

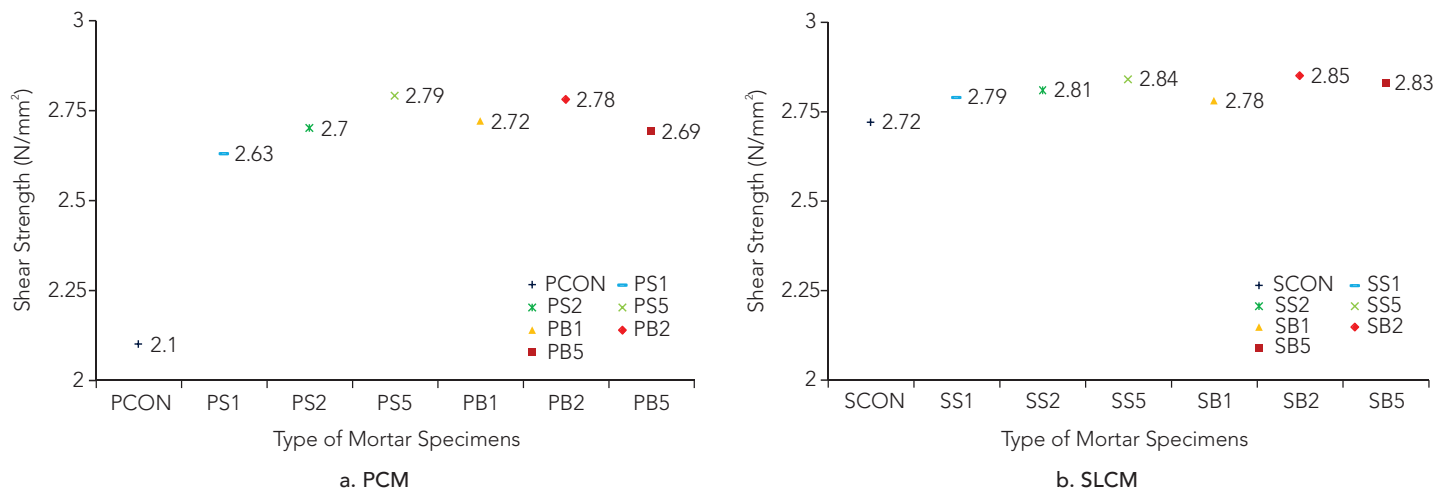


Figure 11: Shear strength of PCM and SLCM specimens with different dosage of inhibitors

Figure 12 shows the comparison of 24 hours water absorption for inhibitor admixed mortar specimens. There was a significant reduction in water absorption for control SLCM at 26% when compared to control PCM. Figure 12a exhibits a marginal reduction in water absorption for WSNI and BPI admixed specimens up to 10% in the tested dosage levels except for 1% BPI. The water absorption was significantly reduced by 23% when BPI is admixed at 1%.

Figure 12b indicates significant reduction of 22 and 27% in water absorption for 2 and 5% WSNI admixed specimens respectively, whereas 1% addition exhibits marginal reduction (8%). The BPI incorporation offered appreciable reduction in water absorption of 11 and 15% upon addition at 2 and 5% respectively. The BPI 1% specimens [SB1] showed insignificant reduction as compared to control specimens [SCON]. It can be concluded that BPI and WSNI specimens exhibited significant reduction in water absorption in PCM and SLCM at higher dosages (2 and 5%).

Figure 13 and Figure 14 shows the performance of PCM and SLCM specimens with and without inhibitor addition in the sorptivity test. It can be inferred that the absorption (*I*) values observed for all the specimens were less than 6mm which was in line with Alexander *et al.* [35]. The SLCM specimens offered reduced water absorption as compared to PCM irrespective of inhibitor addition.

From Figure 13, it can be seen that the specimens with WSNI at 1% (PS1) and 5% (PS5) exhibited significantly reduced rate of absorption (sorptivity) of water (as function of time) as compared to PCON in the initial absorption stage (until 6 hr exposure). The specimens admixed with WSNI 2% (PS2) offered appreciably reduced sorptivity when compared to PCON. In case of BPI admixed PCM specimens, significantly reduced sorptivity was noted upon increasing the dosage of inhibitor from 1 to 5%. The performance is graded as PB5>PB2>PB1>PCON. Despite of type of inhibitor and dosage addition, similar trend in water absorption (*I*) values for PCM specimens post 6 hr period.

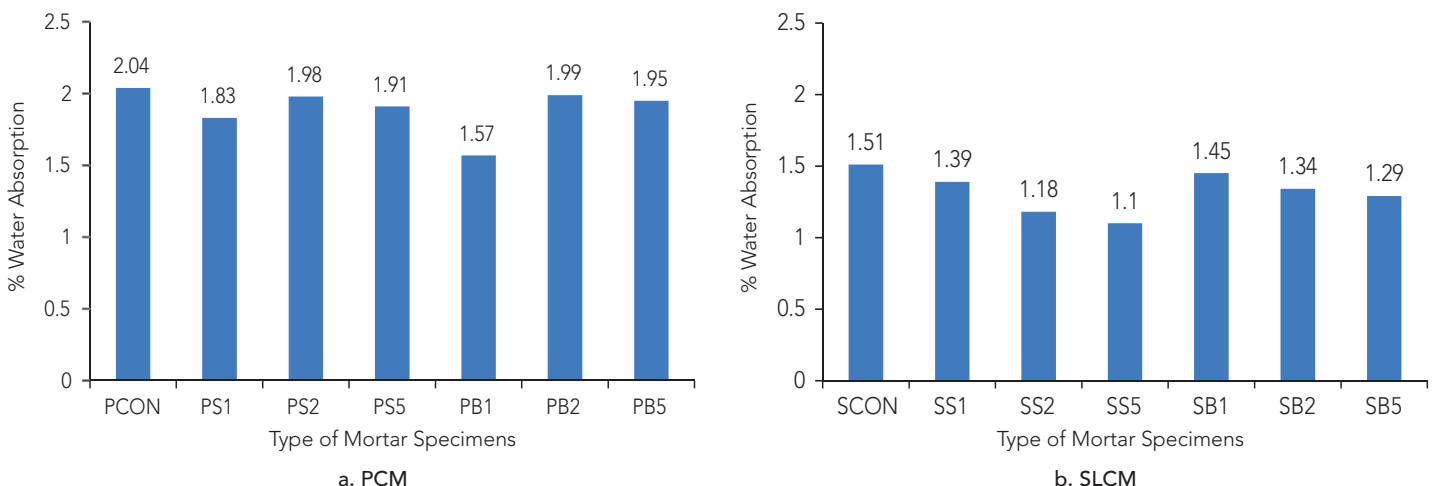


Figure 12: Comparison of 24 hour water absorption for control and inhibitor admixed mortar

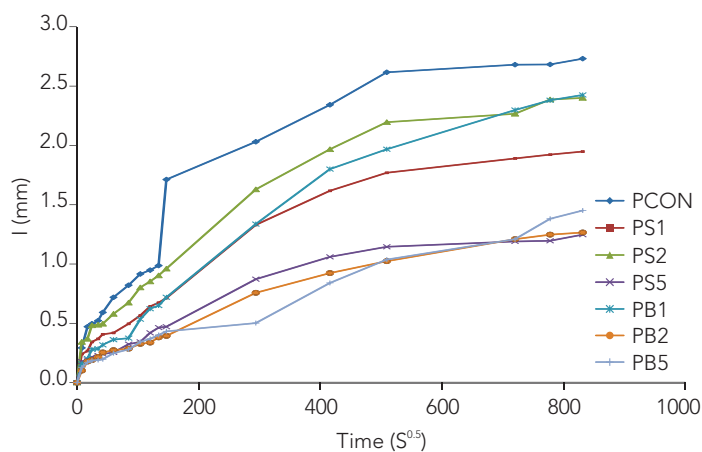


Figure 13: Performance of PCM with and without inhibitor in the sorptivity test

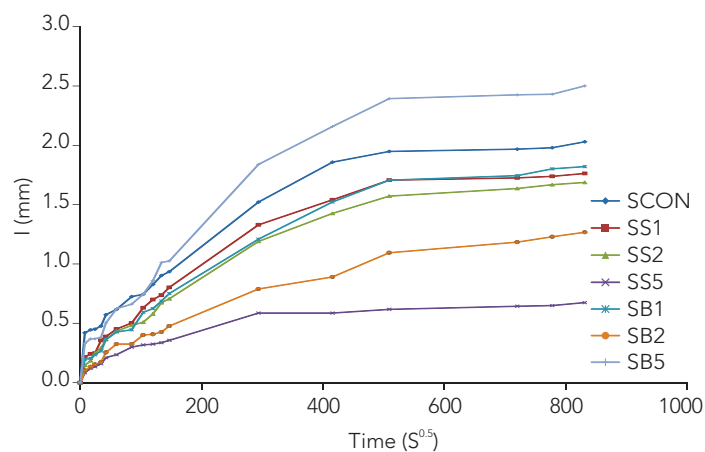


Figure 14: Performance of SLCM with and without inhibitor in the sorptivity test

Figure 14 shows the inferior performance of SB5 specimens since sorptivity values were higher compared to control SCON specimens in both initial and secondary absorption stage which needs further study. Whereas the specimens SB1 and SB2 exhibited significantly improved performance (i.e., highly reduced sorptivity values) throughout the test period. The performance of WSNI admixed specimens in SLCM is graded as SS5>SS2>SS1>SCON. As per ASTM C1585<sup>[29]</sup>, the sorptivity values are also influenced by mineral and chemical admixtures, the superior performance of inhibitor admixed mortar specimens (except SB5) may be due to presence of water reducing agent in the WSNI<sup>[8]</sup> and enhanced pore lining offered by BPI<sup>[5]</sup>.

It can be concluded that SLCM significantly reduced water absorption and the addition of WSNI and BPI further reduced the water absorption (except SB5) appreciably in different dosage levels. The insignificant reduction in water absorption for BPI 5% in SLCM needs further study to understand the reasoning.

Figure 15 shows the average depth of chloride ion penetration in PCM and SLCM with and without inhibitor. It can be seen that there was a 33% reduction in chloride ion penetration in SCON when compared to PCON. The addition of WSNI in PCM reduced the chloride ion penetration of the order of 13% - 33% whereas BPI addition in PCM offered a 10 - 40% reduction. The appreciable durability performance was obtained for WSNI at 2% and BPI at 1% as compared to other dosage levels. A similar trend was observed in the case of BPI and WSNI admixed slag cement mortar. There was a reduction of 7 - 34% and 14 - 21% in chloride ion penetration for WSNI and BPI admixed slag cement mortar respectively.

Table 4 shows the observation on accelerated corrosion test for control and inhibitor admixed mortar specimens. The parameters identified for performance evaluation included corrosion potential before and after the test, maximum current development, cement mortar resistance (at high frequency) at initial and after failure, time taken for crack initiation and

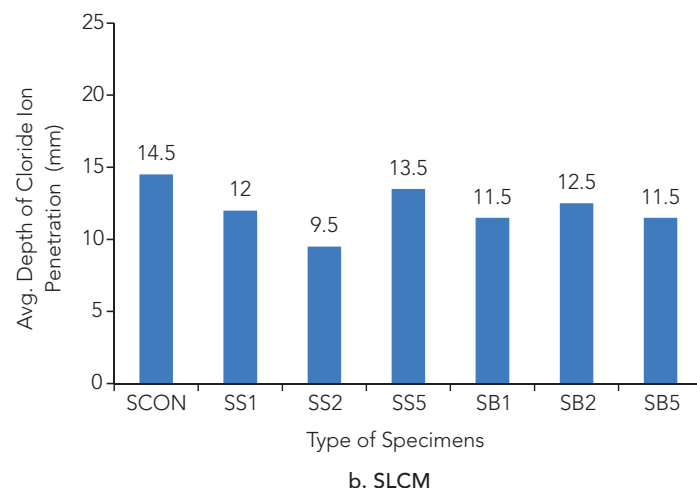
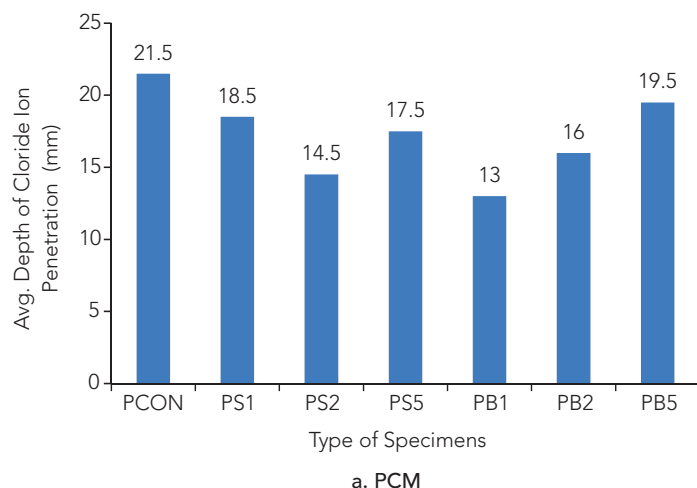


Figure 15: Chloride ion penetration in PCM and SLCM with and without inhibitor



Table 4: Observation on accelerated test for control and inhibitor admixed mortar specimens

S. NO	SPECIMEN DESIGNATION	OPEN CIRCUIT POTENTIAL (mV) Vs. SCE		MAXIMUM CURRENT DEVELOPMENT (mA)	CEMENT MORTAR RESISTANCE ( $\Omega/\text{cm}^2$ )		CHLORIDE TOLERABLE LIMIT (BY WEIGHT OF CEMENT) (%)	TIME TO FAILURE (CRACK INITIATION) (hr)	TIME FACTOR Vs. CONTROL
		INITIAL	AFTER FAILURE		INITIAL	AFTER FAILURE			
1	PCON	-94	-509	37.0	85	74	0.18	31	-
2	PS1	-69	-408	26.8	103	96	0.19	32	1.03
3	PS2	-45	-482	19.5	110	85	0.18	36	1.16
4	PS5	-82	-216	9.30	134	120	0.14	35	1.13
5	PB1	-140	-620	29.60	152	80	0.24	37	1.19
6	PB2	-53	-681	28.30	122	83	0.35	35	1.13
7	PB5	-100	-670	18.90	117	106	0.14	35	1.13
8	SCON	-214	-581	8.50	250	230	0.12	46	-
9	SS1	-140	-629	8.90	267	210	0.30	48	1.04
10	SS2	-269	-583	8.10	285	218	0.29	49	1.07
11	SS5	-165	-420	8.10	315	300	0.36	72	1.57
12	SB1	-112	-467	8.50	318	240	0.15	57	1.24
13	SB2	-153	-459	9.40	295	215	0.18	68	1.48
14	SB5	-388	-440	9.70	276	212	0.41	58	1.26

chloride level near rebar. It can be observed that SLCM mortar offered 1.5 times more resistance to corrosion (in terms of crack initiation) compared with PCM irrespective of inhibitor addition. For PCM specimens, the addition of WSNI and BPI increases the crack initiation time up to 20%, in particular, at higher dosages (2 and 5%). In the case of SLCM specimens, there was a marginal increase in crack initiation time for WSNI specimens at 1 and 2% dosage, whereas addition at 5% significantly increased the crack initiation time up to 57%. For BPI admixed specimens there was an appreciable increase in crack initiation time of the order of 24 - 48% as compared to control mortar.

An enhanced resistance against chloride attack due to inhibitor incorporation in mortar was noticed from the chloride values after the failure of specimens. It can be observed that there was a significant increase in chloride tolerable limit up to two fold for BPI admixed PCM specimens. The scenario was similar for SLCM inhibitor admixed specimens with two fold increase for WSNI specimens and 3 fold for BPI specimens at 5% dosage of addition. The current development at the end of the test period points that there was an appreciable to significant reduction for inhibitor admixed PCM specimens, irrespective of the type, when compared to control mortar specimens; whereas SLCM specimens showed a similar current development irrespective of inhibitor addition. The potential values observed after failure of the specimens exhibited severe corrosion of rebars as per ASTM C 876 – 2009 [36] and confirmed the failure of specimens except PS5. The PS5 specimens offered low corrosion risk since failure of the specimen was observed at the tip and was not

realized during the test. The mortar resistance values observed (both at initial and after failure) in all the specimens revealed an appreciable reduction and this may be due to corrosion initiation and subsequent crack formation in the specimen.

Figure 16 and 17 shows the Nyquist plot of control, WSNI and BPI admixed PCM and SLCM specimens before and after the accelerated corrosion test. It can be visualized that in all the specimens, there was a considerable reduction in cement mortar resistance at high frequency levels after the failure of specimens and this was in line with the observations mentioned in Table 4 with respect to potential values after the test.

Figure 18 shows the view of rebars after subjecting to an accelerated corrosion test. It can be noticed that control PCM specimens were seen with an innumerable number of rust spots throughout the length of the specimen particularly in rib areas. The inhibitor admixed specimens were observed with isolated rust areas at 1 and 2% dosage; and further reduced corrosion at 5% dosage irrespective of the type of inhibitor. In the case of SLCM specimens, difficulty was experienced in noticing the point of failure for inhibitor admixed specimens. These specimens exhibit a small change in behaviour in the surface in the form of oozing out of corrosion products and the formation of very minute cracks. Considering the test duration, accelerating nature and chloride levels near anode (Table 4), it can be inferred that WSNI and BPI admixed mortar at 1, 2 and 5% offered excellent protection to steel reinforcement rods against corrosion.

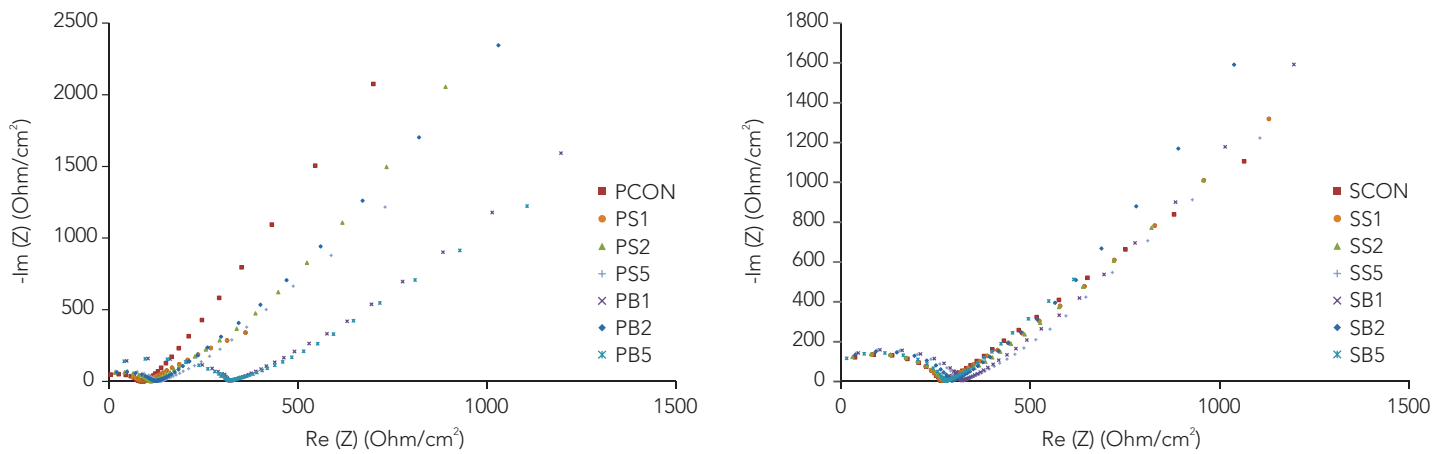


Figure 16: Nyquist plot of PCM and SLCM specimens (Initial: Before ACT)

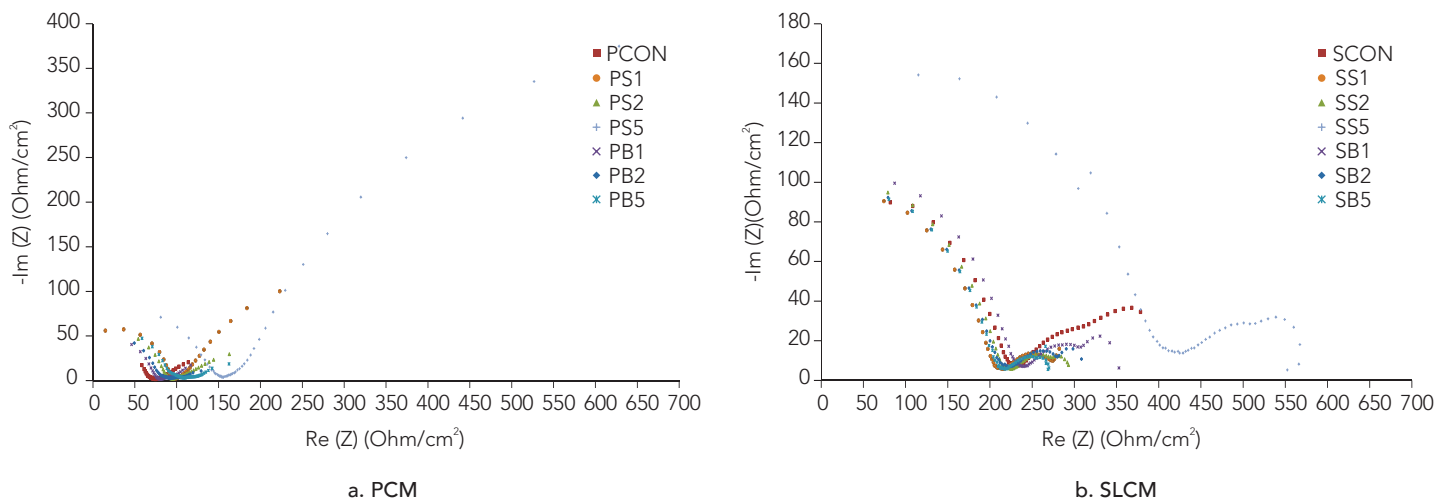


Figure 17: Nyquist plot of PCM and SLCM specimens (Final : After Failure)

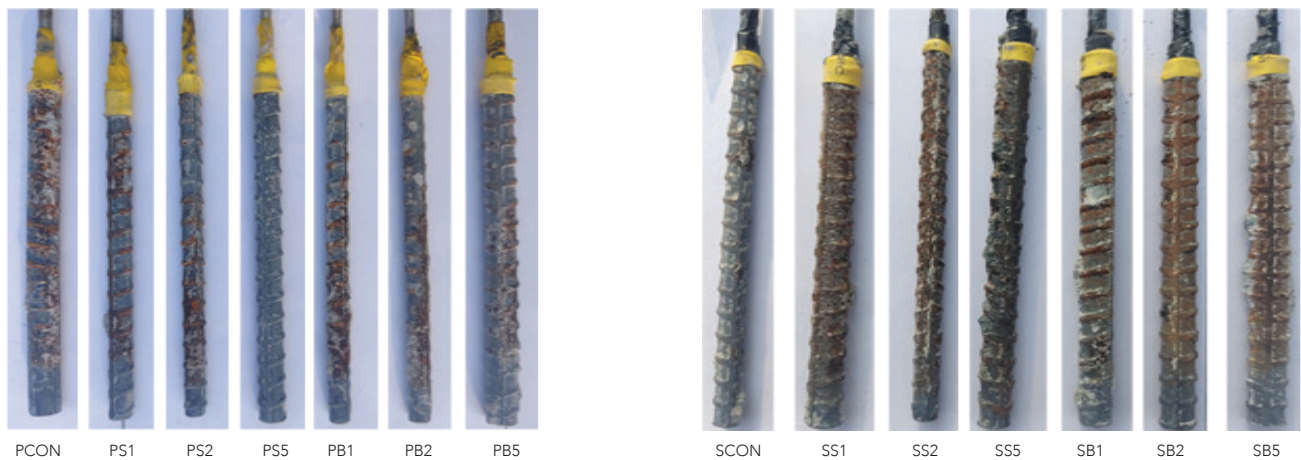


Figure 18: View of rebars after ACT

The improved strength and durability performance of WSNI is due to chloride repelling mechanism exhibited by nitrite ions (due to charge similarity) and improved microstructure of the mortar due to reduction in water cement ratio for the

required workability<sup>[8]</sup>. The improved pore lining and formation of passivation film around the steel can be attributed to the significant performance of the bipolar (dual mechanism corrosion inhibiting admixture) inhibitor<sup>[37]</sup>

## 5. CONCLUSIONS

Based on the test results and further analysis, the following conclusions are drawn:

- Appreciable reduction in water cement ratio for the similar workability due to incorporation of WSNI and BPI.
- The incorporation of inhibitor in the tested dosages, irrespective of the type exhibits reduction in water cement ratio for the target workability. But the observed setting time values were well within the codal provisions for the type of cement.
- Addition of WSNI and BPI significantly increases the early age strength of both PCM and SLCM mixes<sup>[34]</sup>.
- The 28 day compressive strength improved appreciably due to addition of WSNI at higher dosages, whereas 28 day and 56 day strength values for SLCM mixes were similar to control mortar irrespective of type inhibitor and dosage.
- There is a significant increase in splitting tensile strength for WSNI and BPI admixed mortar specimens, irrespective of the type of cement, in all the tested dosages except SB5 specimen.
- Flexural strength of PCM increased up to 30% due to addition of WSNI and BPI at higher dosages.
- PCM exhibited improved shear strength in the range of 25 - 30% due to addition of inhibitors irrespective of type and dosage.
- Reduction in water absorption upto 23% due to the incorporation of WSNI and BPI in cement mortar.
- SLCM shows significant reduction in water absorption in sorptivity test as compared to PCM.
- Admixing of WSNI and BPI at tested dosages appreciably reduced the chloride ion penetration irrespective of the type of cement.
- Accelerated corrosion test results revealed improved tolerable limit for chloride for inhibitor admixed mortar.

## 6. RECOMMENDATION

The addition of WSNI and BPI at 2% by weight of cement is recommended for improved corrosion prevention in reinforced concrete structures in small scale construction sector considering the strength and durability aspects.

## REFERENCES

- [1] Paulo J. M. Monteiro and Povindar Kumar Mehta (2013). *Concrete: microstructure, properties, and materials*, McGraw Hill Professional.
- [2] Cabrera J. G. (1996). "Deterioration of concrete due to reinforcement steel corrosion", *Cement and Concrete Composites*, Vol.18, No.1, pp. 47-59.
- [3] Vaysburd A. M. and Emmons P. H. (2004). "Corrosion inhibitors and other protective systems in concrete repair: concepts or misconcepts", *Cement and Concrete Composites*, Vol. 26, No. 3, pp. 255-263.
- [4] Karuppanasamy J, Pillai R.G. (2017). "A short-term test method to determine the chloride threshold of steel-cementitious systems with corrosion inhibiting admixtures", *Materials and Structures*, Vol. 50, No.4, pp. 205.
- [5] Mahmood Aliofkhazraei, (2018). "Corrosion inhibitors, principles and recent applications", Intech, Croatia.
- [6] Ann K.Y., Jung H.S., Kim H.S., Kim S.S., Moon H.Y. (2006). "Effect of calcium nitrite-based corrosion inhibitor in preventing corrosion of embedded steel in concrete", *Cement and concrete Research*, Vol. 36, pp. 530-535.
- [7] Berke N.S., Hicks M.C., (2004). "Predicting long-term durability of steel-reinforced concrete with calcium nitrite corrosion inhibitor", *Cement and Concrete Composite*, Vol. 26, No.3, pp. 191-198.
- [8] M.S. Haji Sheik Mohammed (2008). Performance evaluation of protective coatings on steel rebars, Thesis submitted to Anna University, India for Ph.D.
- [9] Manu Harilal, V.R. Rathish, B. Anandkumar, R.P. George, M.S. Haji Sheik Mohammed, John Philip and G. Amarendra,(2019). "High performance Green Concrete (HPGC) with improved strength and chloride ion penetration resistance by synergistic action of fly ash, nanoparticles and corrosion inhibitor", *Construction and Building Materials*, Vol. 198, pp. 299-312.
- [10] Umar Mohd, Fathima Naheetha, M.S. Haji Sheik Mohammed and S. Hemalatha , (2019). "Modified cement composites for protection against microbial induced concrete corrosion of marine structures", *Biocatalysis and Agricultural Biotechnology*, Vol. 20, pp.1-7.
- [11] Pillai R.G., Sooraj Kumar A O Nair, Jayachandran K., Dhanya B.S., Manu Santhanam, Ravindra Gettu, (2015). "Enhancing the corrosion resistance of reinforced concrete structures- Indian scenario and challenges ahead", International Conference and Expo on Corrosion, CORCON 2015, India.
- [12] Karavokyros, L., Katsiotis, N., Tzanis, E., Batis, G., Sapalidis, A., Chatzopoulos, A., Sideris, K. and Beazi-Katsioti, M. (2020). "The effect of mix-design and corrosion inhibitors on the durability of concrete", *Journal of Materials Science and Chemical Engineering*, Vol. 8, pp. 64-77. <https://doi.org/10.4236/msce.2020.84005>.



- [13] Schuldyakova, K.V., Kramara, L.Ya., Trofimovadoi, B.Ya. (2016). "The properties of slag cement and its influence on the structure of the hardened cement, paste", *Procedia Engineering*, Vol. 150, pp.1433-1439. DOI: 10.1016/j.proeng.2016.07.202.
- [14] Maria Eugenia Parron-Rubio, Francisca Perez-Garcia, Antonio Gonzalez-Harrera, Miguel Jose Oliveira and Maria Dolores Rubio-Cintas, (2019). "Slag substitution as a cementing material in concrete : mechanical, physical and environmental properties", *Materials*, Vol. 12, No. 2845, pp. 1-15.
- [15] IS 1489 Part 1: 2015 (2020). *Indian standard code of practice for Specification for portland pozzolona cement*, Bureau of Indian Standards, New Delhi.
- [16] IS 455: 2015 (2020). *Indian standard code of practice for portland slag cement - specification*, Bureau of Indian Standards, New Delhi.
- [17] IS 650:1991(2008). *Indian standard code of practice for standard sand for testing cement - specification*, Bureau of Indian Standards, New Delhi.
- [18] Dyana Joseline, Steffy Maryline W and M.S. Haji Sheik Mohammed,(2015). "Sodium nitrite based mixed inhibitor for corrosion protection of steel rebars used in construction", International Conference and Expo on Corrosion, CORCON 2015, YSF28, India.
- [19] IS 4031 - Part 11:1988 (2019). *Indian standard code of practice for methods of physical tests for hydraulic cement – Determination of density*, Bureau of Indian Standards, New Delhi.
- [20] IS 2386 - Part 3:1963 (2016). *Indian standard code of practice for methods of test for aggregates for concrete – specific gravity, density, voids, absorption and bulking*, Bureau of Indian Standards, New Delhi.
- [21] IS 2386 - Part I: 1963 (2002) *Indian standard code of practice for Methods of Test for Aggregates for Concrete – Particle Size and Shape*, Bureau of Indian Standards, New Delhi.
- [22] IS 383- 1970 (2021). *Indian standard code of practice for specification for coarse and fine aggregates from natural sources for concrete*, Bureau of Indian Standards, New Delhi.
- [23] IS 13435 - Part 4:1992 (2017). *Indian standard code of practice for acrylic based polymer waterproofing material - Determination of pH value*, Bureau of Indian Standards, New Delhi.
- [24] IS 4031 - Part 5: 1988 (2019). *Indian standard code of practice for methods of physical tests for hydraulic cement – Determination of initial and final setting times*, Bureau of Indian Standards, New Delhi.
- [25] IS 516: 1959 (2018). *Indian standard code of practice for methods of tests for strength of concrete*, Bureau of Indian Standards, New Delhi.
- [26] IS 5816: 1999 (2018). *Indian standard code – Method of test splitting tensile strength of concrete*, Bureau of Indian Standards, New Delhi.
- [27] JIS A 1171: 2000. *Test methods for polymer-modified mortar*, Japanese Industrial Standard, Tokyo, Japan.
- [28] ASTM C 642: 2006. *Standard test method for density, absorption and voids in hardened concrete*, American Society for Testing and Materials, United States.
- [29] ASTM C 1585: 2013. *Standard test method for measurement of rate of absorption of water by hydraulic-cement concretes*, American Society for Testing and Materials, United States.
- [30] Rengaraju, S., Rathinarajan, S., Ajithakumari, A., Pugal,O., Pillai, R.G. (2015). "Effect of corrosion inhibitors on durability parameters of cement mortar", International Conference and Expo on Corrosion, CORCON 2015, India.
- [31] Aggarwal, L.K., Thapliyal, P.C., Karade, S.R. (2007). "Properties of polymer-modified mortars using epoxy and acrylic emulsions", *Construction and Building Materials*, Vol. 21, pp. 379-383.
- [32] Dyana Joseline, Pillai R.G. (2020). Enhancing service life of prestressed concrete structures by using fly ash and corrosion inhibitors, *Indian Concrete Journal*, Vol. 94, No. 11, pp. 54-67.
- [33] Devi,M. and Kannan, K. (2013). "Evaluation of corrosion inhibition performance of zinc oxide and sodium nitrite in quarry dust concrete", *Asian Journal of Chemistry*, Vol. 25, No. 15, pp. 8690-8696.
- [34] Schutter G. D., Luo L. (2004). "Effect of corrosion inhibiting admixtures on concrete properties", *Construction and Building Materials*, Vol. 18, pp. 483-489.
- [35] Alexander M.G., Mackechnie J.R. and Ballim Y. (1999). "Guide to the use of durability indexes for achieving durability in concrete structures." *Achieving durable and economic concrete construction in the South African context*, Research Monograph, Vol. 2, pp. 5-11.
- [36] ASTM C 876-1999. *Standard test method for half-cell potentials of uncoated reinforcing steel in concrete*, American Society for Testing and Materials, United States.
- [37] Kaur K., Goyal Shweta., Bhattacharjee B., Kumar Maneek. (2016). "Efficiency of migratory-type organic corrosion inhibitors in carbonated environment, *Journal of Advanced Concrete Technology*, Vol. 14, pp. 548-558.



**S. SHAFEER AHAMED** is an Assistant Professor of Civil Engineering and research scholar at B.S. Abdur Rahman Crescent Institute of Science & Technology, Chennai. His current research interests are in corrosion inhibitors for concrete, supplementary cementitious materials, repair and rehabilitation of structures and durability of concrete structures. He is also the Assistant Director of Centre for Prevention and Control of Corrosion in Concrete Structures (PC3S) at Crescent Innovation and Incubation Council, Chennai. Email: shafeer@crescent.education



**J. SHERIN MARIYA** is a graduate of Bachelor of Technology in Civil Engineering from Sathyabama University and Master of Technology in Structural Engineering from B.S. Abdur Rahman Crescent Institute of Science & Technology. Her current research interests are in the durability of concrete structures, corrosion control in RC structures and concrete technology. Email: sherinmariya21@yahoo.com



**V. ROOPA** is an Assistant Professor of Civil Engineering and research scholar at B.S. Abdur Rahman Crescent Institute of Science & Technology, Chennai. Her current research interests are in the service life extension of existing RC roofing systems, cathodic protection of RC structures, galvanized steel rebar, repair and rehabilitation of structures and sustainability in concrete structures. She is also the Assistant Director of Centre for Prevention and Control of Corrosion in Concrete Structures (PC3S) at Crescent Innovation and Incubation Council, Chennai. Email: roopa@crescent.education



**M.S. HAJI SHEIK MOHAMMED** is a Professor of Civil Engineering at B.S. Abdur Rahman Crescent Institute of Science & Technology, Chennai. His current research interests are in the prevention and control of corrosion in RC structures, durable repair composites, repair & rehabilitation of structures, structural behaviour of RC elements and sustainability & affordable housing clusters. He is also the Director of Centre for Prevention and Control of Corrosion in Concrete Structures (PC3S) at Crescent Innovation and Incubation Council, Chennai. Email: hajisheik@crescent.education

---

Cite this article: Shafeer Ahamed, S., Mariya, J. S., Roopa, V. and Haji Sheik Mohammed, M.S. (2021). "Corrosion inhibiting admixture for corrosion prevention in small scale reinforced concrete structures", *The Indian Concrete Journal*, Vol. 95, No. 4, pp. 38-51.

# MECHANICAL AND ELECTROCHEMICAL ASPECTS OF MICROALLOYED STEEL

B. BHUVANESHWARI\*,  
P. PRABHA\*,  
S. SANDHIYA,  
G. S. PALANI

## Abstract

Microalloyed steel is widely used in the automobile sector and recently finding its place in the construction of buildings, bridges and pipelines. It is a special category of low carbon steel with high yield to tensile strength ratio due to the addition of alloying elements, which boost the microstructural and strength related properties of the steel. Tensile tests, chemical analysis, corrosion tests and the morphological studies have been conducted on Titanium microalloyed steel samples to study the mechanical and electrochemical aspects. From these studies, it is understood that the Titanium microalloyed steel has the potential in structural composites applications as the steel stabilities against corrosion is relatively good under chloride contaminated simulated concrete pore solution environment.

**Keywords:** Chemical analysis, Corrosion tests, High-strength low-alloy Steel (HSLA), Microalloyed steel, Tensile strength, Titanium.

## 1. INTRODUCTION

Microalloyed steels or High-Strength Low-Alloy Steels (HSLA) developed in the second half of the twentieth century was one of the biggest breakthroughs in the development of new steels (Villalobos *et al.* 2018). The small additions of alloying elements (< 0.1%) such as niobium, titanium, vanadium and so on to low carbon steels (0.03%-0.15% C and up to 1.5% Mn), helps in achieving higher yield and tensile strengths. The minimum yield and ultimate strength ranges from 300 to 450 MPa and 440 to 590 MPa respectively and has the potential to exceed ultimate strength more than 1000 MPa (Xie *et al.* 2014). The HSLA range of steel products are available in hot and cold rolled grades. Due to its higher fatigue resistance, this steel is superior to other heat-treated steels. The disadvantages lie with relatively low ductility and toughness compared to quenched and tempered alloys. Normal steels can be substituted with light weight HSLA steel to reduce the quantity of steel usage and the

fabrication costs when the design codes permit the use of it. The application of microalloyed steel includes construction sector, pipeline industry, automotive sectors etc.

One of the most efficient methods that is used to improve and control the properties of microalloyed steel is the thermomechanical processing (TMP) followed by accelerated cooling. A careful selection of microalloy and its optimization are the two important things to be considered while making excellent and high strength microalloyed steels for various applications. Also controlled processing ease the difficulties faced during the manufacturing process of steels. As per the report, the solid solution strengthening is mainly based on the contents of microalloying and the properties related to grain size refinement, while precipitation upon hardening are due to the interaction between microalloying elements and the strain induced during controlled thermomechanical processes (TMCPs) (Villalobos *et al.* 2018). The basic principle behind this technique is to have control on the austenite grain size refinement, defect density strengthening, micro-alloying element precipitation reaction and modulation in phases formed (HE *et al.* 2007). TMCP process is relatively simple as it produces microstructurally tuned steels with cost-effective manner. In general, uncontrolled process temperature or the low temperature rolling causes negative impact on fracture toughness. Also, the compromise on resistance to sour environments is inevitable in the uncontrolled processing of steels. Hence, the controlled processing is the need of the hour on producing steel with high strength and durability. The micro-alloying plays a major role in providing the high strength and durability to the microalloyed steel. Recent studies majorly focused on nanoprecipitates formed during the manufacturing process as it contributes to the enhanced yield strength of the microalloyed steel (Gladman 1997). Interesting to note that the presence of precipitates formed by Ti, V, Nb and C, N contribute in inhibiting the austenitic grain boundary movements and hinders the grain growth, which occurs at high temperature (Xie *et al.* 2012). Hence it results in the movement of dislocations, thereby increased steel strength.



Rasouli *et al.* (2008) studied the effect of hot deformation temperature on microstructure and mechanical properties of microalloyed steel. The results indicated that by decreasing the deformation temperature, final microstructure is refined and the volume fraction of grain boundary ferrite is increased and some pearlite is produced. Therefore, both the yield and ultimate tensile strength are increased, while the toughness is preserved in comparison to ferritic-pearlitic microstructure. Skobir (2011) reviewed the development and basic characteristics of microalloyed steels and concluded that at least three strengthening mechanisms contribute to the final achieved strength and its relative contribution is determined by the composition and thermomechanical treatment. Also the finishing temperature for rolling determines the grain size and the strength level reached for a particular steel. Sherif and Seikh (2012) studied the effects of grain refinement on the corrosion resistance property of BSK 46 microalloyed steel in 1N H<sub>2</sub>SO<sub>4</sub> solution under different microstructural conditions. The repeated quenching of BSK 46 steels was found to increase the refining in their microstructures. Seikh Asiful Hossain (2013) studied the properties of microalloyed steel and reported that very fine grained microstructure is the reason behind the combination of strength and ductility. Liu *et al.* (2013) oxidized a microalloyed steel at different temperature between 900°C and 1200°C in 80% N<sub>2</sub>-15% CO<sub>2</sub>-5% O<sub>2</sub> atmosphere. As compared with the pure iron, an additional layer between matrix and oxide scale was detected in micro-alloyed steel. Bandgar *et al.* (2019) studied the fatigue crack growth rate behavior of HSLA Steel at varying load amplitudes to study its adequate resistance to propagation of fatigue cracks, as majority of the failures in service are due to metal fatigue. Janardhan Gorti *et al.* (2020) studied the tensile and fatigue behavior of resistance spot-welded HSLA steel

sheets by microstructural examination and micro-hardness measurements across the weld joints in as-received and pre-strained conditions.

Most of the research works reported in the literature are on the metallurgical aspects of HSLA steel. Though HSLA steel has varied applications in the automotive industry worldwide, its application in construction industry is still in development stage. Hence, it is mandatory to study the basic mechanical and electrochemical aspects of HSLA steel for its application in structural engineering. This paper presents the details regarding the chemical analysis, mechanical properties, corrosion and electrochemical aspects of microalloyed steel sample specimens. This study aims to find the application of microalloyed steel based on the strength and electrochemical corrosion aspects.

## 2. CHEMICAL ANALYSIS

Chemical analysis is conducted for determining the proportion of Carbon, Manganese, Sulphur, Phosphorous, Aluminium, Silicon, Copper, Titanium and Iron. Optical emission spectroscopy technique is used to determine the composition of Hot Rolled Steel, Cold Formed Steel and Microalloyed steel and the results are presented in Table 1. The maximum limit prescribed by the code is compared with the actual values obtained from the chemical analysis and are found well within the limits. All the three steels contain Carbon, Sulphur, Manganese, Phosphorous. In addition to these elements, cold formed steel contains Aluminium whereas hot rolled steel contains Silicon and microalloyed steel contains Titanium. The microalloyed steel sample conforms to Grade CR0-“Hard” grade according to IS: 513 (2008). Increased carbon and manganese

Table 1: Results from chemical analysis

ALLOYS	COLD ROLLED STEEL		HOT ROLLED STEEL		MICROALLOYED STEEL	
STANDARDS	IS: 513 (2008)		IS: 2062 (2011)		IS: 513 (2008)	
COMPOSITION	MAX	ACTUAL	MAX	ACTUAL	MAX	ACTUAL
Carbon	0.08%	0.01%	0.22%	0.19%	0.25%	0.08%
Manganese	0.40%	0.14%	1.50%	1.21%	1.70%	1.64%
Sulphur	0.030%	0.006%	0.045%	0.002%	0.045%	0.001%
Phosphorous	0.020%	0.003%	0.045%	0.009%	0.050%	0.012%
Aluminium	0.070%	0.060%	–	–	–	–
Silicon	–	–	0.40%	0.18%	–	–
Copper	–	–	–	–	–	–
Titanium	–	–	–	–	0.20%	0.123%
Iron	Rest (%)					

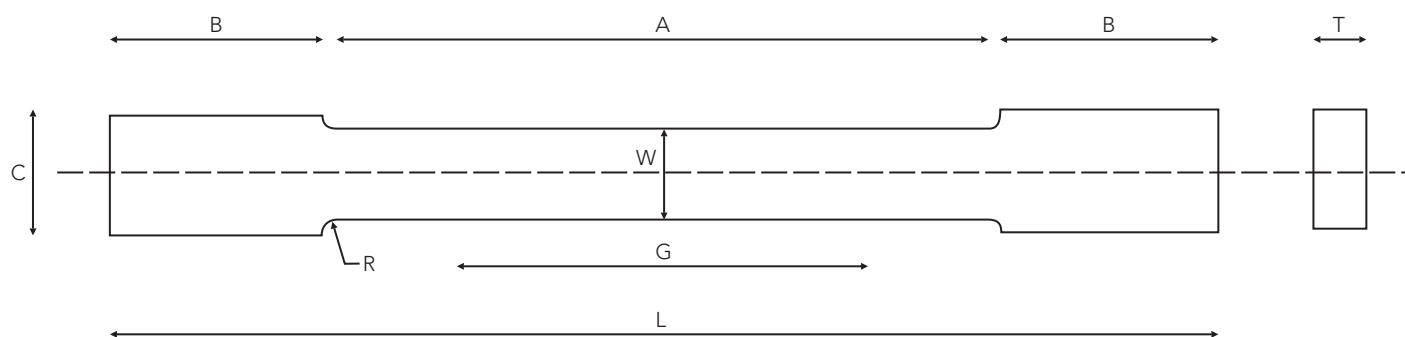


Figure 1: Dimension of tension test coupon

content in microalloyed steel produces a material with higher strength and lower ductility. Addition of Phosphorus of 0.10% improves the strength and corrosion resistance. Presence of Titanium leads to stabilization of steel and it improves resistance to inter-granular corrosion. Titanium added in amounts of 0.1-0.2% which combines with carbon to form titanium carbides, which are quite stable and hard to dissolve in steel, this tends to minimize the occurrence of inter-granular corrosion. For the sample considered, the titanium proportion is 0.123% which is well within the limit.

### 3. TENSILE TESTS

Tensile test is conducted on hot rolled, cold formed and Titanium microalloyed steel samples for determining the mechanical properties (Table 2) as per ASTM E8/E8M-11: Standard Test Methods for Tension Testing of Metallic Materials.

The dimensions of the tensile coupon are shown in Figure 1. The overall length of the coupon (L) is 410 mm. The length of the reduced section (A) is 230 mm. The length (B) and width (C) of grip section is 75 and 50 mm respectively. The width (W) and thickness (T) of the coupon is 40 and 10 mm respectively. During a tension test, it is desirable to apply forces to the specimen large enough to break it and the rate of the force should be in such a way that the rate of the strain of the steel specimen less than 0.1%. The test is conducted in a Universal Testing Machine (UTM) of 50 Tons capacity. Four specimens are tested for each category and the specimen id's are given as S1, S2, S3 and S4. The tensile coupons, fracture of the microalloyed steel sample and the failure surface of the specimen are shown in Figure 2 (a-c). The stress-strain curve for three different types of steel are shown in Figure 3. The yield stress is indicated by star symbol and the respective strain is the yield strain. Microalloyed steel reported the highest yield strength  $f_y$  of 802 MPa compared to

Table 2: Results from tensile tests

TYPES OF STEEL	YOUNG'S MODULUS	YIELD STRENGTH	ULTIMATE STRENGTH	% ELONGATION	POISSON'S RATIO $\mu$
	$E$ (N/mm <sup>2</sup> )	$f_y$ (N/mm <sup>2</sup> )	$f_u$ (N/mm <sup>2</sup> )		
Hot rolled steel	200000	275	426	25.9	0.3
Cold formed steel	205000	290	489	23.7	0.3
Microalloyed steel	210000	802	839	12.1	0.29



Figure 2: Tensile tests on microalloyed steel a) Test specimens b) Fracture c) Failure surface

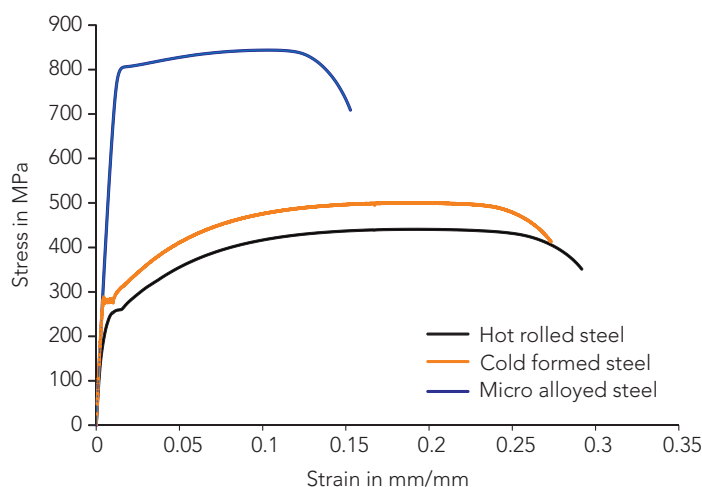


Figure 3: Stress-strain behaviour of hot rolled, cold formed and microalloyed steel

other types of steel due to the presence of alloying element, Titanium. Also, it undergoes less plastic deformation (12.1%), while hot rolled and cold formed steel undergoes large deformation before failure. This indicates that microalloyed steel samples tested possesses high strength and low ductility compared to hot rolled and cold formed steel.

## 4. CORROSION TESTS

Corrosion properties of microalloyed steel in different corrosive environments are studied electrochemically. The electrolytes used are hydrochloric acid solution (1.0M), nitric acid solution (1.0M) and 3.0% sodium chloride with Simulated Pore Solution (SPS). Saturated calcium hydroxide,  $\text{Ca}(\text{OH})_2$  with a pH equal to 12.5 is used to simulate the concrete pore solution. Sodium chloride (NaCl) is added in to the simulated pore solution electrolyte to create sea water environment, in order to understand the chloride attack on microalloyed steel. The microalloyed steel samples (1 cm x 1 cm) are abraded by using successive grit size of SiC-coated abrasive papers (220, 320, 400, 600, 800, 1000, 1200 and 1500 respectively), followed by 0.1  $\mu\text{m}$  diamond paste until it reaches mirror finish. Then thorough rinsing with deionized water and acetone are carried out on the steel samples. The polished microalloyed specimens are shown in Figure 4.

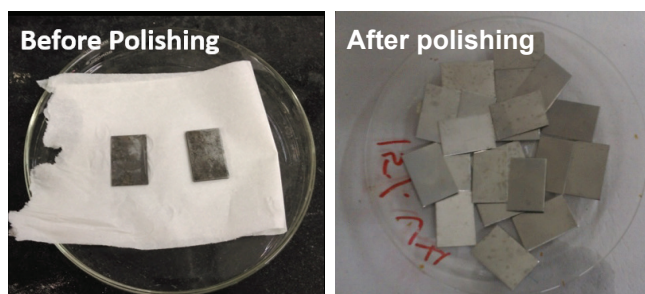


Figure 4: Microalloyed steel specimens before and after polishing

## 4.1 Electrochemical corrosion of microalloyed steel in various corrosive medium

The electrochemical technique employed is potentiodynamic polarisation (anodic and cathodic polarization). The steel samples are put in a special holder electrochemical cell for measurements. The corrosion tests are performed in an Autolab Potentiostat and Galvanostat (PG STAT 100) workstation with electrochemical cell supporting 100 mL electrolyte (corrosive solutions) at 298 K. The Luggin capillary bridge arrangement present in the set-up is to minimize ohmic polarization (Bhuvaneshwari et al. 2015; Balasubramaniam et al. 2018). The  $P_t$  foil and calomel electrode are used as the counter and reference electrodes, respectively. The steel sample having a mirror finished surface forms the working electrode (1 cm x 1 cm). All the three electrodes are placed in the cell containing corrosive solution for 30 min and the corrosion potential is automatically recorded. The polarization studies are conducted with the potential range from  $\pm 250$  mV to the OCP with 1 mV/s scan rate. The studies are conducted with static working electrode, naturally aerated electrolytes at a controlled temperature of  $298 \pm 1$  K. Reading is taken every 24 hours continuously for ten days. The above steps are repeated for other two acids. The corrosion experiment data is based on the triplicate experiments conducted.

Automatic generation of graph is obtained and saved by using NOVA software. In general, for corrosion system, the Tafel extrapolation method is used to describe the anodic and cathodic reactions of process, which forms basic for the Butler-Volmer equation, as shown in Equation 1.

$$I = I_a + I_c = I_{corr} [e^{(2.3(E-E_{oc})/\beta_a)} - e^{(-2.3(E-E_{oc})/\beta_c)}] \quad (1)$$

where,

$I$  = measured cell current (amps);  $I_{corr}$  = corrosion current (amps);  $E$  = electrode potential (volts),  $E_{oc}$  = corrosion potential (volts);  $\beta_a$  = anodic Beta Tafel Constant in volts/decade;  $\beta_c$  = the cathodic Beta Tafel Constant in volts/decade.

### 4.1.1 Potentiodynamic polarization measurements

The electrochemical workstation and three cell electrodes corrosion set up used for conducting corrosion studies of the microalloyed steel is shown in Figure 5. The anodic and cathodic polarization behavior of microalloyed steel exposed in 1M HCl, 1M  $\text{HNO}_3$  as well as 3% NaCl contaminated pore solution are shown in Figure 6. It is clear from the Tafel plots that both anodic and cathodic reactions of microalloyed steel electrodes are seriously corroded with increase in the duration of exposure time especially in the harsh environmental conditions. Heavy metal loss is also noticed, which results in the exposure area

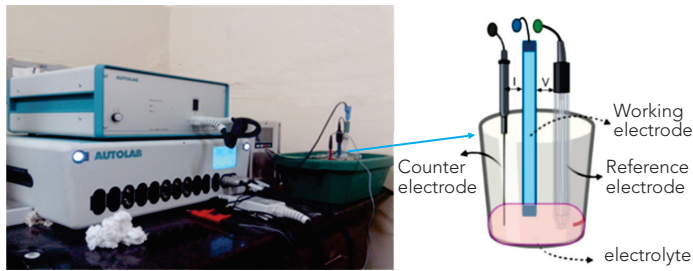


Figure 5: Electrochemical workstation and corrosion set up with three cell electrodes

reduction, thereby decrease in corrosion current is noticed. However, the severe damage is occurred at initial stage itself (within 24 hrs exposure). It is obvious that the polarization plots display a cathodic region of Tafel behavior. On the other hand, the anodic polarization curves do not display an extensive Tafel region, which may be due to the deposition of the corrosion products or impurities on the steel (e.g.,  $\text{Fe}_3\text{C}$ ) to form a non-passive surface film. The electrochemical parameters like corrosion potential ( $E_{\text{corr}}$ ) and corrosion current density ( $I_{\text{corr}}$ ) according to potentiodynamic polarization studies are presented in Table 3.

Results mainly point out the following: The  $I_{\text{corr}}$  values decreased with increase in exposure time. Initial high value of corrosion current is corresponding to the active sites of steel surfaces, which is very high for the microalloyed steel exposed to harsh acidic environments. The corrosion current progressively declines as a result of passivity due to native oxide layers up to some extent and then majorly due to the reduction of exposed surface area. Hence, the grain boundaries might have affected heavily in the case of steels exposed in acidic medium at the initial days of exposure itself, that promoted the metal loss. This may affect the long-term properties as well as strength of the microalloyed steel, when it is used for harsh environment-based applications. However, the initial days of exposure of steel into the chloride contaminated concrete pore solution does not create much corrosion loss to the metal, as observed from the corrosion current. The reactivity is explored in the order as  $\text{HNO}_3$  and  $\text{HCl} > 3\% \text{ NaCl} + \text{pore solution}$ , which reiterates that the corrosive species is more reactive to the metal. Also,  $E_{\text{corr}}$  value has shifted towards more negative potential. As it is known that corrosion is a steady state condition, however the corrosion potential is dynamic situation and depends on the

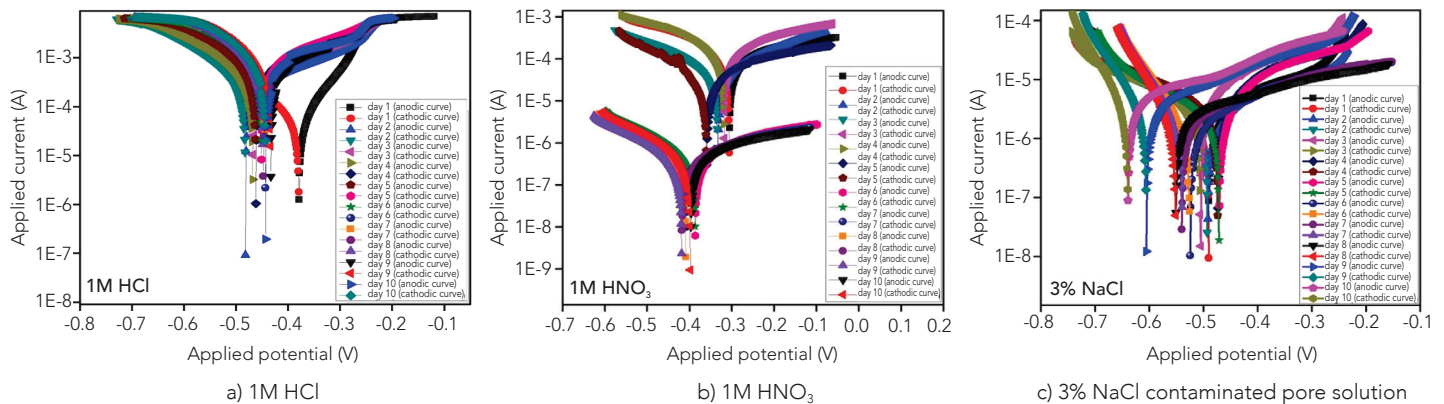


Figure 6: Tafel plots for the corrosion of microalloyed steel in various corrosive mediums

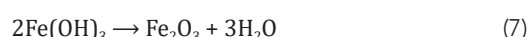
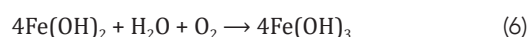
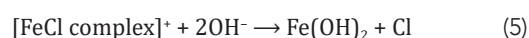
Table 3: Electrochemical parameters of microalloyed steel in various corrosive mediums

EXPOSURE TIME	HCl MEDIUM		HNO <sub>3</sub> MEDIUM		NaCl + SCP MEDIUM	
	$I_{\text{corr}}$ (mA/cm <sup>2</sup> )	$-E_{\text{corr}}$ (mV)	$I_{\text{corr}}$ (mA/cm <sup>2</sup> )	$-E_{\text{corr}}$ (mV)	$I_{\text{corr}}$ (mA/cm <sup>2</sup> )	$-E_{\text{corr}}$ (mV)
Day 1	22.74	379.01	23.67	318.33	49.431	506.28
Day 2	10.01	429.72	12.52	305.87	44.851	471.28
Day 3	5.91	433.56	2.11	359.83	41.986	473.94
Day 4	3.19	443.43	1.42	333.30	25.112	490.62
Day 5	-	-	0.15	408.76	22.192	492.31
Day 6	2.42	452.49	0.14	398.16	6.2847	524.61
Day 7	1.22	447.89	-	-	4.4621	540.17
Day 8	1.00	451.51	0.14	386.60	2.7074	551.25
Day 9	0.18	462.24	-	-	2.4098	605.25
Day 10	0.12	468.19	1.27	418.76	1.8992	639.31



thermodynamic parameters of the system. Also, the metals exposed to harsh acidic environmental conditions, mainly in  $\text{HNO}_3$  medium, have shown a drastic change in potential shift which depicts the interference of corrosion products formed in-situ. That could be due to formation or depletion of native oxide layer; or mainly by the nature of the corrosion product itself. The decrease in corrosion current density is due to the severe reduction in the original area of the metal. This difference indicates the behavior of grain boundary attacks due to acidic medium exposure. In order to bring discussion on the corrosion effect of grain boundaries and the metallurgical phases of microalloyed steels under harsh acidic environmental conditions, X-ray diffractational study is needed to understand their metallurgical property correlation. That study is beyond the scope of this paper. McCafferty (2005) had presented a valuable study concerning validity of the Tafel extrapolation method for measuring corrosion rates by using both the anodic and cathodic Tafel regions. It is inferred from the present study that, when corrosion reaction time is more than the anodic dissolution of steel, the cathodic hydrogen evolution reaction will also be increased. From the potentiodynamic polarization curves of microalloyed steel exposed to acidic mediums, as shown in Figure 6, there is no sharp slope in the anodic range, which mentions about the less or no passive films formation on the metal surface (John *et al.* 2011). As per corrosion theory, the shift noticed in the cathodic curves of the microalloyed steel in the acidic environments explains that the corrosion process mainly occurs by the cathodic reactions (Seikh 2013). However, in the case of microalloyed steel exposed to chloride simulated pore solution environment, both the anodic and cathodic shifts are visible, which may be due to the grain refinement happening at the time of corrosion reaction, enhancing the passive film formation at some point and also resist the further dissolution of iron. The following mechanism explains the steel oxidation reaction (Seikh 2013) during corrosion process.

As far as steel is concerned, iron gets oxidized at the anodic site and releases electrons in the presence of oxygen (Equation 2). At the cathode side, generally oxygen combines with moisture, and form hydroxyl ions upon the release of electrons at the anode (Equation 3).



- While chloride ions present in the solution, iron at the anode side gets oxidized (Equation 3) and it forms a

soluble iron-chloride complex as the ferrous ions react with chloride ions (Equation 4). After that, formation of ferrous hydroxide occurs due to the reaction of iron-chloride complex with hydroxyl ions (Equation 5), resulting in a greenish black product.

- Next, oxidation of ferrous hydroxide to ferric hydroxide happens, which in turn dehydrates to form ferric oxide (Equations 6 and 7).
- In the cathode side, formation of hydroxyl ions occurs due to the reaction of oxygen with moisture, then the release of electrons begins at the anode side as explained before (Equation 3). According to the reaction stated in Equations 4 and 5, the chloride ions are still present in the solution, which contributes further for the occurrence of corrosion.

The initial dissolution of metal in the harsh acidic environments as noticed from the polarisation results indicate that the Titanium microalloyed steel used in this study may not be suitable for harsh environment applications namely pipeline construction, where the acidic and gaseous environment dominates; however, the initial stability of the microalloyed steel in the chloride contaminated simulated pore solution environment is quite high compared to the acidic environment exposures. Hence, based on the electrochemical studies, it can be concluded that the microalloyed steel can be a good choice for structural construction applications. With proper corrosion protection coating, the use of Titanium microalloyed steel in harsh environment needs to be explored as well.

## 5. VISUAL AND SCANNING ELECTRON MICROSCOPE (SEM) ANALYSIS

The corrosion effect on microalloyed steel under different environmental conditions are shown in Figure 7. Based on the visual observations, it is found that the corrosion effect is much higher on the microalloyed steel exposed to harsh acidic environments as it developed more pits (indicated by white arrows) and large holes (indicated by circles) as shown in Figure 7. Most of the exposed steel surfaces are completely damaged or the area is reduced, thereby less corrosion current is resulted during the electrochemical studies of microalloyed steel under acidic environments. In the case of microalloyed steel exposed to SCP+NaCl medium, the corrosion attack is less significant and not much damage noticed. Hence, the corrosion current has gradually decreased. The reason for the decrease in the corrosion current of steel with respect to exposure days in the harsh acidic environmental exposure is due to the severe corrosion attack occurred in the early stage itself, thereby the area exposed got significantly reduced. So, the drastic changes in corrosion current are noticed. Otherwise, the scenario would be different. Further, SEM study is conducted to identify the

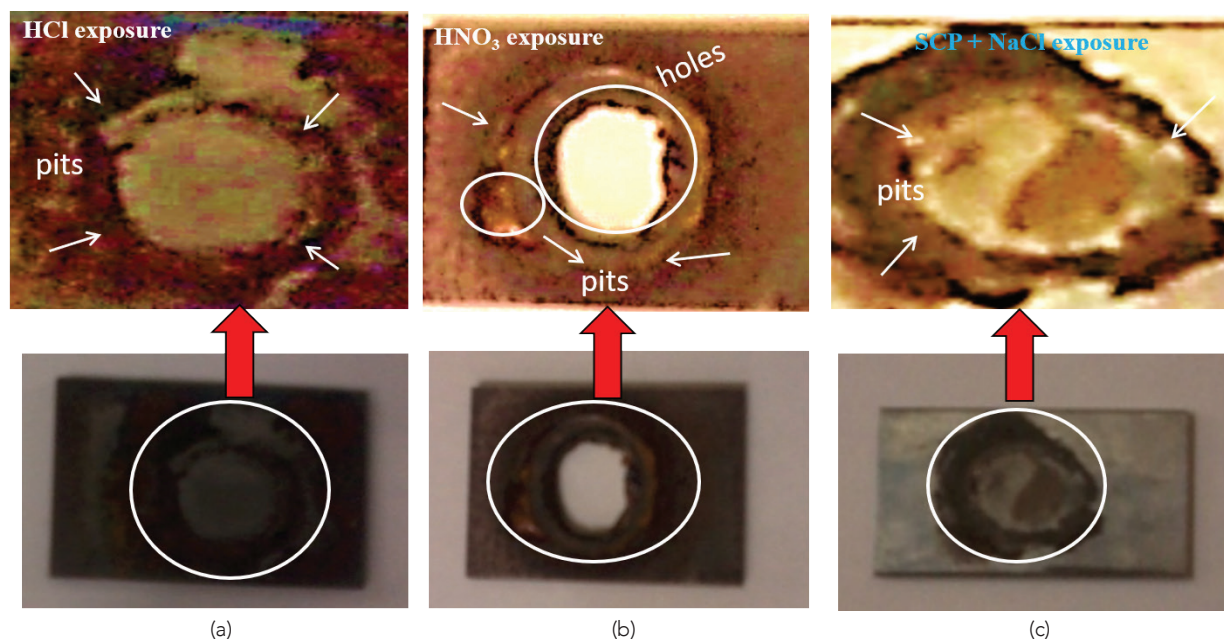


Figure 7: Visual observation on the corrosion of microalloyed steel exposed to (a) HCl, (b) HNO<sub>3</sub> and (c) SCP+NaCl mediums

micro and macro structural damages occurred on steel surfaces in the presence of corrosive medium. SEM images are acquired on a Hitachi S3200N (Tokyo, Japan) system. The secondary electron images are taken at a chamber pressure of 50 Pa with an electron beam of 20 kV. Microstructural studies on steel surfaces, before and after the performing the corrosion tests are shown in Figure 8. The clean, polished microalloyed steel surface depicts the defect free surfaces without any sign of pits and holes (Figure 8a). After the occurrence of corrosion, the microalloyed steel surfaces exposed in corrosive solutions became heterogeneous in nature which is evident in the general and pitting corrosion related corrosion attacks. These pits as indicated by arrows in Figure 8b and c are full of black corrosion products. These observations can be explained

on the basis of corrosive ion activity and the extent of its contribution in acceleration of metal dissolution (Figure 8b and 8c). As evidenced from Figure 8c, the large and small holes (as indicated by circles) expose the severity of the HNO<sub>3</sub> environment on the corrosion of microalloyed steel. However, only less microstructural damages are evidenced from SEM images of the microalloyed steel exposed to chloride simulated pore solution environment (Figure 8d). The corrosion pits and holes are marked in the corresponding SEM figures of the microalloyed steel exposed to HCl, HNO<sub>3</sub> and SCP+NaCl mediums. Further, SEM studies also support the findings from polarisation experiments. Based on the morphological studies, it can be concluded that the microstructural damages observed for the microalloyed steel exposed to harsh acidic environments are very high compared to the chloride simulated concrete pore solution environment. Hence, the Titanium microalloyed steel employed in the present study can be a good or alternate choice for concrete or steel composite applications, however their usage in pipeline construction (where the acidic and gaseous environment dominates) and marine related applications need further experimental investigations with proper corrosion protection coating.

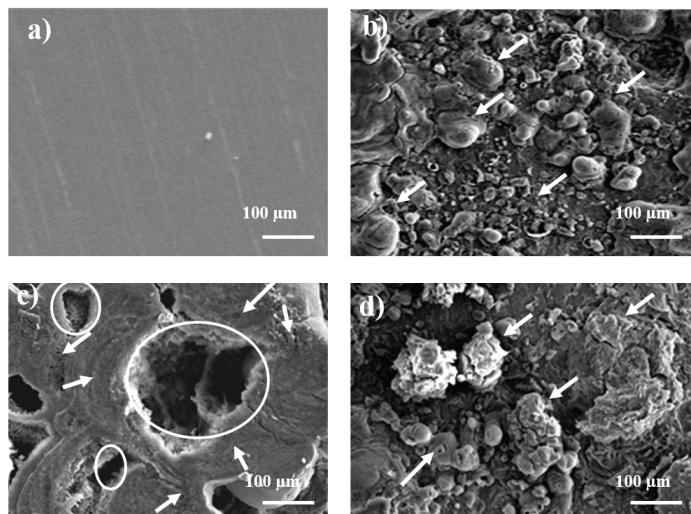


Figure 8: SEM observations on the surface morphology of microalloyed steel exposed to various environments (a) after polishing (b) HCl medium (c) HNO<sub>3</sub> medium (d) SCP+NaCl medium

## 6. SUMMARY AND CONCLUSIONS

The various properties of microalloyed steel are studied by conducting chemical analysis, tensile tests, corrosion tests by electrochemical analysis and SEM analysis of steel sample specimens. Chemical analysis is carried out by optical emission spectroscopy. Tensile test is conducted by using a universal testing machine. The following conclusions are drawn from the studies.

- Chemical analysis results confirm the presence of Ti microalloying in the microalloyed steel.
- Tensile tests revealed the very high yield strength and reduced ductility of HSLA steel samples compared to hot rolled and cold formed steel samples.
- Polarization measurements indicate that the corrosive nature of steel under highly acidic environments is very high compared to the chloride attack simulated with the concrete pore solution environment. High corrosion current is observed in the initial days of exposure in itself for the microalloyed steel exposed in the harsh acidic environments due to the heavy metal loss.
- The surface morphological studies also supported the high corrosion damages occurred in the microalloyed steel exposed to harsh acidic environments compared to the specimens subjected to chloride induced corrosion.

Based on the results from the present study, microalloyed steel showed a good tensile strength and as far as corrosion is concerned, not much severity is noticed when exposed to concrete pore solution environment. However, in an acidic environment, more severe corrosion is evident. The Titanium microalloyed steel used in this study can be a good choice for steel/concrete composite applications as the steel stabilities against corrosion is comparatively well in the simulated concrete environments. At present microalloyed steel is not used commonly in structures in India. Further studies investigating various other physical, chemical, mechanical and durability properties of microalloyed steel need to be conducted to promote the usage of HSLA steel in India.

## ACKNOWLEDGMENTS

The authors express their gratitude to the Director, CSIR-SERC for their support. The authors acknowledge CSIR-Structural Engineering Research Centre Grant No: 12<sup>th</sup> FYP eNano-Tics and I HEAL. The assistance provided by the Project Assistants & Students of Steel Structures Laboratory and Chemistry Lab of CSIR-SERC are also acknowledged. Dr. B. Bhuvaneshwari acknowledges the DST Women Scientist Fellowship (Award Number: SR/WOS-A/CS-17/2017).

## REFERENCES

- [1] Villalobos., Julio, C., Adrian Del-Pozo., Bernardo Campillo., Jan Mayen. and Sergio Serna. (2018). "Microalloyed Steels through History until 2018: Review of Chemical Composition, Processing and Hydrogen Service", *Metals*, Vol. 8, pp. 351.
- [2] Xie, H., Du, L.X., Hu, J. and Misra, R.D.K. (2014). "Microstructure and mechanical properties of a novel 1000 MPa grade TMCP low carbon microalloyed steel with combination of high strength and excellent toughness", *Mater. Sci. Eng. A*, Vol. A612, pp. 123–130.
- [3] HE., Xin-lai., Cheng-jia SHANG., Shan-wu YANG., Xue-min WANG. and Hui GUO. (2007). "High performance low carbon bainitic steel—refinement principle and application [J]", *Heat Treatment of Metals*, pp. 12.
- [4] Gladman, Terrence. "The physical metallurgy of microalloyed steels", Maney Publications.
- [5] Xie, Kelvin. Y., Tianxiao Zheng., Julie, M. Cairney., Harold Kaul., James, G. Williams., Frank, J. Barbaro., Chris, R. Killmore., and Simon, P. Ringer. (2012). "Strengthening from Nb-rich clusters in a Nb-microalloyed steel", *Scripta Materialia*, Vol. 66, pp. 710-13.
- [6] Rasouli., Dariush., Shahab Asl., Akbarzadeh, a., and Daneshi, G. (2008). "Effect of cooling rate on the microstructure and mechanical properties of microalloyed forging steel", *Journal of Materials Processing Technology*, Vol. 206, pp. 92-98.
- [7] Skobir, Danijela. (2011). "High-strength low-alloy (HSLA) steels, *Materials and Technologies*, Vol. 45, pp. 295-301.
- [8] Sherif, El-Sayed. and Asiful Seikh. (2012). "Effects of Grain Refinement on the Corrosion Behaviour of Microalloyed Steel in Sulphuric Acid Solutions", *International Journal of Electrochemical Science*, pp. 7.
- [9] Seikh Asiful Hossain. (2013). "Influence of Heat Treatment on the Corrosion of Microalloyed Steel in Sodium Chloride Solution", *Journal of Chemistry*, 587514.
- [10] Liu, Sheng., Di Tang., Huibin Wu., and Lidong Wang. (2013). "Oxide scales characterization of micro-alloyed steel at high temperature", *Journal of Materials Processing Technology*, Vol. 213, pp. 1068-75.
- [11] Bandga. R, Sachin., Chiradeep Gupta., Gaurav Rao., Pranshu Malik., Singh, R.N., and Sridhar, K. (2019). "Fatigue Crack Growth Rate Behaviour of HSLA Steel at Varying Load Amplitudes", *Procedia Structural Integrity*, Vol. 14, pp. 330-36.
- [12] Janardhan Gorti., Kaushal Kishore., Krishna Dutta., and Goutam Mukhopadhyay. (2020). "Tensile and fatigue behavior of resistance spot-welded HSLA steel sheets: Effect of pre-strain in association with dislocation density", *Materials Science and Engineering: A*, Vol. 793: 139796.
- [13] IS 513. (2008). "Indian Standard for Cold Reduced Low Carbon Steel Sheet And Strip", Bureau of Indian Standards, New Delhi.

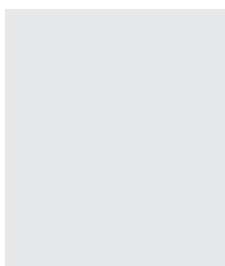
- [14] ASTM E8/E8M-11. (2011). "Standard Test Methods for Tension Testing of Metallic Materials", West Conshohocken, (Pennsylvania): ASTM International. doi: [https://doi.org/10.1520/E0008\\_E0008M-11](https://doi.org/10.1520/E0008_E0008M-11).
- [15] IS 2062. (2011). "Indian Standard for Hot Rolled Medium And High Tensile Structural Steel - Specification", Bureau of Indian Standards, New Delhi.
- [16] Bhuvaneshwari, B., Selvaraj, A., Iyer, N.R., and Ravikumar, L. (2015). "Electrochemical investigations on the performance of newly synthesized azomethine polyester on rebar corrosion", *Materials and Corrosion*, Vol. 66, pp. 387-95.
- [17] Balasubramaniam, Bhuvaneshwari., Athiramu Selvaraj., Nagesh R. Iyer., Lingam Ravikumar., Prabhat K. Rai., Mondal, K., and Raju Kumar Gupta. (2018). "Electrochemical and microstructural analysis of azomethine polyamides as inhibitor for rebar corrosion under chloride contaminated pore solution", *Frontier Research Today*, Vol. 1, pp. 1004.
- [18] McCafferty, E. (2005). "Validation of corrosion rates measured by the Tafel extrapolation method", *Corrosion Science*, Vol. 47, pp. 3202-15.
- [19] John, SAM., Mohammad Ali., and Abraham Joseph. (2011). "Electrochemical, surface analytical and quantum chemical studies on Schiff bases of 4-amino-4H-1, 2, 4-triazole-3, 5-dimethanol (ATD) in corrosion protection of aluminium in 1N HNO<sub>3</sub>", *Bulletin of Materials Science*, Vol. 34, pp. 1245-56.



**B. BHUVANESHWARI** is a DST Women Scientist at the Department of Chemical Engineering, Indian Institute of Technology, Kanpur, India. She completed her Ph.D. in Chemistry (2013) in India. Her research interests include polymer synthesis, corrosion analysis, nanocomposites for energy applications, cryogenic treatment of metals, repair and retrofitting of structures, computational modelling and environmental applications. Email: [bhuvib@iitk.ac.in](mailto:bhuvib@iitk.ac.in).



**P. PRABHA** is presently Principal Scientist at CSIR-Structural Engineering Research Centre Chennai and has more than 13 years of R&D experience. Her field of research includes Cellular lightweight foamed concrete, Hot rolled and cold formed steel structures, Steel-concrete composite Structures, Prefab/precast technology for housing, Finite Element Modelling. Email: [prabha@serc.res.in](mailto:prabha@serc.res.in)



**S. SANDHIYA** has completed her B.E in University College of Engineering, Ramanathapuram, India. She did her project work at CSIR- Structural Engineering Research Centre, Chennai. She gained experience in the field of steel characterisation methods. Email: [sandhiyadce@gmail.com](mailto:sandhiyadce@gmail.com)



**G. S. PALANI** is presently Chief Scientist at CSIR-Structural Engineering Research Centre, Chennai and has R&D experience of more than 32 years. His field of research interest include finite element analysis, fatigue and fracture analysis, steel structures, design and testing of transmission line and communication towers. Email: [pal@serc.res.in](mailto:pal@serc.res.in)

**Cite this article:** Bhuvaneshwari, B., Prabha, P., Sandhiya, S., and Palani, G.S. (2021). "Mechanical and electrochemical aspects of microalloyed steel", *The Indian Concrete Journal*, Vol. 95, No. 4, pp. 52-60.



# CATHODIC PROTECTION OF STEEL REINFORCEMENT: PAST EXPERIENCE, PERFORMANCE AND FUTURE OPPORTUNITIES

GEORGE SERGI\*

## Abstract

Impressed current cathodic protection (ICCP), following on from its early success in buried pipelines and submerged structures, was trialled on atmospherically exposed steel reinforced structures in the 1970's, first in the USA on bridge decks and then more extensively in the UK as new and better performing inert anodes were developed. Cathodic Protection (CP) of steel reinforced concrete soon became a well-established technique for controlling reinforcement corrosion of structural elements. Long-term maintenance of ICCP systems, however, started to be seen as a burden to most structure owners and managers as it involves additional and continual costs. A requirement arose, therefore, for simpler CP systems to be made available which will involve less maintenance and monitoring requirements. As a first stage to simpler systems, galvanic cathodic protection anodes were developed in the 1990's, first, only to protect steel reinforcement immediately around patch repairs but subsequently to control reinforcement corrosion over wider areas where corrosion risk was found to be high. It was the combination of ICCP and galvanic anode systems, however, that set the benchmark for a simpler alternative long-term method for corrosion control of steel reinforcement. This paper attempts to follow the development of all CP systems utilized for atmospherically exposed steel reinforced structural elements and looks at recently developed simpler systems and methodologies that would likely form the future of the CP industry.

**Keywords:** Cathodic Protection, Cathodic Prevention, Galvanic CP, Corrosion Arrest, Two-Stage CP.

## 1. INTRODUCTION

Concrete normally contains an alkaline pore liquid phase which protects embedded steel from corrosion by allowing a highly dense passive oxide film to develop on its surface when oxygen is available. This form of protection can be lost, however,

if the concrete undergoes either carbonation or chloride contamination in the vicinity of the steel. Such effects can lead to cracking and spalling of the cover concrete. In cases of chloride-induced corrosion, pitting develops at localised sites, whilst the remainder of the surface remains passive providing a large cathodic area for oxygen reduction which drives the corrosion.

For alkaline concrete, corrosion of steel may be expected to vary with potential and chloride content of the concrete, as illustrated by Bertolini *et al.* <sup>(1)</sup> and summarised in Figure 1. Domain A represents conditions that can lead to the initiation and propagation of pits on initially passive steel. Domain B signifies conditions that allow pre-existing pits to propagate but do not favour the initiation of new pits on initially passive steel. Domain C indicates conditions that do not allow the initiation and propagation of pits, so that pre-existing pits tend to repassivate. Finally, Domains D and E represent conditions that lead to highly negative potentials and are sufficiently reducing to render the passive film unstable. In such cases, hydrogen is formed cathodically, increasing the risk of hydrogen embrittlement of pre-stressed steel tendons. Thermodynamically, therefore, forcing the potential of the steel into Domain C by applying sufficient cathodic current (4 to 6) would ensure that no new pits will propagate, and existing pits will gradually repassivate. Even if polarisation is only sufficient to place the steel potential in Domain B (4 to 5), the development of new pits cannot occur and a reduction in the intensity of corrosion in any pre-existing pits will diminish depending on the level of polarisation.

What Figure 1 also demonstrates quite elegantly is that an increasing level of chloride reduces the steel potential at which pitting can occur (pitting potential) and at which repassivation is possible (repassivation potential) so that an increasing cathodic current is required to force the potential of the steel below these levels as the chloride contamination rises. At the other extreme, there is a minimum concentration of chloride below which pitting is not possible. This, of course, assumes a fixed level of alkali in the concrete. Applying a cathodic current to steel,

\*Corresponding author : George Sergi, Email: georges@Vector-Corrosion.com

however, ensures the production of hydroxyl ions on the surface of the steel from the cathodic reaction (Equation 1).



The applied electric field also attracts alkali cations, present in the pore electrolyte, such as  $\text{Na}^+$ ,  $\text{K}^+$  and  $\text{Ca}^{2+}$ , to the now negatively charged steel. The opposite occurs with the negatively charged  $\text{Cl}^-$  anions which are repelled away from the steel. The reduction of the destructive  $\text{Cl}^-$  ions renders the surrounding electrolyte less aggressive to the steel. Aided by the increase in alkali, which maintains the steel passive, the thermodynamic equilibrium moves to the left, as indicated in Figure 1 by the thick arrow. It would be reasonable to suggest that the chloride concentration axis can be changed to a ratio of chloride to hydroxyl ionic concentration, enabling the potential passivation of the steel with time as  $[\text{Cl}^-]/[\text{OH}^-]$  reduces, even if the level of steel polarisation remains the same (5 to 7 to 8, Figure 1). These aspects will be elaborated further later in the article.

Understanding of these principles was essential for the development and evolution of CP of reinforcing steel in concrete. As an example, the recognition that the primary objective of CP, unlike cases such as buried pipelines and submerged steel structures where total immunity is required (Domains D and E in Figure 1), is simply to reduce the susceptibility of the metal to pitting in the presence of chloride ions was a major development. To achieve adequate CP in a structure in which chloride-induced corrosion has been occurring for some time, it is only necessary to polarize the steel from its condition of pitting (Domain A) to Domain C where pitting is unstable. Thus, complete repassivation of the steel can be achieved.

A development in Italy, which demonstrated a clear understanding of the principles of CP in reinforced concrete, was the application of CP on prestressed concrete viaducts as a means of preventing the initiation of corrosion. In such cases, even though the structures may be exposed to chlorides, their

low concentrations near the reinforcement as they are being repelled away are unlikely to cause depassivation, so only modest polarization is needed, typically an impressed current density of about  $0.4\text{--}2 \text{ mA/m}^2$  (1 to 2 in Figure 1), to maintain the steel at a potential where pits cannot initiate. Bertolini et al termed this Cathodic Prevention<sup>[1]</sup>. As chloride penetration progresses, it must of course be ensured that the potential remains below the upper boundary of the imperfect passivity domain (2 to 3 in Figure 1) but much higher chloride levels can be tolerated at the steel before corrosion can initiate.

Further interesting proposals have also surfaced at different times. Intermittent CP in marine tidal locations, where remote anode systems in seawater might be employed, and the use of solar powered impressed current CP where low levels of polarisation are required<sup>[2]</sup> are examples of this. Another interesting application on which this paper will concentrate on, is the use of galvanic anodes to protect both regions of the steel reinforcement susceptible to corrosion following a conventional patch repair in chloride-contaminated concrete and as a means of reducing the corrosion activity of the steel reinforcement where chlorides have penetrated the cover concrete to the steel and have initiated corrosion<sup>[3,4]</sup>. The use of galvanic anodes to prevent re-initiation of corrosion of the steel following a short period of intense ICCP with the intension of arresting corrosion is perhaps the major recent development in the technology which may drive the future of CP.

## 2. HISTORICAL DEVELOPMENT OF CP FOR STEEL REINFORCED CONCRETE

The earliest recorded applications of CP to steel in concrete were for buried pipelines<sup>[5,6]</sup>. In such cases, where the material is surrounded by a conductive electrolyte such as groundwater or damp soil, it is possible to use discrete anode systems to distribute the current to the steel reinforcement. Several such uses of CP have been described involving both impressed current and sacrificial anodes<sup>[7]</sup>.

In atmospherically exposed reinforced concrete, it is technically much more difficult to apply CP because of the need to ensure a reasonably uniform current distribution in a concrete electrolyte of fairly high resistivity. To comply with this requirement, initially only externally applied DC power supplies were considered which required the necessary development of inert anode systems that meet the following conditions:

- capable of being applied to concrete surfaces or cover concrete in such a way as to allow uniform electrolytic conduction,
- acceptable in terms of weight, cost and durability in service under a wide range of environmental exposure conditions,
- resistant to corrosion and acidification of the surrounding concrete owing to anodic reactions on its surface.

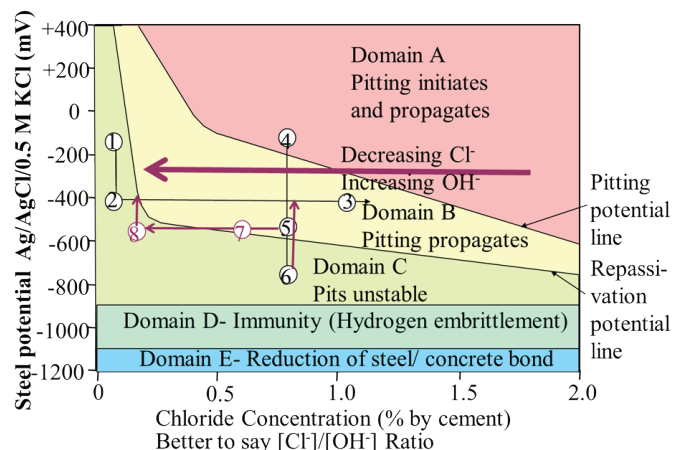


Figure 1: Approximate domains of electrochemical behaviour of steel in concretes with increasing levels of chloride contamination



Figure 2: Graphite-based organic coating applied to the surface of a concrete cross beam (left) and decorative overcoating (right)

Progress in achieving these requirements has been rapid since the earliest reported successful application of CP to a reinforced concrete bridge deck in the USA in 1974<sup>[8]</sup>. In this and other similar cases, the anode system consisted of high silicon cast iron primary anodes in a thick conductive asphalt overlay. A non-conductive asphalt wearing course was applied over the top to prevent wear. The added weight, as well as difficulties of applying the conductive medium in vertical surfaces, effectively prevented the system from being used for structures other than bridge decks and car parks. In the early 1980's, many alternative anode systems were developed which enabled CP to be applied to reinforced concrete in a much wider range of situations, including highway bridge substructures, buildings and marine structures<sup>[9]</sup>. A number of these systems have now been used quite extensively for decades and are considered sufficiently well-proven to be described in some detail in ISO EN 12696: 2016<sup>[10]</sup>. The Standard recognizes that further new and effective anode systems are likely to become available for CP of atmospherically exposed reinforced concrete.

Amongst the anode systems described by the Standard are the following:

- i. organic conductive coatings, normally applied to a dry film thickness in the range 0.25 to 0.5 mm,
- ii. metallic conductive coatings of thermally sprayed zinc, normally applied to a thickness in the range 0.2 to 0.4 mm,
- iii. activated titanium, in various forms such as mesh mounted on the surface of the structure and embedded in a cementitious overlay, thin ribbon buried in continuous slots cut in the cover concrete and lengths of fine mesh rolled in the form of a tube which can be buried in drilled holes in the concrete,
- iv. ceramic conductive titanium oxide tubes inserted in drilled holes in the concrete.

Organic conductive coatings containing graphite have shown variable performance but have a range of effective service lives

of 5 to 15 years when properly applied and operated at current densities below  $20 \text{ mA/m}^2$  in an appropriate environment<sup>[9]</sup>. They do not withstand conditions of continuous wetting or abrasion and undergo gradual degradation at a rate dependent on the applied current density. Reported failure mechanisms involve disbondment, blistering and flaking related to degradation of the cementitious matrix by anodic acidity and oxidation of the organic binder<sup>[11]</sup>. The carbon present in the coating is consumed by the anodic reaction so that enough carbon for the desired lifetime should be incorporated into the coating. They are relatively easy to reapply and are commonly overcoated with grey or white paint to improve appearance, to provide UV protection and to limit heat gain to the structure (Figure 2).

Thermally sprayed zinc may be applied to reinforced concrete by arc or flame spraying (Figure 3) and shows greater tolerance than that of organic conductive coatings to conditions of moisture at the time of application or during service. Poor adhesion of the zinc coating to the concrete substrate is often experienced, however, if the coating thickness exceeds about 0.4 mm<sup>[10]</sup>. Calculated rates of zinc anode consumption suggest that sustained operation at  $20 \text{ mA/m}^2$  would oxidise completely



Figure 3: Thermally sprayed zinc anode applied to the surface of a steel reinforced concrete element



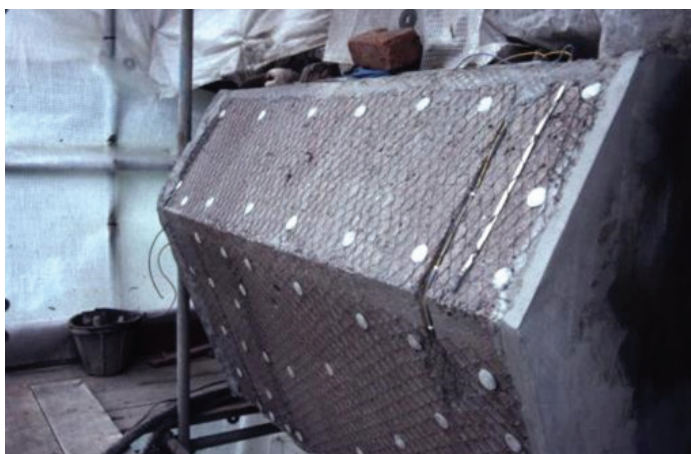


Figure 4: Activated mesh anode fixed on the steel reinforced concrete element prior to the application of a cementitious overlay

a 0.2 mm coating in less than 6 years<sup>[9]</sup>. The reported failure mechanism involves gradual increase in the resistance of the coating owing to zinc corrosion so that the current distribution is likely to become ineffective<sup>[11]</sup>. A range of thickness 0.2-0.4 mm is recommended for optimum performance<sup>[10]</sup> and the current density should not exceed 10 mA/m<sup>2</sup> over significant timescales. This should ensure a lifetime of the order of 25 years for a 0.4 mm coating thickness.

Activated titanium electrodes with proprietary electrocatalytic coatings are available in several forms, the most widely used being an expanded mesh which is normally attached to the surface of reinforced concrete by means of non-metallic fixings and covered with a cementitious overlay of appropriate low resistivity (Figure 4). A variety of such overlays, applied by different means, have been used and their performance is critical to the durability of the anode system. Some failures have occurred due to disbondment of the overlay and these have generally been attributed to deficiencies in surface preparation, pre-treatment or application procedures. Evidence as to whether the substrate/overlay bond strength may be significantly affected by sustained application of CP in certain instances is

somewhat inconclusive<sup>[11]</sup>. The ability of the activated titanium anodes themselves to operate at high current densities (up to 220 mA/m<sup>2</sup>) for short periods is well established but can give rise to acid attack of the surrounding cementitious material<sup>[10]</sup>. This needs to be considered particularly when such anodes are not applied to the surface of a structure but inserted in holes drilled into the concrete and embedded in a cementitious repair mortar with or without a graphite-based backfill. The inclusion of saturated lithium hydroxide in the cementitious mortar has been suggested for the use of discrete titanium oxide anodes which decreases the risk of acidification of the encasement mortar allowing current densities in excess of 220 mA/m<sup>2</sup><sup>[12]</sup>.

All these ICCP systems require the installation of external power supplies such, as transformer rectifiers. To comply with CP standards (see later) carefully controlled long-term current distribution and zoning of the anodes to deliver the required current are essential requirements with the necessity of continual monitoring of the systems.

### 3. CORROSION CONTROL WITH THE USE OF GALVANIC ANODES

A parallel development since the early 1990's has been the introduction and gradual establishment of galvanic anodes, firstly, to control the formation of incipient anodes, often described as the 'ring effect', around the periphery of patch repairs, simply by attaching galvanic anodes to the exposed steel around the perimeter of patch repairs prior to the application of the repair material (Figure 5). Subsequently, more and more applications of continuously improving galvanic anodes have been established with anodes placed in a grid formation (Figure 6) or along the exposed steel reinforcement where applicable (Figure 7).

That galvanic anodes control steel reinforcement corrosion adequately was demonstrated elegantly in large slabs in India<sup>[13]</sup>. These had dimensions of 1 m x 1 m x 0.25 m. Some had nine galvanic anodes attached to the steel members in a 3 x 3 grid



Figure 5: Alkali activated galvanic anodes, as in inset, attached to steel reinforcement prior to the application of the repair material

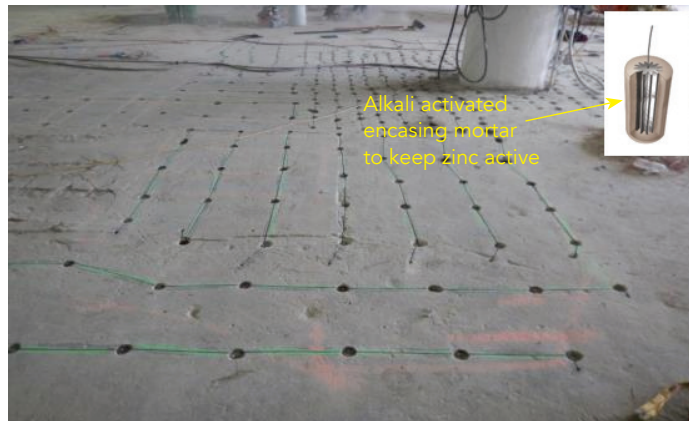


Figure 6: Chains of alkali activated galvanic anodes, as in the inset, placed in drilled holes in the concrete in a grid formation to control corrosion of the steel reinforcement





Figure 7: Alkali activated 'rod' galvanic anodes positioned along steel reinforcement in an expansion joint prior to the placing of the repair mortar

configuration and some were cast with no anodes (Figure 8). All had 2% chloride by weight of cement additions in the mix water, a level that would normally cause significant corrosion of the steel reinforcement. After 10 years of exposure in the outdoor warm and humid conditions of Mumbai, the slabs containing the anodes remained intact (Figure 9) while the slabs with no anodes had suffered from severe corrosion and cracking of the concrete cover (Figure 10).

The mean 24-hour depolarised potential of the protected steel measured from the top surface of the concrete using a saturated calomel reference electrode (SCE) remained passive throughout its life (mean of around -150 mV) whereas that in the non-protected slab was of the order of -400 mV to -600 mV indicating significant corrosion. Corrosion current density values of the steel determined by linear polarisation after around 9 years confirmed the large disparity of the corrosion rate between the two slabs, the protected steel showing insignificant corrosion ( $<0.5 \text{ mA/m}^2$ ) whereas the corrosion current density of the non-protected steel was a very high  $6 \text{ mA/m}^2$ . Anodes were still delivering a protective current density of the order of  $0.4 \text{ mA/m}^2$  by area of steel at the later years, comfortably within the cathodic



Figure 9: Slab protected by galvanic anodes (lines are wires connecting individual anodes and/or steel bars)

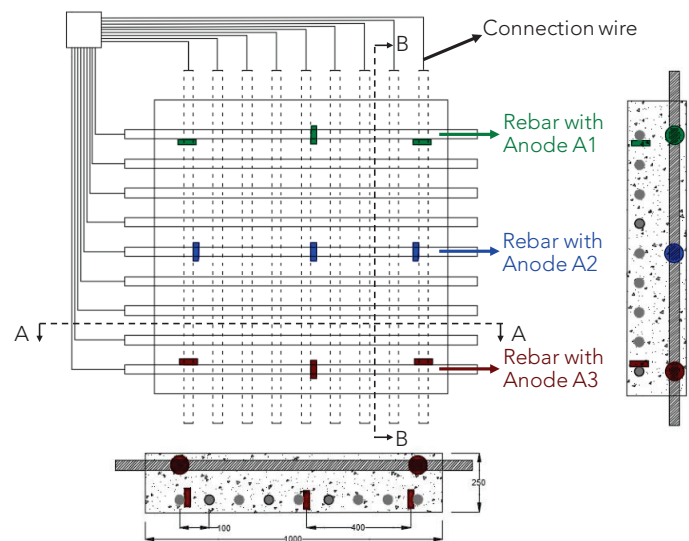


Figure 8: Schematic of concrete slabs showing the position of the 18, 32mm dia steel bars and of the 9 galvanic anodes. Steel bars and anodes were connected externally via a junction box which allowed monitoring of the current and potential of the steel bars 24 hours after disconnection of the anodes (depolarised potential)

prevention current density range of  $0.2\text{-}2.0 \text{ mA/m}^2$  suggested in ISO 12696: 2016<sup>[10]</sup>.

Owing to the relatively low current delivery of galvanic anodes compared to impressed current systems, depolarisation values do not always exceed or reach 100 mV as indicated in Figure 11<sup>[14]</sup>. In the case of ICCP systems, the current output can be adjusted so that it can achieve 100 mV depolarisation, as required by standards<sup>[10]</sup>, and appears to be a limitation with galvanic CP. What is apparent, however, is that the level of polarisation is directly related to the logarithm of current (Figure 11). This is described by the Butler Volmer equation (Equation 2) which relates applied current density to level of polarisation of the steel.

$$i_{corr(app)} = \frac{i_{appl}}{\exp\left(\frac{2.3\eta}{\beta_a}\right) - \exp\left(\frac{-2.3\eta}{\beta_c}\right)} \quad (2)$$



Figure 10: Corroded slab without anode protection showing extent of cracking of the concrete caused by steel corrosion after exposure to outdoor warm and humid conditions for 10 years<sup>[13]</sup>

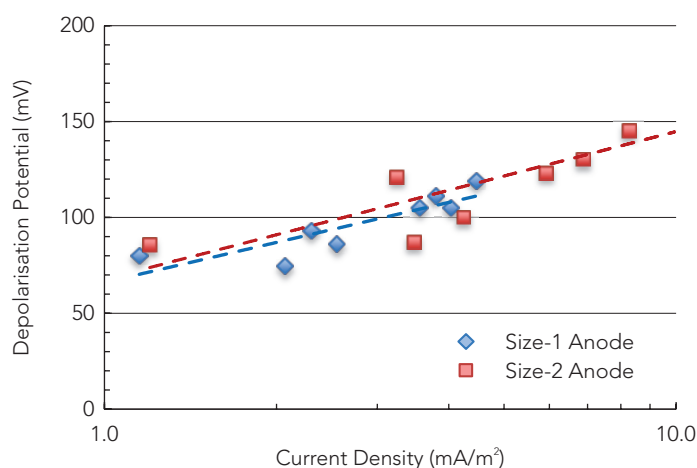


Figure 11: Typical 24-hour depolarisation potentials of steel protected by galvanic anodes of Size 1 (x1 current output) and Size-2 (x2 current output) at a spacing of 300 mm on centre

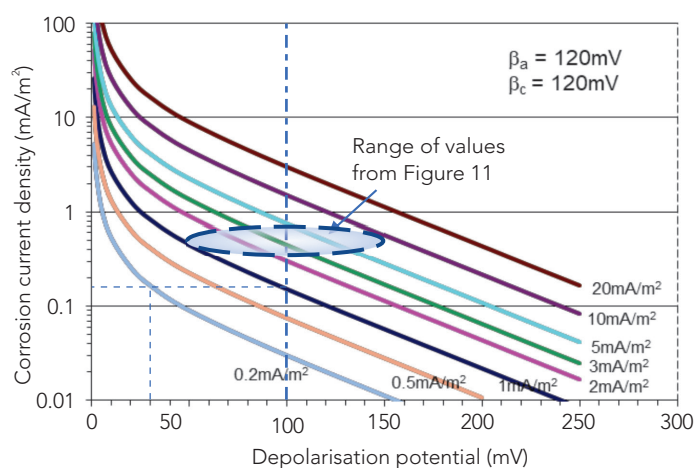


Figure 12: Theoretical corrosion current density of steel as a variant of its 24-hour depolarisation at a range of applied cathodic current densities

Where,

$i_{corr(app)}$  is the apparent corrosion current density,

$i_{appl}$  is the applied current density,

$\eta$  is the observed potential shift (depolarisation potential),

$\beta_a$  is the anodic Tafel slope (can be assumed as 120mV) and

$\beta_c$  is the cathodic Tafel slope (can be assumed as 120mV).

The equation allows an estimation of the average apparent corrosion current density of the steel if both the depolarisation potential and the applied current density are known. There is a large error involved in estimating the corrosion current density in this way as the total area of steel affected is not easily determined, small areas of intense corrosion could be greatly masked by the very large area under consideration and low oxygen availability renders the equation non-applicable.

The equation could, however, be helpfully used to understand the suitability of the depolarisation criterion. If the apparent corrosion current density is plotted against the level of depolarisation as a series of lines representing the applied current density (Figure 12) a number of conclusions can be drawn. For example, the steel corrosion current density applicable at a 100 mV depolarisation potential depends on the applied cathodic current density required to achieve that level of polarisation (vertical broken line in Figure 12). Consequently, the steel corrosion current density would be shown to be very high if the required applied current density is 20 mA/m² but very low if it is 0.2 mA/m². Furthermore, the corrosion current density of the steel would be shown to be the same if the level of depolarisation achieved at an applied current density of 1 mA/m² is 100 mV as it would be if the depolarisation was 30 mV but at a current density of only 0.2 mA/m² (horizontal broken line in Figure 12). At such a low steel corrosion current density it would not be necessary to apply the higher current density to achieve 100 mV of depolarisation but a lower current density of 0.2 mA/m², would be sufficient to prevent any future corrosion of

the steel. This defines cathodic prevention and it shows that the level of depolarisation in cathodic prevention applications can be much lower than 100 mV.

Indicating in Figure 12 the relative levels of applied current density and depolarisation shown in Figure 11, it can be seen that they fall within a band represented by an ellipse which suggests an essentially unchanging level of corrosion current density. Obviously, owing to the large errors involved, as explained earlier, the numbers shown are only indicative but the change of an apparent corrosion current density with time as estimated by the Butler Volmer equation can act as a useful indicator about the trend of the level of corrosion. This can be aided by the 24-hour depolarised potential so that a gradually decreasing apparent corrosion current density in combination to a 24-hour depolarised potential moving in a less negative direction would indicate that the CP system is at least reducing the level of corrosion of the protected steel reinforcement.

A major discovery with regard to galvanic anodes has been made from their long-term monitoring. Results from a 20-year field trial in the UK has indicated that the current output of alkali-activated galvanic anodes diminished approximately exponentially<sup>[15]</sup>. Furthermore, even though the size of anode had some effect, the spacing at which the anodes were positioned in the concrete structure primarily determined the speed of reduction of the current output. This is clearly shown in Figure 13<sup>[16]</sup> where anode spacing of only 300 mm delivered the best long-term performance and a spacing of 750 mm performed worse. The slope of the current over time can be used to determine an Aging Factor which describes the number of years at which the current output of the anodes is halved<sup>[15]</sup>. By studying long term results from over a dozen monitored sites of alkali-activated anodes, the values determined for the Aging Factor were found to vary between 5 and 14 years with a mean of 10 years. This compares very favourably with halide activated anodes, where the zinc is kept active by chloride, bromide etc.,

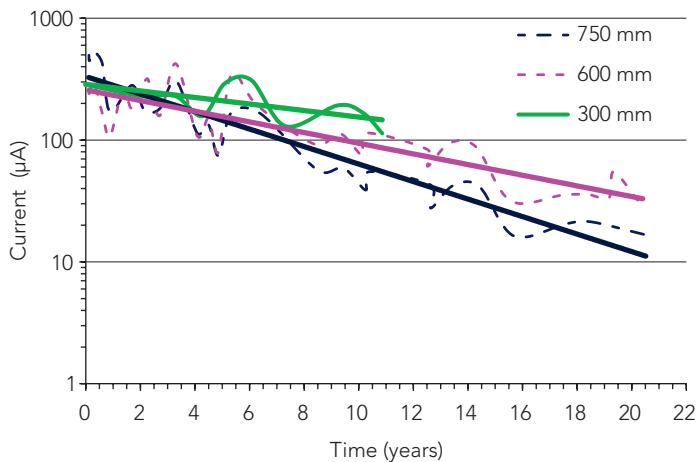


Figure 13: Reduction of current output of galvanic anodes embedded in structural elements of a bridge in the UK

which achieve an Aging Factor of less than 3 years. The reduced performance of halide activated anodes is thought to be caused by the relative insolubility of the zinc corrosion products which tend to block the pore structure of the encasing mortar close to the zinc/mortar interface and interfere with current flow (17). The importance of the Aging Factor in the design of galvanic CP systems is considerable as the current density at a future time can be accurately estimated in order to design for long-term protection. Figure 14 demonstrates this elegantly<sup>[15]</sup>. An alkali-activated anode set is, in this case, required to achieve a specific current density of 2 mA/m<sup>2</sup> at 20 years. For an Aging Factor of 13 years, the current density would need to be designed to deliver an early current density of around 7 mA/m<sup>2</sup>. Furthermore, the design will maintain a current density above 1 mA/m<sup>2</sup> even beyond 30 years. A typical halide anode set would require an initial current density of over 2000 mA/m<sup>2</sup> in order to achieve the required 2 mA/m<sup>2</sup> at 20 years, clearly an improbability.

The current density was also found to vary with concrete temperature. Analysis of data sets of current output of galvanic anodes in relation to the concrete temperature had shown

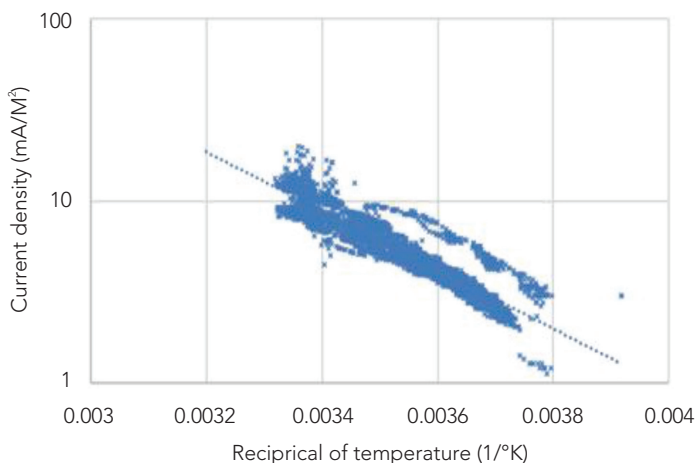


Figure 15: Relationship between the logarithm of current density of a galvanic anode set and the reciprocal of concrete temperature in Kelvin

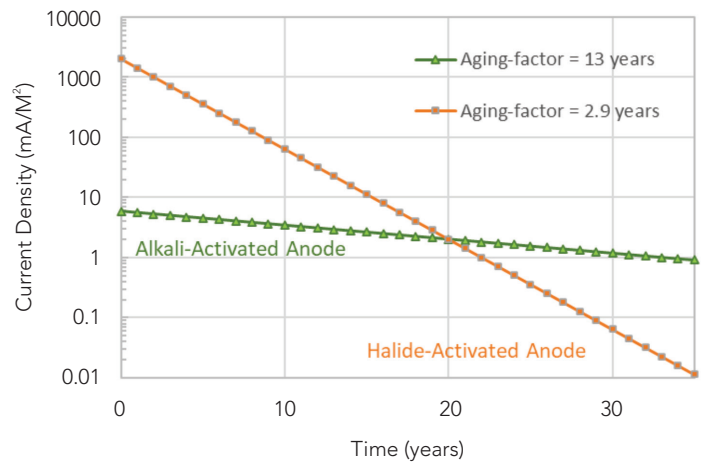


Figure 14: Anode current density vs time for two types of anodes with different Aging Factors such that both anodes provide a current density of 2 mA/m<sup>2</sup> at 20 years

that the level of current output is related to the reciprocal of the absolute temperature according to the Arrhenius equation (Equation 3) as depicted in Figure 15.

$$k = Ae^{-\frac{Ea}{RT}} \quad (3)$$

Where,

$k$  = Rate constant

$A$  = Frequency factor

$Ea$  = Activation energy

$R$  = Universal gas constant

$T$  = Absolute temperature (K)

A form of the equation<sup>[18]</sup> relates the corrosion rate, i.e. the current output from the zinc, to the reciprocal of temperature (Equation 4).

$$\text{Log } i_{\text{corr}} = \text{Log } A - \left( \frac{\Delta Ea}{2.303RT} \right) \quad (4)$$

Where,

$i_{\text{corr}}$  = Corrosion current of zinc metal

$\Delta Ea$  = Apparent activation energy of the corrosion process

The relationship shown represents a doubling of current density every 10-15°C increase in temperature over ambient conditions. The same variation of current output with temperature was seen in all monitored galvanic CP installations (see, for example, Figure 13). This knowledge allows a better calculation of the required current density for particular climatic conditions, for example, a higher current output will be expected in tropical conditions compared to cooler climates.

#### 4. THE NEED FOR SIMPLER ICCP SYSTEMS

There is no doubt that ICCP of steel reinforced concrete has, over the last decades, become a well-established technique for controlling reinforcement corrosion of structural elements. The expectation of long life protection has, however, been somewhat

Table 1: Cathodic Charge required to passivate steel at the chloride levels and current densities shown

Current Density (mA/m <sup>2</sup> )	30			50	
% Cl <sup>-</sup> in Mortar	1	2	3	2	4
Cathodic Charge (kC/m <sup>2</sup> )	15	120	190	74	108

reduced as some anode systems fail, monitoring equipment become antiquated and lack of adequate maintenance makes the systems inoperable with the average service life of any CP system falling to 15 years<sup>[19]</sup>. Inevitable additional costs are involved in maintaining and prolonging correct operation of the system. It appears that there is a requirement by structure managers and owners for simpler CP systems which will involve less maintenance and monitoring requirements.

ISO EN 12696:2016<sup>[10]</sup> has clear performance criteria that need to be continuously satisfied to ensure that the system is working. A much-used criterion is that a depolarisation potential of 100 mV should be achieved when the system is temporarily turned off for a period of 24 hours. The standard also defines that a successful CP system either passivates the steel or reduces the corrosion rate of the steel reinforcement which implies, correctly, as shown earlier, that achieving 100 mV of polarisation does not necessarily mean that corrosion has been arrested short-term. Nonetheless, it has been shown in several cases that if a CP system is running for an extended period, e.g. 5 years, and is then turned off, corrosion of the steel does not reinitiate over a significant time period<sup>[20]</sup>. As briefly mentioned earlier, this phenomenon is believed to be caused by some secondary effects, primarily, the increase in alkalinity and reduction in chloride concentration at the steel/concrete interface<sup>[21]</sup> which in effect reduces the [Cl<sup>-</sup>]/[OH<sup>-</sup>] ratio considerably below the critical ratio for initiation or maintenance of corrosion. It has also been suggested that realkalisation of the acidified pits occurs which allows steel repassivation within them<sup>[22]</sup>. Once repassivation of the steel is achieved, the application of cathodic prevention can then maintain the passive conditions long-term<sup>[23]</sup>.

It was soon realised that a system that can arrest steel corrosion relatively early and can then switch to cathodic prevention mode over the longer term is realistically possible. It was important, however, to identify the desired current density and overall charge delivery to the steel reinforcement for successful corrosion arrest to occur before the current density is reduced to the lower cathodic prevention current density levels (0.4-2 mA/m<sup>2</sup>) which have been shown to be easily achieved by galvanic anodes<sup>[14,23]</sup>.

To develop a viable Stage-1 procedure in which corrosion arrest of corroding steel can be achieved, a series of experiments were conducted, the results of which are published elsewhere<sup>[24]</sup>. What was discovered was very interesting. At two constant current levels, 30 mA/m<sup>2</sup> and 50 mA/m<sup>2</sup>, the corrosion of pre-corroded steel plates in mortars containing increasing doses of chloride by weight of cement as NaCl, was arrested after a length of time under polarisation. The required charge (current

multiplied by time) delivered to the steel until passivation of the steel was achieved increased with the level of chloride but was lower at the higher current density of 50 mA/m<sup>2</sup>, as summarised in Table 1.

Passivity of the steel was assumed when the 24-hour depolarised potential had reached -150mV vs Ag/AgCl, 0.5M KCl (-141mV vs SCE) as indicated in EN 12696: 2016<sup>[10]</sup>.

As revealed in the introduction, work by Pedeffferri<sup>[25]</sup> and Presuel-Monreno *et al.*<sup>[26]</sup> had demonstrated that passivity of the steel can be maintained in a corrosive environment for considerable periods, by a process they termed Cathodic Prevention, by applying a current density of 0.4-2 mA/m<sup>2</sup>. Even constant exposure to highly corrosive environments could not initiate corrosion at a current density of 1 mA/m<sup>2</sup><sup>[27]</sup>. Once corrosion is arrested, it would appear reasonable to suggest that a second stage of a process, based on Cathodic Prevention, is likely to protect the steel from further corrosion. Thus, a CP system based on a Two-Stage process appears to be a viable corrosion mitigation method.

This understanding formed part of a process that has enabled the recent development of a simple to install and operate Two-Stage Corrosion Mitigation system<sup>[28,29]</sup> as illustrated in Figure 16.

A field trial on a real structural element, a column underneath a bridge in the UK (Figure 17), was performed which demonstrated the effectiveness of the system.

All cracked and spalled concrete that had occurred on two edges of the column had been removed and repaired with an appropriate repair mortar. A total of six anodes were installed in a grid formation at a spacing of 600 mm in such a way so as to surround the repaired areas. Two silver/silver chloride standard reference electrodes were embedded within the test areas in-between the anodes to enable monitoring of the steel potentials both during application of the current and following disconnection. A junction box connected the anodes to the steel externally, so disconnection of the anodes, either the ICCP component or the galvanic component, was possible at any stage. The main results are detailed in Figure 18. The range of current densities applied either during Stage-1 (ICCP anodes) or Stage-2 (galvanic anodes) is indicated at the top of the graph. All potentials shown are 24-hour depolarised potentials, i.e. the current was interrupted for 24 hours before the steel potential was recorded. The anodes were disconnected for two longer periods starting at 130 days and 260 days to allow extended



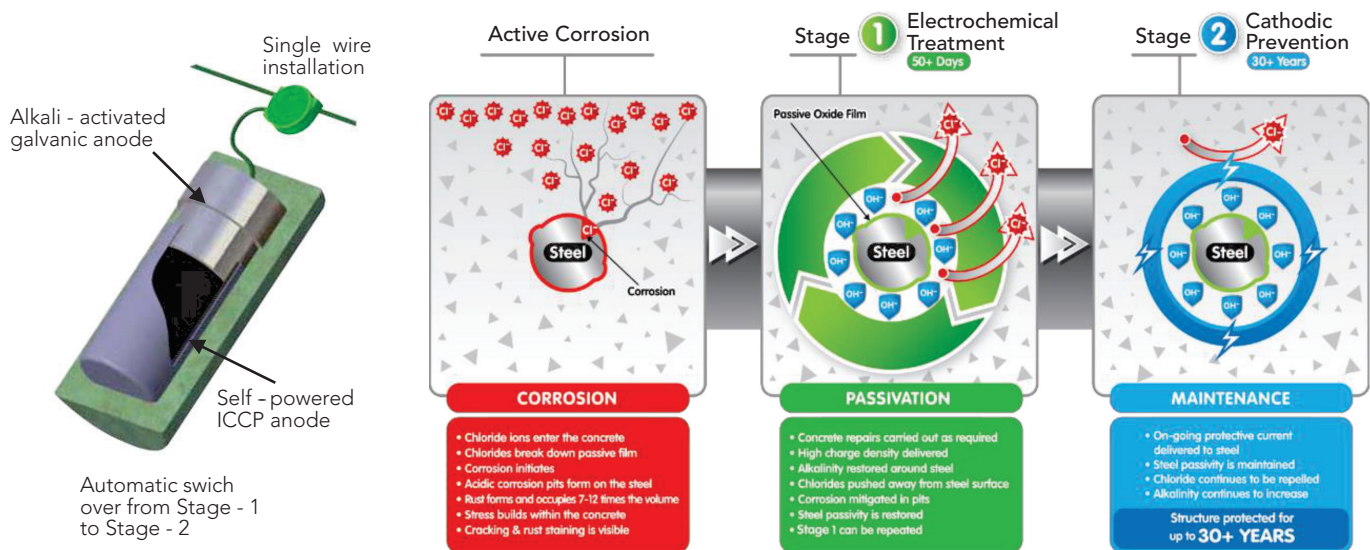


Figure 16: Two-Stage anode and schematic of its operation

depolarisation of the steel. The cumulative charge delivered to the steel obviously accrued much faster during the application of current from the ICCP component and it was already evident that even after the current was interrupted when  $130 \text{ kC/m}^2$  of charge was delivered to the steel, which was based on the laboratory results for passivating steel in a 2%  $\text{Cl}^-$  environment (Table 1), the steel had clearly passivated ( $>-150\text{mV}$  vs  $\text{Ag}/\text{AgCl}$ , 0.5 M KCl) and remained passive throughout even after a lengthy lower current delivery from the galvanic anodes at cathodic prevention mode.

Depolarisation levels during the ICCP periods were in the range of 150-200 mV as the current density was maintained at higher than the recommended range of  $2-20 \text{ mA/m}^2$  but it is this higher current density that changes the electrolyte around the steel to low, passive-inducing ratios of  $[\text{Cl}^-]/[\text{OH}^-]$ . Depolarisation during

the galvanic current delivery was considerably lower (50-75 mV) but passivation of the steel had already been achieved so a 100 mV depolarisation was not necessary during this cathodic prevention stage.

## 5. THE FUTURE OF CP- CONCLUDING REMARKS

Judging by advancements in the last 5-10 years, it is inevitable that further developments will occur in the field of cathodic protection of steel reinforcement. It is likely that reliable and greatly simplified cathodic prevention systems will become more of a norm in new construction where corrosion prevention would be considered more desirable and cost-effective than eventual corrosion mitigation and repair. Considerably less power would be required to drive cathodic prevention systems



Figure 17 Installation of a Two-Stage anode system in a column suffering from reinforcement corrosion from up to 2% chloride by weight of cement

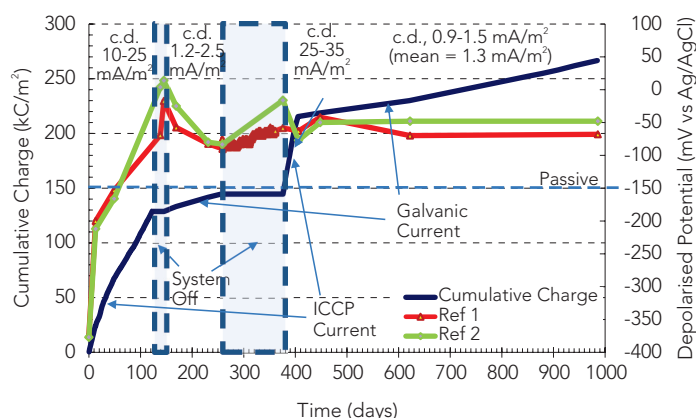


Figure 18: Details of the monitoring results since the installation of the system indicating current density, cumulative charge delivered to the steel and 24-hour depolarised potentials of the steel as measured by two standard embedded reference electrodes

as the current density does not need to exceed 1-2 mA/m<sup>2</sup>. Such levels of current density can be easily achieved by galvanic anodes. Furthermore, intelligent monitoring systems may be set up to predict when steel reinforcement corrosion initiation risk increases and activate an already installed cathodic prevention system. A move in that direction will be driven by the requirement for more environmentally acceptable procedures for structure management. Such a need will make the replacement of existing structures, buildings and infrastructure in general, environmentally very costly, so maintenance of existing structures and their conversion to new use is likely to become standard practice. For steel reinforced structural elements, extensive repairs to reinstate corroded areas would have to be reduced and cathodic protection would be a prime candidate for maintaining the structure to a safe condition with minimal repairs. For the same environmental reasons, low emission power generation will start to proliferate and self-powered localised CP systems, i.e. driven by solar and wind energy or rechargeable components, will likely become the norm.

The concept of cathodic protection would likely also evolve as a two-stage process similar to what was described in this article. Allowing a higher than what is currently considered to be a normal long-term cathodic current density of less than 20 mA/m<sup>2</sup> will inevitably arrest corrosion owing to the rapid build-up of alkali ions and the depletion of the aggressive chloride ions after which cathodic prevention would again be viable. As an example of power use, the long-term charge required to achieve 30-year protection with an ICCP system at a mean current density of 6 mA/m<sup>2</sup> to maintain a minimum of 100mV depolarisation as required by standards, is estimated to be of the order of 5,500 kC/m<sup>2</sup> of steel area. An equivalent 2-stage CP system where an early current density of 25 mA/m<sup>2</sup> for 2 months is applied to arrest corrosion and a long-term current density of 1 mA/m<sup>2</sup> up to 30 years to maintain steel passivity would use just 1,000 kC/m<sup>2</sup>, achieving a substantial saving in power consumption.

The continual development of galvanic anodes would likely increase the Aging Factor to well beyond 20 years by a combination of the better design of the metallic sacrificial element and of the encasing activating mortar. This would allow a much longer service life of galvanic anodes at designable current densities for specific environmental conditions and particularly, ambient temperature.

## REFERENCES

- [1] Bertolini, L., Bolzoni, F., Cigada, A., Pastore, T. & Pedferri, P. "Cathodic protection of new and old reinforced concrete structures." *Corros. Sci.*, 35, (1993), pp 1633-1639.
- [2] Hassanein, A. M., Glass, G. K. & Buenfeld, N. R. "Intermittent cathodic protection of concrete structures." *Corrosion of reinforcement in concrete construction*, eds. C. L. Page, P. B. Bamforth & J. W. Figg, The Royal Society of Chemistry, Cambridge, (1996), pp 407-414.
- [3] Page, C. L. and Sergi, G. "Developments in cathodic protection applied to reinforced concrete" *J. Mat. in Civil Eng.*, 12, 1, Sp. Issue, Durability of Construction Materials (Feb. 2000), pp 8-15.
- [4] Sergi, G. and Page, C. L. "Sacrificial anodes for cathodic protection of reinforcing steel around patch repairs applied to chloride-contaminated concrete" *Proc. EUROCORR'99 European Corrosion Congress*, Aachen, Aug-Sept 1999.
- [5] Unz, M., "Cathodic Protection of prestressed concrete pipe" *Corrosion*, 16, 6, (1960), pp. 289-297.
- [6] Heuze B., "Cathodic protection of steel in prestressed concrete" *Materials Performance* 11, (1965), pp. 57-62.
- [7] Cherry, B. W. "Cathodic protection: theory and practice", eds. V. Ashworth & C. Googan, Ellis Horwood, Chichester, (1993), 326-350.
- [8] Stratfull, R. F., "Experimental cathodic protection of a bridge deck" *Transportation Research Record*, 500, (1974), pp. 1-15.
- [9] Wyatt, B. S. "Anode systems for cathodic protection of reinforced concrete." *Cathodic protection: theory and practice*, eds. V. Ashworth & C. Googan, Ellis Horwood, Chichester, (1993), pp. 293-311.
- [10] ISO EN 12696:2016 "Cathodic protection of steel in concrete".
- [11] Weale, C. J. (1992). "Cathodic protection of reinforced concrete" Ph.D. thesis, Aston University, 415 pp.
- [12] Sergi, G., Simpson, D. & Hayfield, PCS. "Long Term Behaviour of Ceramic Tubular Shaped Anodes for Cathodic Protection Applications" *NACE Corrosion 2008*, Paper 1327.

- [13] Krishnan, N., Kamde, D., Pillai, R., Sergi, G., Shah, D. & Velayudham, R. "8-year performance of cathodic protection systems in reinforced concrete slabs and life-cycle cost benefits" Proc. Int. Conf. Sustainable Materials, Systems and Structures RILEM (SMSS2019) Durability, Monitoring and Repair of Structures, 20-22 March 2019 – Rovinj, Croatia pp. 611-618.
- [14] Rathod, N., Slater, P. Sergi, G., Seneviratne G. & Simpson D. "A fresh look at depolarisation criteria for cathodic protection of steel reinforcement in concrete" MATEC Web Conf. 289, 03011, (2019), Concrete Solutions.
- [15] Sergi, G., Seneviratne, G. & Simpson, D. "Monitoring Results of Galvanic Sacrificial Anodes in Steel Reinforced Concrete over 20 Years" Construction & Building Materials, 269, (2021) 121309.
- [16] Whitmore, D. & Sergi G. "Long-term Monitoring Provides Data Required to Predict Performance and Perform Intelligent Design of Galvanic Corrosion Control Systems for Reinforced Concrete Structures" NACE Corrosion 2021.
- [17] Sergi, G. & Seneviratne, G. "Improved design considerations for steel reinforcement corrosion control with galvanic anodes following performance evaluation from analysis of site data" Submitted in Structural Faults and Repair, Edinburgh, UK, 2021.
- [18] Emran, K. M. "Effects of concentration and temperature on the corrosion properties of the Fe–Ni–Mn alloy in HCl solutions", Research on Chemical Intermediates (2015) 41, pp. 3583–3596.
- [19] Polder RB, Leegwater G, Worm D, Courage W. Service life and life cycle cost modelling of cathodic protection systems for concrete structures. Cem Concr Compos. 47 (2014) pp. 69-74.
- [20] Christodoulou, C., Glass, G., Webb, J., Austin, S. and Goodier, C. "Assessing the long term benefits of Impressed Current Cathodic Protection" Corrosion Science, 52 (8), (2010) pp. 2671-2679.
- [21] Sergi G, Seneviratne AM. Extending the service life by electrochemical treatment of steel reinforcement. In: Proceeding of the RILEM International workshop on performance-based specification and control of concrete durability. (2014). pp. 385-92.
- [22] Glass GK, Davison N. "Pit Realkalisation and its Role in the Electrochemical Repair of Reinforced Concrete". J Corros Sci Eng. 9 (2006) 10.
- [23] Sergi G. Ten-year results of galvanic sacrificial anodes in steel reinforced concrete. Mater Corros. 62 (2011) pp. 98-104.
- [24] Rathod, N., Slater, PR., Sergi, G. and Seneviratne, G. "A Suggestion for a Two-Stage Corrosion Mitigation System for Steel Reinforced Concrete Structures" Proc. EUROCORR 2018, 102036, Kraków, Poland, 9 September 2018.
- [25] Pedefferri P. Cathodic protection and cathodic prevention. Constr Build Mater. 10 (1996) pp. 391-402.
- [26] Presuel-Monreno FJ, Sagues A. Steel Activation in Concrete Following Interruption of Long-Term Cathodic Polarization. Corrosion. 61 (2005) 428-36.
- [27] Bertolini L, Bolzoni F, Gastaldi M, Pastore T, Pedefferri P, Redaelli E. Effects of cathodic prevention on the chloride threshold for steel corrosion in concrete. Electrochim Acta. 54 (2009) pp. 1452-63.
- [28] Arnesen T, Beaudette M, Simpson D, Sergi G. Modular Corrosion Protection System for Mitigating Corrosion of Reinforced Concrete Structures. In: Forensic Engineering 8th Congress - Forging Forensic Frontiers. (2018).
- [29] Whitmore, D., Simpson, D., Beaudette, M and Sergi, G., "Two-Stage, Self-Powered, Modular Electrochemical Treatment System for Reinforced Concrete Structures" Corrosion & Materials, August 2019, pp 28-32.



**GEORGE SERGI** is Technical Director at Vector Corrosion Technologies heading the Research and Development Department which develops products for durability of concrete and steel reinforcement protection and offers corrosion mitigation techniques for the Civil Engineering and Construction Industries. He is author of several international patents and has developed noble products for corrosion protection of steel reinforcement. He was formerly Technical Director and Head of Corrosion at the Building Research Establishment, UK and Technical Director at Aston Material Services Ltd. He had originally spent 20 years researching the fundamentals of concrete durability and corrosion as applied to steel reinforced concrete at Aston University. He is Editor of the Construction and Building Materials Journal. He is a member of Cathodic Protection Committee GEL/603 assisting in the editing and publication of BSI and EN Standards. Email: georges@vector-corrosion.com

**Cite this article:** Sergi, G., (2021). "Cathodic protection of steel reinforcement: Past experience, performance and future opportunities", *The Indian Concrete Journal*, Vol. 95, No. 4, pp. 61-71.



www.icjonline.com

# THE INDIAN CONCRETE JOURNAL

## TAKE A CONCRETE DECISION. SUBSCRIBE TO ICJ TODAY.

Write to us at [info@icjonline.com](mailto:info@icjonline.com) and order your copy now!

### SUBSCRIPTION FORM [For Indian Nationals]

☐ Collector's Edition

☐ New subscriber

☐ Renewal (Please tick one)

Name: \_\_\_\_\_  
(Please fill in block letters)

Date of birth: 

d	d	m	m	y	y
---	---	---	---	---	---

Address: \_\_\_\_\_

Designation: \_\_\_\_\_  
(Leave this blank if it is a residential address)

\_\_\_\_\_  
\_\_\_\_\_  
\_\_\_\_\_

Company / Organisation: \_\_\_\_\_  
(Leave this blank if it is a residential address)

\_\_\_\_\_  
\_\_\_\_\_

City: \_\_\_\_\_

Cell no.: \_\_\_\_\_  
(MOBILE NUMBER IS COMPULSORY)

State / Province: \_\_\_\_\_

Pin Code: \_\_\_\_\_  
(PIN CODE IS COMPULSORY)

E-mail: \_\_\_\_\_  
(EMAIL IS COMPULSORY)

Subscription Tariff, Rupees (Inclusive of postage & handling)	1 year
Collector's Edition	1000/-
Online E-Journal*	1200/-
Paper edition	1800/-
Online E-Journal* & paper edition	2800/-

\*In Online E-Journal there will be no hard copy, subscribers can view the journal online at [www.icjonline.com](http://www.icjonline.com) with username and password

Send this form or write to [info@icjonline.com](mailto:info@icjonline.com) Website: [www.icjonline.com](http://www.icjonline.com)

#### DETAILS OF OTHER PAYMENT OPTIONS AND GENERAL TERMS AND CONDITIONS

##### TERMS AND CONDITION:

1. Advance payment needed 2. We are currently only accepting online payments. Details for the transfer are given below:  
**Account Name** - ACC LIMITED **Account Number** - 57500000308512 **Branch Address** - Fort, Mumbai **IFSC Code** - HDFC0000060  
3. After completion of each transaction, kindly inform us of the amount, transaction date and senders name, senders bank account number by email. 4. Payment once received will not be refunded or adjusted. 5. Please note that the subscription will be started / renewed from the next month of the receipt of the payment. We do not offer backdated subscriptions. 6. For any extra hard copy of the past 10 years, write to us for applicable charges, subject to availability, until stocks last. 7. ICJ is ordinarily posted to all subscribers by ordinary post on the 1st of every month from the Mumbai Post office. If you do not receive your copy by the end of the month, you can email us for a free replacement copy in the next month. A free replacement copy will not be entertained thereafter. For example, a free replacement copy for the March 2019 issue will be entertained only in April 2019, neither earlier, nor later. A free replacement copy for the March 2019 issue will not be entertained after April 2019. 8. Only one replacement copy will be entertained per year (12 months). 9. ICJ is posted to all subscribers by ordinary post. If you want to opt for courier service / registered post parcel, kindly add Rs. 2400 per year to the final amount.

(Please note that we have no branches)



# **ACC GOLD WATER SHIELD**

## **पानी से करें SHIELD**



Engineered with cutting-edge technology, **ACC GOLD WATER SHIELD** is an innovative water-repellent cement. Its unique formula offers your home a 360-degree shield against harmful effects of water seepage - making sure it remains strong and stylish, and continues to be admired, for years to come.



Strong & Durable



Scientifically  
Formulated



Innovative  
Technology

# **ACC**

करें कुछ कमाल